

UPSTREAM OPEN READING FRAMES DIFFERENTIALLY REGULATE GENE-
SPECIFIC TRANSLATION IN THE INTEGRATED STRESS RESPONSE

Sara Kathryn Young

Submitted to the faculty of the University Graduate School

in partial fulfillment of the requirements

for the degree

Doctor of Philosophy

in the Department of Biochemistry and Molecular Biology

Indiana University

July 2016

Accepted by the Graduate Faculty, Indiana University, in partial fulfillment of the requirements for the degree of Doctor of Philosophy.

Ronald C. Wek, Ph.D., Chair

Murray Korc, M.D.

Doctoral Committee

Amber L. Mosley, Ph.D.

May 13, 2016

John J. Turchi, Ph.D.

© 2016

Sara Kathryn Young

ACKNOWLEDGEMENTS

I am foremost indebted to Dr. Ronald C. Wek for being an extraordinary mentor who has worked to mold me into a capable research scientist. I appreciate the time and dedication of my research committee: Dr. Murray Korc, Dr. Amber L. Mosley, and Dr. John J. Turchi. Past and current members of the Wek lab were paramount to the work presented in this thesis, particularly Dr. Thomas D. Baird with his invaluable contribution to the EPRS project and overall support. I would also like to thank the faculty and staff of the Department of Biochemistry for their generous support and guidance. This work was supported by National Institutes of Health Grant GM049164 to R.C.W.

Sara Kathryn Young

UPSTREAM OPEN READING FRAMES DIFFERENTIALLY REGULATE GENE-SPECIFIC TRANSLATION IN THE INTEGRATED STRESS RESPONSE

Gene expression is a highly coordinated process that relies upon appropriate regulation of translation for protein homeostasis. Regulation of protein synthesis largely occurs at the initiation step in which the translational start site is selected by ribosomes and associated initiating factors. In addition to the coding sequences (CDS) for protein products, short upstream open reading frames (uORFs) located in the 5'-leader of mRNAs are selected for translation initiation. While uORFs are largely considered to be inhibitory to translation at the downstream CDS, uORFs can also promote initiation of CDS translation in response to environmental stresses. Multiple transcripts associated with stress adaptation are preferentially translated through uORF-mediated mechanisms during activation of the Integrated Stress Response (ISR). In the ISR, phosphorylation of α subunit of the translation initiation factor eIF2 α (eIF2 α -P) during environmental stresses results in a global reduction in protein synthesis that functions to conserve energy and nutrient resources and facilitate reprogramming of gene expression.

Many key regulators of the ISR network are subject to preferential translation in the response to eIF2 α -P. These preferentially translated genes include the pro-apoptotic transcriptional activator *Chop* that modifies gene expression programs, feedback regulator *Gadd34* that targets the catalytic subunit of protein phosphatase 1 to dephosphorylate eIF2 α -P, and glutamyl-prolyl tRNA synthetase *Eprs* that increases the charged tRNA pool and primes the cell for resumption of protein synthesis after stress remediation. Ribosome bypass of at least one inhibitory uORF is a common theme between *Chop*, *Gadd34*, and *Eprs*, which allows for their regulated expression in response to cellular stress. However, different features encoded within the uORFs of

the *Chop*, *Gadd34*, and *Eprs* mRNAs provide for regulation of their inhibitory functions, illustrating the complexities of uORF-mediated regulation of gene-specific translation. Importantly, preferentially translated ISR targets can also be transcriptionally regulated in response to cellular stress and misregulation of transcriptional or translational expression of *Gadd34* can elicit maladaptive cell responses that contribute to disease. These mechanisms of translation control are conserved throughout species, emphasizing the importance of translation control in appropriate gene expression and the maintenance of protein homeostasis and health in diverse cellular conditions.

Ronald C. Wek, Ph.D., Chair

TABLE OF CONTENTS

LIST OF FIGURES	x
ABBREVIATIONS	xiii
CHAPTER 1. INTRODUCTION	1
1.1 Regulation of gene expression by uORFs	1
1.2 uORFs and their function in the regulation of downstream translation initiation	5
1.3 Translation regulation during the Integrated Stress Response	7
1.4 Preferentially translated mRNAs play diverse roles in response to cellular stress	8
1.5 Ribosome reinitiation in the ISR.....	12
1.6 Ribosome bypass in the ISR.....	15
1.7 Cross-regulation between the ISR and other cellular stress pathways.....	18
CHAPTER 2. EXPERIMENTAL PROCEDURES	21
2.1 Cell culture and generation of stable cell lines.....	21
2.2 Mice	22
2.3 Immunoblot analyses	22
2.4 mRNA measurements by qPCR	23
2.5 Total RNA and DNA measurements	25
2.6 Polysome profiling and sucrose gradient ultracentrifugation	25
2.7 Plasmid constructions and luciferase assays	25
2.8 <i>In vitro</i> transcription and translation assays.....	30
2.9 Cell number and viability assays.....	31
2.10 Statistical analyses	32
CHAPTER 3. RESULTS: RIBOSOME REINITIATION DIRECTS GENE-SPECIFIC TRANSLATION AND REGULATES THE INTEGRATED STRESS RESPONSE	33
3.1 eIF2 α ~P is required for <i>Gadd34</i> transcription and translation, but <i>Crep</i> expression occurs independent of eIF2 α ~P	33

3.2 Preferential translation of <i>Gadd34</i> features an inhibitory uORF	37
3.3 <i>Gadd34</i> translation control involves bypass of an inhibitory uORF	41
3.4 The inhibitory function of <i>Gadd34</i> uORF2 is reliant on Pro-Pro-Gly juxtaposed to the uORF2 stop codon	42
3.5 <i>Crep</i> translation is dampened by an inhibitory uORF in an eIF2 α ~P independent manner	50
3.6 Regulatory properties of <i>Gadd34</i> uORF2 are transferable to a heterologous 5'-leader derived from <i>Crep</i>	54
3.7 Alterations in the regulatory features of <i>Gadd34</i> uORF2 affect cell viability during ER stress	58
CHAPTER 4. RESULTS: RIBOSOME ELONGATION STALL DIRECTS GENE- SPECIFIC TRANSLATION CONTROL IN THE INTEGRATED STRESS RESPONSE	
	63
4.1 The inhibitory function of <i>Chop</i> uORF is reliant upon an Ile-Phe-Ile sequence	63
4.2 Translation of an Ile-Phe-Ile sequence in the <i>Chop</i> uORF results in an elongation stall.....	73
4.3 Alterations in <i>Chop</i> uORF translation control change the dynamics of CHOP expression.....	79
4.4 Alterations in <i>Chop</i> uORF translation control affect cell viability.....	85
CHAPTER 5. RESULTS: TRANSLATION REGULATION OF THE GLUTAMYL- PROLYL TRNA SYNTHETASE GENE EPRS THROUGH BYPASS OF UORFS WITH NON-CANONICAL INITIATION CODONS	
	88
5.1 <i>Eprs</i> expression is increased in response to eIF2 α ~P through enhanced translation	88
5.2 Preferential translation of <i>Eprs</i> features two uORFs with non-canonical initiation codons	89

5.3 <i>Eprs</i> translational control involves bypass of two uORFs with non-canonical initiation codons	98
5.4 Translation control of <i>Eprs</i> during treatment with the drug halofuginone.....	106
CHAPTER 6. RESULTS: NMP4 IS A NOVEL REGULATOR OF RIBOSOME BIOGENESIS AND CONTROLS THE UNFOLDED PROTEIN RESPONSE VIA REPRESSION OF <i>Gadd34</i>	111
6.1 Loss of <i>Nmp4</i> in MSPCs results in increased expression of <i>Gadd34</i>	111
6.2 Loss of <i>Nmp4</i> in MSPCs increases protein synthesis	114
6.3 Deletion of <i>Nmp4</i> in MSPCs increases ribosome biogenesis.....	115
6.4 Deletion of <i>Nmp4</i> sensitizes MSPCs to chronic ER stress	118
CHAPTER 7. DISCUSSION	122
7.1 Differential translation control of <i>Gadd34</i> and <i>Crep</i>	122
7.2 Roles of uORFs in regulating the ISR and cellular resistance to stress	125
7.3 Translation control of <i>Chop</i> through a ribosomal elongation stall	125
7.4 Role of uORFs in regulating cell viability	128
7.5 Translation control of <i>Eprs</i> through non-canonical initiation codons.....	129
7.6 Expression of <i>Eprs</i> is induced during diverse cellular stresses	133
7.7 NMP4 regulates protein synthesis through transcriptional repression of <i>Gadd34</i> ..	136
7.8 The link between uORF-mediated translation regulation and mRNA abundance ..	140
7.9 Evolutionary conservation of uORF-mediated translation mechanisms	141
REFERENCES	146
CURRICULUM VITAE	

LIST OF FIGURES

Figure 1. uORFs regulate translation initiation at downstream coding sequences	4
Figure 2. The Integrated Stress Response features a global reduction in translation initiation concomitant with preferential translation of stress remediation transcripts	10
Figure 3. uORF regulation of downstream translation through the Delayed translation reinitiation mechanism.....	14
Figure 4. uORF regulation of downstream translation through the Bypass mechanism.....	17
Figure 5. eIF2 α ~P is required for induced <i>Gadd34</i> translation, but <i>Crep</i> expression occurs independent of eIF2 α ~P	35
Figure 6. Preferential translation of <i>Gadd34</i> features an inhibitory uORF	39
Figure 7. <i>Gadd34</i> translation control involves bypass of an inhibitory uORF that relies on a Pro-Pro-Gly juxtaposed to the uORF2 stop codon.....	46
Figure 8. <i>Gadd34</i> translation control involves bypass of an inhibitory uORF	48
Figure 9. <i>Crep</i> translation is dampened by an inhibitory uORF in an eIF2 α ~P-independent manner	52
Figure 10. Regulatory properties of <i>Gadd34</i> uORF2 are transferable to a heterologous 5'-leader derived from <i>Crep</i>	56
Figure 11. Alterations in the regulatory features of <i>Gadd34</i> uORF2 affect cell viability during ER stress	61
Figure 12. <i>Chop</i> translation control involves bypass of an inhibitory uORF due in part to poor start codon context	67
Figure 13. <i>Chop</i> translation control involves an inhibitory uORF that relies on an encoded Ile-Phe-Ile sequence	69
Figure 14. <i>Chop</i> translation control involves bypass of an inhibitory uORF	71

Figure 15. Translation of the <i>Chop</i> uORF results in a ribosome elongation stall that is dependent on an Ile-Phe-Ile sequence	76
Figure 16. Alterations in <i>Chop</i> uORF translation control change the dynamics of <i>Chop</i> expression.....	83
Figure 17. Alterations in <i>Chop</i> uORF translation control lower cell viability during stress	86
Figure 18. <i>Eprs</i> translational expression is increased in response to eIF2 α -P	92
Figure 19. The 5'-leader of the <i>Eprs</i> mRNA directs preferential translation	94
Figure 20. Preferential translation of <i>Eprs</i> features two uORFs with non-canonical initiation codons	96
Figure 21. <i>Eprs</i> translation control involves bypass of an uORF with a non-canonical CUG initiation codon.....	102
Figure 22. <i>Eprs</i> translational control involves bypass of uORFs with non-canonical initiation codons	104
Figure 23. <i>Eprs</i> translation control is regulated in response to halofuginone treatment.....	108
Figure 24. GCN2 confers protection against halofuginone-induced toxicity	110
Figure 25. Expression of <i>Gadd34</i> is increased upon deletion of <i>Nmp4</i>	113
Figure 26. Deletion of <i>Nmp4</i> in MSPCs increases ribosome biogenesis and protein synthesis	117
Figure 27. Deletion of <i>Nmp4</i> facilitates maintenance of global translation during activation of the UPR	120
Figure 28. Deletion of <i>Nmp4</i> sensitizes MSPCs to pharmacological induction of ER stress	121
Figure 29. Models for <i>Gadd34</i> and <i>Crep</i> translational control	124
Figure 30. Model for <i>Chop</i> translational control	127

Figure 31. Model for <i>Eprs</i> translational control	132
Figure 32. Model depicting gene regulation downstream of the eIF2 kinase GCN2 during halofuginone treatment	135
Figure 33. Model for NMP4 regulation of ribosome biogenesis and the UPR	139
Figure 34. uORF mechanisms of translation control are evolutionarily conserved	144

ABBREVIATIONS

ATF	Activating Transcription Factor
bZIP	Basic Leucine Zipper
CDS	Coding Sequence
CHOP	C/EBP Homologous Protein
CHX	Cycloheximide
CReP	Constitutive Repressor of eIF2 Phosphorylation
eIF	Eukaryotic Initiation Factor
eIF2 α ~P	Phosphorylation of the α Subunit of Eukaryotic Initiation Factor 2
EPRS	Glutamyl-Prolyl-tRNA Synthetase
ER	Endoplasmic Reticulum
FRT	Flp Recombination Target
GADD34	Growth Arrest and DNA Damage-Inducible Protein 34
GCN	General Control Nonderepressible
GEF	Guanine Nucleotide Exchange Factor
HF	Halofuginone
ISR	Integrated Stress Response
MEF	Mouse Embryonic Fibroblast
MSPC	Mesenchymal Stem Progenitor Cell
NMP4	Nuclear Matrix Protein 4
ORF	Open Reading Frame
PCR	Polymerase Chain Reaction
PERK	PKR-like Endoplasmic Reticulum Kinase
qRT-PCR	Quantitative Real-Time PCR
SAL	Salubrinal
TG	Thapsigargin

tRNA	Transfer RNA
TUN	Tunicamycin
uORF	Upstream Open Reading Frame
UPR	Unfolded Protein Response
UTR	Untranslated Region
WT	Wild-Type

CHAPTER 1. INTRODUCTION

1.1 Regulation of gene expression by uORFs

Multiple genome-wide analyses, including those utilizing ribosome and polysome profiling and mass spectrometry approaches, have provided evidence to suggest that translation is a major regulator of gene expression (1-5). Ribosome profiling, for instance, has revealed multiple previously uncharacterized translation initiation sites, including those that result in N-terminal protein extensions and truncations and likely functionally distinct protein isoforms (4,6). Another class of open reading frames (ORFs) suggested to be translated at high frequency are short, upstream ORFs (uORFs) that are located within the 5'-leader of mRNAs (3-5). uORFs are denoted by an in-frame initiation and termination codon and contain at least one additional codon in between. Over 40% of mammalian mRNAs contain uORFs, illustrating that uORFs are prevalent genome-wide and can serve as major regulators of translation (5,7,8). Approximation of uORF prevalence has relied upon the use of an AUG to denote the uORF start codon, however, recent ribosome profiling studies indicate that non-canonical initiation codons (e.g. CUG, UUG, and GUG) can also serve as competent sites of translation initiation (3,4). These findings suggest that the magnitude of uORF prevalence and the contribution of uORF translation in the regulation of gene expression have likely been underestimated.

Typically, uORFs are considered to be inhibitors of downstream translation initiation at the functional protein coding sequence (CDS). The inhibitory effect of uORFs is attributed to the fact that in eukaryotes the 43S preinitiation complex binds to the 5'-cap structure of the mRNA and scans processively 5' to 3' and initiates translation preferentially at the first encountered initiation codon that is an optimal context (9). The 43S preinitiation complex is composed of multiple factors including eukaryotic initiation factor (eIF) -3, eIF1, eIF1A, the eIF2/GTP/Met-tRNA_i^{Met} ternary complex, and the small

40S ribosomal subunit (10). Disassociation of the eIF2 ternary complex and other critical initiation factors during translation of constitutively repressing uORFs is suggested to be the cause of the low levels of subsequent translation reinitiation at downstream coding sequences.

While uORFs can serve as repressors of CDS translation in a constitutive manner, there are also examples of uORFs that serve as dampeners in a controlled fashion or even promote translation initiation at the CDS in response to environmental stresses (4,11). Based on these studies, uORFs can have one or more core properties that are critical for translational control (Figure 1). These properties include those that: 1) enhance reinitiation after uORF translation, allowing for degrees of translation initiation at the downstream CDS; 2) direct ribosome elongation stalling during translation of the uORF and, as a consequence, thwart translation at the downstream CDS and possibly subsequent ribosome scanning of the 5'-leader of the affected mRNA; 3) promote ribosome dissociation from the mRNA and therefore diminish subsequent CDS translation; 4) position uORFs out-of-frame with the CDS, resulting in ribosome termination downstream of the CDS start codon; and 5) allow for scanning ribosomes to bypass the uORF in either a largely constitutive fashion or upon induction of physiological signals (Figure 1). These uORF properties, which can be incorporated individually or in combination within mRNAs, help determine the specific mechanism of translational control of a given gene (5,11-15).

Frequently the uORF-mediated mechanisms of translation control are featured in mRNAs that encode proteins important for the cellular response to stress and control of cell fate (5,11-15). This is well illustrated in the examples of preferential translation of mRNAs involved in adaptation to cellular stress by phosphorylation of eukaryotic initiation factor 2 on its α subunit at serine 51 (eIF2 α -P). Because eIF2 α -P can direct translational control in response to a range of different environmental stresses, this

pathway is often referred to as the Integrated Stress Response (ISR) (16). This thesis highlights the mechanisms by which uORFs can modulate translation at the CDS, and the processes by which uORFs with these diverse properties can be incorporated individually or in combination into mRNAs to facilitate preferential translation in response to eIF2 α -P in the ISR.

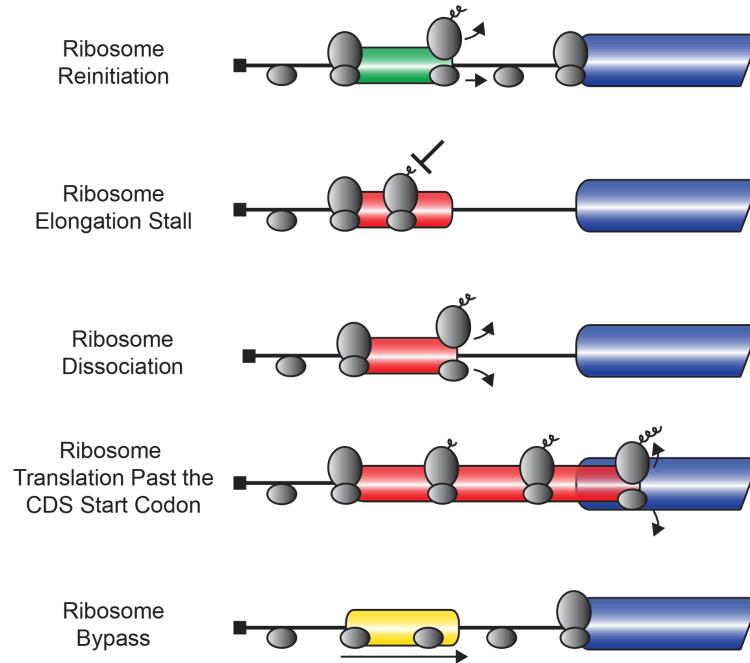


Figure 1. uORFs regulate translation initiation at downstream coding sequences.

uORFs can have multiple core properties, including promoting ribosome reinitiation after uORF translation, ribosome elongation stalling while translating the uORF, ribosome dissociation from the mRNA, ribosome translation past the CDS start codon, or ribosome bypass of the uORF. The CDS is represented by the blue bar; positive-acting uORFs are represented by a green bar, negative-acting uORFs are represented by a red bar; and uORFs that have no effect on downstream translation are represented by a yellow bar. Scanning and elongating ribosomes are illustrated by the gray ovals.

1.2 uORFs and their function in the regulation of downstream translation initiation

The observation that uORFs can function in distinct ways that promote, inhibit, or have no effect on downstream translation initiation suggests that it is the specific features of the uORFs themselves that determine their regulatory functions. Promotion of ribosome reinitiation following translation of an uORF, for instance, has been shown to rely upon the length of the uORF, the distance between the uORF stop codon and the CDS, and/or the nucleotide sequences surrounding the uORF termination codon (17-20). Long uORFs are usually considered to be inhibitory to downstream translation and result in low amounts of ribosome reinitiation. Long uORFs are thought to inhibit downstream translation due to the increased time that the ribosome spends translating the uORF, thus allowing for the loss of critical initiation factors that are required for efficient translation reinitiation (18). Mutations in eIF3 further exacerbate the low levels of translation reinitiation observed after uORF translation, suggesting that eIF3 may be a critical initiation factor that functions to promote ribosome reinitiation (21). Furthermore, retention of eIF3 by the 40S ribosomal subunit post-translation termination is suggested to allow the 40S subunit to maintain its interaction with the mRNA being translated (22-24). Maintenance of the 40S-mRNA interaction would thus allow for the small ribosomal subunit to reacquire a new eIF2 ternary complex and facilitate reformation of the 43S preinitiation complex, resumption of scanning, and translation initiation at a downstream start codon (22,24,25).

Because the time spent translating the uORF is considered to help determine the ability of ribosomes to reinitiate downstream, it is perhaps not surprising that uORFs that induce ribosome elongation stalls are largely inhibitory to downstream translation. Pauses in elongation have been shown to be reliant upon both nucleotide and polypeptide sequences encoded in the uORF, as well as the interaction of trans-acting factors, such as polyamines, with the nascent uORF peptide (26,27). Stable RNA

secondary structures, for instance, can slow uORF translation elongation sufficiently to reduce downstream translation reinitiation (18). Codon usage bias in the uORF also likely regulates efficiency of the uORF ribosome elongation (27). In the translational control of the gene encoding S-adenosylmethionine decarboxylase, involved in polyamine biosynthesis, high levels of the end-product polyamines are suggested to facilitate an interaction between the uORF nascent polypeptide and the ribosome exit channel that ultimately results in a potent ribosome elongation stall (26).

Ribosome dissociation from the mRNA post-uORF translation is also regulated by the nucleotide sequence or polypeptide sequence encoded at the uORF (19,23,25,28,29). Bicistronic calicivirus mRNAs, for instance, promote retention of the 40S ribosomal subunit after translation of an ORF through an interaction that occurs between the nucleotides located in the 3'-portion of the ORF and the 18S rRNA. Retention of the 40S subunit by this cis-acting mRNA element is suggested to allow sufficient time for the ribosomal subunit to reacquire a new eIF2 ternary complex and reinitiate translation downstream (23,25). Nucleotide sequences that promote ribosome dissociation have also been described and are suggested to rely upon interactions between the nucleotide sequence 3' of the uORF stop codon and the 40S ribosomal subunit that disrupt efficient translation termination (20,29).

The presence of an uORF that overlaps and is out-of-frame with the CDS is also an efficient barrier to mRNA translational expression. In this case, translation of the uORF results in translation termination and resumption of 40S subunit scanning that occurs past the initiation codon for the CDS. Since translating ribosomes are suggested to only 'backup' in a 3' to 5' fashion for a small number of nucleotides, this results in low translation of the CDS (13,18).

The mere presence of an uORF in the 5'-leader of a mRNA does not necessarily mean that the uORF will be efficiently translated. Ribosomes may also bypass the

uORF and initiate instead at the downstream CDS (12,14,30,31). This ability is thought to be due at least in part to the nucleotide sequences flanking the AUG initiation codon (9,32). Deviations from the so-called Kozak consensus sequence result in decreased translation initiation and increased uORF ribosome bypass. In addition to the start codon context, the specific initiation codon utilized can result in ribosome bypass (4,33). Non-canonical initiation codons (CUG, UUG, and GUG) can also serve as functional sites of translation initiation, although this was previously considered to occur less frequently than translation initiation at an AUG (3,4,34). Bypass of uORFs with non-canonical initiation codons has recently been shown to be a feature of several mRNAs that are subject to preferential translation during cellular stress (4,33).

1.3 Translation regulation during the Integrated Stress Response

During the initiation phase of translation, eIF2 associates with initiator Met-tRNA_i^{Met}, GTP, the 40S small ribosomal subunit, and additional initiation factors to form the 43S preinitiation complex that scans the mRNA and facilitates start codon selection (35). Phosphorylation of eIF2 α inhibits the exchange of GDP for GTP that decreases formation of the 43S preinitiation complex and triggers a global reduction in translation initiation. As mentioned previously, eIF2 α -P can direct translational control in response to a range of different environmental stresses, and as a result this pathway is often referred to as the Integrated Stress Response (ISR) (16). Phosphorylation of eIF2 α occurs through the actions of multiple stress-sensing eIF2 kinases. To illustrate, eIF2 α is phosphorylated by PKR-like ER kinase (PERK) in response to an accumulation of unfolded protein in the lumen of the endoplasmic reticulum (ER), whereas amino acid deprivation is sensed by the General Control Non-derepressible 2 (GCN2) kinase in the cytosol (16,36).

In addition to repression of protein synthesis that is incurred through eIF2 α -P, a subset of mRNAs experience enhanced translation during cellular stress (Figure 2A) (5). Many preferentially translated mRNAs rely on uORF-mediated mechanisms that promote expression of the CDS-encoded protein during cellular stress (12,13,30,37,38). However, genome-wide analysis of mRNA translation during cellular stress revealed that uORFs are roughly equally distributed between those mRNAs that are repressed, resistant, or preferentially translated during cellular stress and eIF2 α -P (Figure 2A) (5). These findings emphasize that it is the specific aforementioned properties of the uORFs that are critical for their regulatory capabilities in translation. Furthermore, the proper mixing and matching of these uORF features are critical for uORF-mediated translational control mechanisms that appropriately regulate gene expression for optimal adaptation to environmental stress. Examples of how these uORF features can be combined to produce complex mechanisms of translational control will be highlighted in the Ribosome reinitiation and Ribosome bypass sections of this thesis.

1.4 Preferentially translated mRNAs play diverse roles in response to cellular stress

Importantly, the encoded CDS products of mRNAs that are preferentially translated through uORF-mediated mechanisms play diverse roles in remediation of cellular stress (Figure 2B). Included among the ISR preferentially translated gene transcripts are *Atf4* (*Creb2*), *Chop* (*Ddit3/Gadd153*), *Atf5*, and *C/ebp α* and β that each encode basic leucine zipper (bZIP) transcription factors that act to modify gene expression programs to address cellular stress (Figure 2B) (12-15,37,38). *Gadd34* (*Ppp1r15a*) is also preferentially translated and combines with the catalytic subunit of protein phosphatase 1 (PP1c) to regulate dephosphorylation of eIF2 α -P and restore protein synthesis after amelioration of stress damage (Figure 2B) (30,39,40). Other

preferentially translated mRNAs include those that encode nutrient transporters SLC35A4 and CAT1, as well as the bifunctional glutamyl-prolyl tRNA synthetase EPRS, which together serve to increase available nutrients and prime the cell for resumption of protein synthesis once cellular stress is remediated (Figure 2B) (11). Finally, cell fate regulator IBTK α was shown to be subject to preferential translation through a mechanism involving uORFs (Figure 2B) (5). uORF-mediated preferential translation thus serves to promote expression of key ISR genes involved in stress alleviation and maintenance of protein homeostasis in diverse cellular conditions.

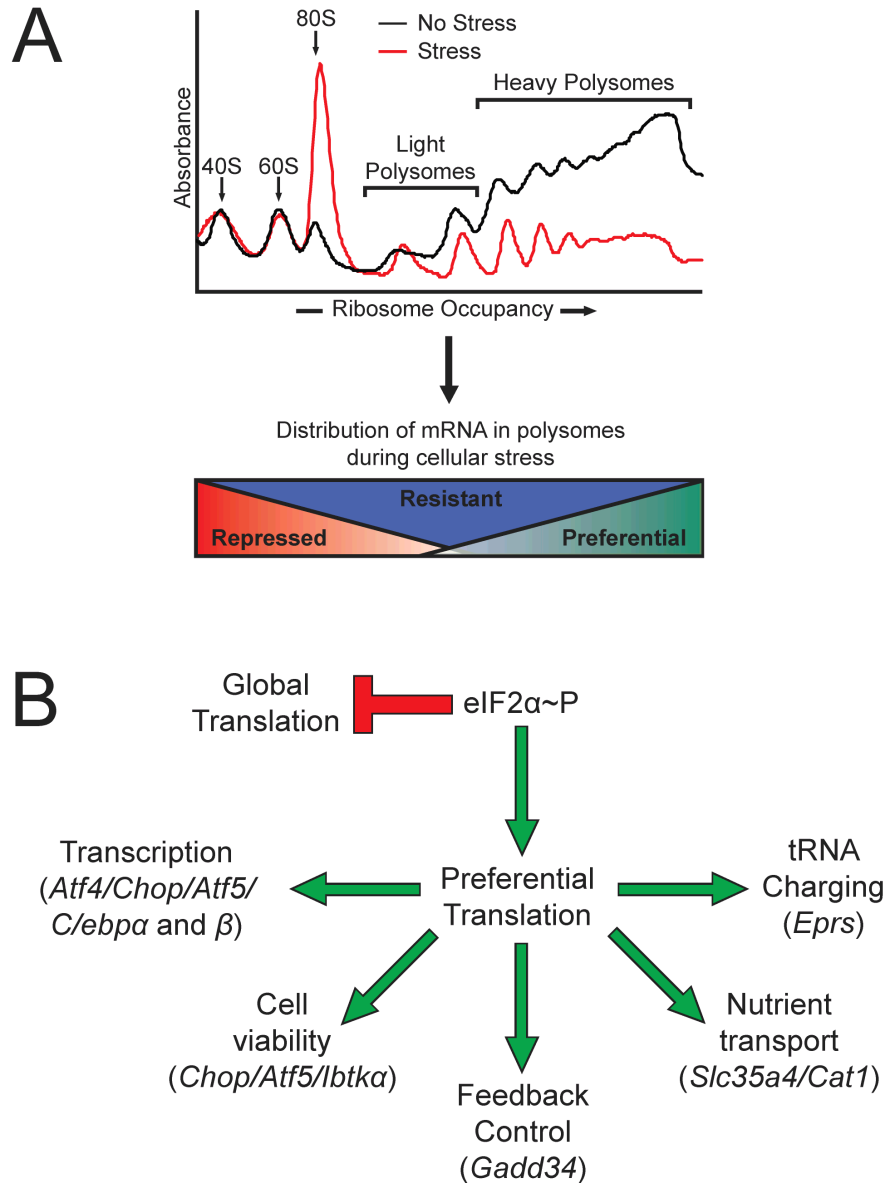


Figure 2. The integrated Stress Response features a global reduction in translation initiation concomitant with preferential translation of stress remediation transcripts. A, Depiction of polysome profiles from mouse embryonic fibroblast cell lysates that were left untreated (black line) or subjected to the ER stress inducer thapsigargin (red line). Basal polysome profiles feature distinctive peaks for the 40S and 60S ribosomal subunits and the 80S monosome, with large peaks observed for heavy polysomes, which is indicative of high levels of global translation. Polysome

profiles from cells subjected to ER stress feature decreased heavy polysomes and an elevated 80S monosome peak, indicative of a reduction in global translation initiation during eIF2 α -P. Those mRNAs that are preferentially translated during cellular stress are largely found associated with heavy polysomes, whereas those mRNAs that are repressed during cellular stress are largely associated with 80S monosomes and light polysomes during endoplasmic reticulum stress. The mRNAs that are translated constitutively are associated with polysomes independent of stress. B, Depiction of the preferentially translated mRNAs and their function in stress remediation. Multiple preferentially translated mRNAs encode transcription factors that promote stress alleviation (*Atf4/ C/ebp α* and β). If the cellular stress is too great to overcome, a subset of transcription factors promotes a pro-apoptotic signaling cascade (*Chop/Atf5*). Feedback dephosphorylation occurs through the activity of the preferentially translated *Gadd34*. Priming of the cell for resumption of global translation occurs through the activity of the preferentially translated nutrient transporters *Slc35a4* and *Cat1*, as well as the glutamyl-prolyl tRNA synthetase *Eprs*. Cell fate regulator *Ibtk α* is also preferentially translated by an uORF-mediate mechanism.

1.5 Ribosome reinitiation in the ISR

One of the predominant mechanisms of uORF-mediated regulation of CDS expression involves the ability of the 40S ribosome to resume scanning after uORF translation and reinitiate at downstream ORFs. Increasing the distance between the stop codon of the uORF and the CDS initiation codon can enhance CDS translation (17). This finding was attributed largely to the ability of the scanning ribosome to reacquire critical initiation factors such as the eIF2 complex, following uORF translation. The extended distance between the uORF stop codon and CDS initiation codon allows more time for the scanning 40S to reacquire a new eIF2/GTP/Met-tRNA_i^{Met} ternary complex, a significant feature of the Delayed translation reinitiation model that was originally identified in the yeast *Saccharomyces cerevisiae* for the transcriptional activator GCN4 (19,41).

Translational control mechanisms for yeast *Gcn4* and mammalian *Atf4* are well-understood mechanisms for translation reinitiation by uORFs. Both genes encode transcription factors that increase expression of genes involved in nutrient import, metabolism, and alleviation of oxidative stress (13,38,42-45). The 5'-leader of the mammalian *Atf4* contains two uORFs: the 5'-proximal uORF1 that is three codons in length and the fifty-nine codon long uORF2 that overlaps out-of-frame with the *Atf4* coding region (Figure 3). The 5'-leader of yeast *Gcn4 mRNA* contains four uORFs, each encoding polypeptides two to three residues in length (Figure 34C) (19,29). In the Delayed translation reinitiation model, the 5'-proximal uORF1 in the *Atf4* and *Gcn4* 5'-leaders acts as a positive element that promotes downstream translation reinitiation (13,19,28). During unstressed cellular conditions, the 40S ribosome resumes scanning after translation of uORF1 and reacquires a new eIF2/GTP/Met-tRNA_i^{Met} complex in sufficient time to reinitiate translation at the next uORF initiation codon. In the case of *Atf4*, translation initiation at the overlapping out-of-frame uORF2 results in translation

termination 3' of the *Atf4* CDS. After translation of uORF2, the ribosome dissociates from the *Atf4* mRNA, thereby reducing expression of the *Atf4* coding region (Figure 3) (13). Similar to the inhibitory nature of *Atf4* uORF2, translation of one of the downstream *Gcn4* uORFs 2, 3, or 4 thwarts expression of the *Gcn4* CDS during nonstressed conditions (Figure 34C) (20,29). The inhibitory property of uORF4 relies upon a 10-nucleotide sequence 3' of the uORF4 stop codon that is suggested to interact with the 40S ribosomal subunit to promote ribosome dissociation (20).

During cellular stress, eIF2 α ~P results in lowered levels of eIF2/GTP that is required for delivery of Met-tRNA_i^{Met} for reinitiating ribosomes. As a consequence, after translation of uORF1 the scanning 40S ribosomal subunit takes a longer amount of time to reacquire a new eIF2 ternary complex that is required for recognition of the next translation initiation codon in the 5'-leaders of the *Atf4* and *Gcn4* mRNAs. The delay in eIF2 ternary complex acquisition allows the 40S ribosomal subunit to scan through the inhibitory uORFs in the two mRNAs and instead promote translation initiation at the *Atf4* or *Gcn4* CDS (Figures 3 and 34C) (13,41). The delayed reinitiation results in the preferential translation of the *Atf4* and *Gcn4* CDS during cellular stress that promotes production of ATF4 and GCN4 proteins that serve to transcriptionally enhance genes important for remediation of the stress damage (13,19,46).

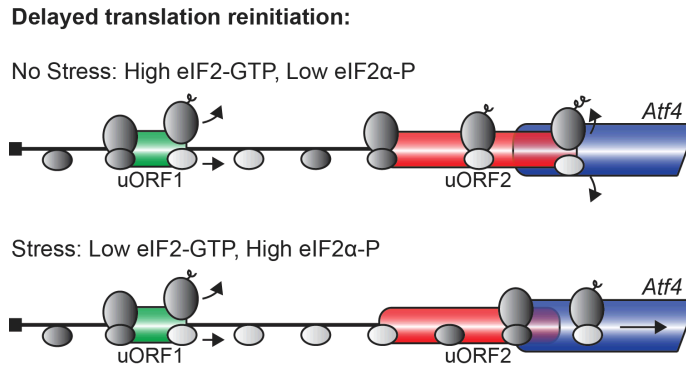


Figure 3. uORF regulation of downstream translation through the Delayed translation reinitiation mechanism. During no stress conditions, there are low levels of eIF2 α -P and high levels of eIF2-GTP. Ribosomes scanning the *Atf4* mRNA initiate at the 5'-proximal uORF1 and following termination, quickly reacquire a new ternary complex. Competent 43S scanning ribosomes (dark gray oval) then reinitiate translation at uORF2, which overlaps out-of-frame with the *Atf4* CDS. Translation of uORF2 results in ribosome termination and dissociation 3' of the *Atf4* initiation codon, resulting in low *Atf4* expression. During cellular stress, elevated eIF2 α -P results in low levels of eIF2-GTP. Ribosomes scanning the *Atf4* mRNA initiate at uORF1 and post-uORF translation resumes scanning. Due to the low levels of eIF2 ternary complex, the 40S ribosome (light gray oval) scans past the initiation codon of the inhibitory uORF2 before reacquiring a new ternary complex (dark gray oval). Delayed acquisition of the eIF2 ternary complex results in translation initiation at the *Atf4* CDS and an increase in *Atf4* expression during cellular stress.

1.6 Ribosome bypass in the ISR

During translation initiation, the competent 43S preinitiation complex must select the start codon in order for translation to commence (47). The optimal nucleotide context surrounding the start codon, termed the Kozak consensus sequence, is GCC(A/G)CCAUGG of which the most important residues are the purines in the -3 and +4 positions (9,32). These two residues have been shown to interact with the eIF2 α subunit and the 18S rRNA contained within the small ribosomal subunit (48). Both of these interactions are, thus, proposed to promote recognition of the initiation codon. Additionally, deviation from the Kozak consensus sequence, or poor uORF start codon context, has been associated with those mRNAs that are preferentially translated, whereas mRNAs that are repressed during eIF2 α -P typically contain an uORF in strong Kozak consensus sequence (5). These findings suggest that start codon context plays a significant role in uORF-mediated translation regulation.

An important example in the ISR of ribosome bypass of an uORF is that of *Chop* (Figure 4) (12,37). Preferential translation of *Chop* is thought to occur during times of extended stress when the cellular stress is too great to overcome, thereby promoting the upregulation of pro-apoptotic signaling networks directed by CHOP (49,50). Bypass of the inhibitory *Chop* uORF is suggested to rely upon poor start codon context of the uORF, allowing for preferential translation of *Chop* during stress (49,50). During nonstressed conditions, translation of the uORF is considered to be inhibitory to *Chop* CDS expression (Figure 4) (12). The inhibitory nature of the *Chop* uORF during basal conditions is not well understood, however, and is a focus of this thesis.

Another important question is how bypass of the uORF is facilitated. Structural analysis of the conformation of the 40S small ribosomal subunit with the initiation factors required for start site selection revealed that eIF2 α -P may disrupt the stability of the interaction between the scanning 43S and the mRNA at the -3 position of the start codon

(51). An additional possibility is that eIF2 α -P may modify the nature of the interaction between eIF2 and the Met-tRNA_i^{Met} that ultimately results in decreased start codon selection at initiation codons in poor Kozak consensus sequence (51). *In vitro* analysis of translation initiation also revealed that loss of eIF1 impaired the 43S scanning ribosome from discriminating between AUG initiation codons in poor or strong Kozak consensus sequence, suggesting that changes in the stoichiometry or post-translational modifications of other initiation factors may play a role in translation start site selection (52).

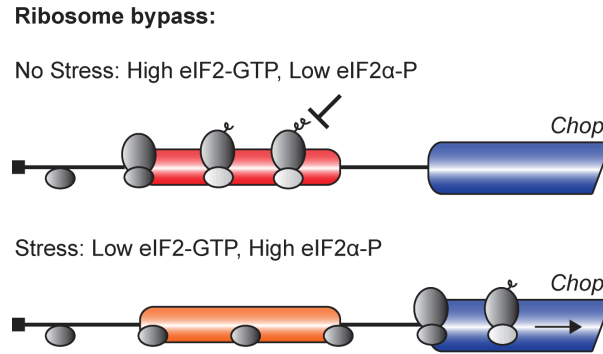


Figure 4. uORF regulation of downstream translation through the Bypass mechanism. During no stress conditions, scanning ribosomes initiated translation at the *Chop* uORF. Translation of the uORF is suggested to result in a ribosomal elongation stall that causes low levels of basal *Chop* expression. During cellular stress, elevated eIF2 α -P results in a ribosomal bypass of the inhibitory uORF due to its poor start codon context. Bypass of the inhibitory uORF results in increased translation initiation at the *Chop* CDS and an increase in *Chop* expression during times of extended cellular stress.

1.7 Cross-regulation between the ISR and other cellular stress pathways

Phosphorylation of eIF2 α and the ISR signaling pathway can also be integrated with other cellular stress pathways. As mentioned previously, induced eIF2 α ~P by PERK occurs in response to the accumulation of unfolded protein in the ER. In addition to PERK, accumulation of unfolded proteins also results in activation of IRE1 (ERN1) and ATF6 which are situated in the ER and, combined with PERK, serve as the three arms of the Unfolded Protein Response (UPR) (36). Induction of the UPR leads to a program of translational and transcriptional gene expression that collectively serve to expand the processing capacity of the ER to effectively manage an expanded ER client load (36).

UPR-directed transcription can be driven by IRE1, a ribonuclease that facilitates splicing of *Xbp1* mRNA, leading to translation of an activated version of the XBP1 transcription factor. In response to ER stress, ATF6 is transported from the ER to Golgi for proteolytic cleavage that allows for release of the amino-terminal portion of ATF6 to enter the nucleus and also direct transcription of targeted UPR genes (36). PERK phosphorylation of eIF2 α results in the aforementioned repression of global translation initiation that reduces influx of newly synthesized proteins into the overloaded ER (53,54). Coincident with dampening of global protein synthesis, eIF2 α ~P leads to preferential translation of *Atf4* that activates transcription of UPR genes involved in nutrient import, metabolism, and alleviation of oxidative stress (13,42,46). Appropriate activation of the UPR is especially important in professional secretory cells that balance the synthesis, folding, and trafficking of proteins to insure optimal protein export. The timing of eIF2 α ~P dephosphorylation and the global resumption of protein synthesis is also central to the health of professional secretory cells and is largely regulated by the expression of *Gadd34*, the protein product of which targets type 1 protein phosphatase (PPc1) for dephosphorylation of eIF2 α ~P (30,40,55,56). The mechanism behind the

regulated expression of *Gadd34* and the consequence of misregulated expression on cell health is a focus of this thesis.

Emphasizing the importance of the key UPR regulators in secretory cells, loss of function of *Perk*, *Atf4*, *Ire1*, or *Xpb1* disrupts the health and secretory functions of osteoblasts and subsequent bone formation (57-59). Treatment of precursor osteoblasts with bone morphogenetic protein BMP2 is suggested to activate each of the UPR branches, directing expression of target genes that contribute to secretion and bone formation (57,58,60). Given the central role of the UPR in protein homeostasis and expansion of secretory capacity, there is a growing consensus that the UPR functions in conjunction with additional regulators of bone development (57-62). For example, ATF4 is an essential regulator of osteoblast biology and there are likely to be additional regulatory networks integrating the UPR to bone development (57,61). Zinc finger transcription factor NMP4 (ZNF384) was previously reported to function in the suppression of bone anabolism, partially through the repression of genes such as *Plaur*, *Spp1*, and *Col1a1* that play important roles in osteogenic lineage commitment and mineralization (62-64). Targeted deletion of *Nmp4* in mice enhances bone response to PTH and BMP2 and protects these animals from osteopenia. Furthermore, ChIP-Seq analyses of NMP4-binding sites in preosteoblasts, embryonic stem cells, and two blood cell lines, suggested that NMP4 binds to the promoters of genes encoding UPR regulators and modulates their gene expression (62,65).

This thesis addresses the transcriptional and translational mechanisms that serve to regulate the expression of key ISR and UPR genes that encode proteins important for the cellular response to stress and control of cell fate. Many regulators of the ISR and UPR networks are subject to preferential translation through uORF-mediated mechanisms in the response to eIF2 α -P. Included among those preferentially translated genes that are highlighted in this thesis are the pro-apoptotic transcriptional

activator *Chop* that modifies gene expression programs, feedback regulator *Gadd34* that targets the catalytic subunit of protein phosphatase 1 to dephosphorylate eIF2 α -P, and glutamyl-prolyl tRNA synthetase *Eprs* that increases the charged tRNA pool and primes the cell for resumption of protein synthesis after stress remediation. This thesis addresses the mechanisms by which uORFs can modulate translation at the CDS of these key genes, and the processes by which uORFs with diverse properties can be integrated individually or in combination into mRNAs to facilitate preferential translation in response to eIF2 α -P in the ISR. Furthermore, this thesis describes the novel role of NMP4 in the regulation of the UPR and its control of transcription and protein synthesis processes. Importantly, misregulation of transcriptional or translational expression of ISR and UPR genes elicits maladaptive cell responses emphasizing the importance of transcriptional and translational control in appropriate gene expression and the maintenance of protein homeostasis and health in diverse cellular conditions.

CHAPTER 2. EXPERIMENTAL PROCEDURES

2.1 Cell culture and generation of stable cell lines

WT and A/A mouse embryonic fibroblast (MEF) cells, which express a WT version of eIF2 α and eIF2 α -S51A, were cultured in Dulbecco's Modified Eagle Medium (DMEM) as previously described (66). *Gadd34* ^{Δ C/ Δ C} MEF cells were kindly provided by David Ron (University of Cambridge, UK) and were previously described (39). Stable Flp-In *Gadd34* ^{Δ C/ Δ C} cells lines were generated by using the Flp-In System (Invitrogen) and full-length *Gadd34* cDNAs including 1-kb of the *Gadd34* promoter and mutant versions of the *Gadd34* 5'-leader that were integrated into the genome following the manufacturer's instructions. *Gadd34* ^{Δ C/ Δ C} FRT, *Gadd34*-WT2, *Gadd34*-OPT2, *Gadd34*-AAA2, and *Gadd34*- Δ 2 MEFs were grown in DMEM supplemented with 10% (v/v) fetal bovine serum, 100 units/mL penicillin, 100 μ g/mL streptomycin, 1X nonessential amino acids, and 55 μ M β -mercaptoethanol.

Chop^{-/-} MEF cells were provided by David Ron (University of Cambridge, UK) and were previously described (49). Stable Flp-In *Chop*^{-/-} cells lines were generated by using the Flp-In System (Invitrogen) and full-length *Chop* cDNAs, including 1-kb of the *Chop* promoter and either a WT version of the *Chop* 5'-leader or one with mutated *Chop* uORF initiation codons, which were integrated into the genome of the *Chop*^{-/-} cells following the manufacturer's instructions. The *Chop* uORF has two in-frame initiation codons at codons 1 and 4, with the second ATG being the primary site for translation initiation (12). In the mutant *Chop* uORF, both of these ATG codons were substituted to AGG, thus eliminating translation of the uORF. The resulting MEF cells with a WT uORF *Chop* and those with a version containing the Δ uORF *Chop* were cultured in DMEM supplemented with 10% (v/v) fetal bovine serum, 100 units/mL penicillin, 100 μ g/mL streptomycin, and 1 mM nonessential amino acids. ER stress was induced by the addition of 1 μ M thapsigargin, as indicated.

Gcn2^{+/+} and *Gcn2*^{-/-} MEF cells were previously described (66) and were cultured in DMEM supplemented with 10% (v/v) fetal bovine serum, 100 units/mL penicillin, 100 µg/mL streptomycin, and 1X nonessential amino acids. For halofuginone treatments, both control and treatment groups were cultured in DMEM supplemented with 10% (v/v) dialyzed fetal bovine serum (Gibco). Multipotent stem progenitor cells (MSPCs) were isolated as described (62). Briefly, bone marrow was isolated from euthanized mice that were six to eight weeks of age. A Ficoll gradient was used to isolate bone marrow mononuclear cells that were plated and cultured in Mesencult Media with Mesencult Stimulatory Supplement (StemCell Technologies). MSPCs were maintained in culture for three to four weeks without passage and supplemented with fresh media every five to seven days by removing 50% of the old media and adding 50% fresh media. At approximately 80% confluence, MSPCs were passaged at a 1:3 dilution and for an additional two more passages before MSPCs were frozen for storage. Cells were used for experiments between passages 8 and 10.

2.2 Mice

WT and *Nmp4*^{-/-} mice are as previously described (62). *Nmp4*^{-/-} mice were generated by incorporating a *Neo* gene cassette into the *Nmp4* coding exons 4 through 7. The local Institutional Animal Care and Use Committee approved all husbandry practices and described experimental procedures.

2.3 Immunoblot analyses

MEF cells were treated with 1 µM thapsigargin for up to 6 hours, or left untreated. Alternatively, MEF cells were treated with 20, 50, or 100 nM halofuginone for 6 hours or left untreated. Protein lysates were collected and quantitated and immunoblot analyses were carried out as previously described (67). Antibodies used for the immunoblot

analyses include: GADD34 (Proteintech Cat No 10449-1-AP), CReP (Proteintech Cat No 14634-1-AP), CHOP (Santa Cruz Biotechnology Cat No sc-7351), EPRS (Abcam Cat No ab31531), eIF2 α ~P (Abcam Cat No ab32157), and β -actin (Sigma Cat No A5441). Monoclonal antibody measuring total eIF2 α was kindly provided by Dr. Scott Kimball (Pennsylvania State University College of Medicine, Hershey, PA). Immunoblots were developed either using chemiluminescence with X-ray film or LI-COR Odyssey (LI-COR Biosciences) imaging.

MSPCs were treated with 2 μ M tunicamycin for up to 9 hours, 10 μ M salubrinal for 6 hours, or left untreated. Spleen, liver, and bone marrow tissues were isolated from *Nmp4*^{+/+} and *Nmp4*^{-/-} mice, and protein lysates were collected and quantified from the tissues and MSPCs, followed by immunoblot analyses as previously described. Antibodies used for the immunoblot analyses include: NMP4 (Sigma Cat No HPA004051), GADD34 (Proteintech Cat No 10449-1-AP), CReP (Proteintech Cat No 14634-1-AP), ATF4 (Santa Cruz Cat No sc-22800), eIF2 α ~P (Abcam Cat No ab32157), RPS6~P (Cell Signaling Cat No 2211), RPS6 Total (Cell Signaling Cat No 2317), RPL11 (Cell Signaling Cat No 18163), c-Myc (Cell Signaling Cat No 5605), and β -actin (Sigma Cat No A5441). Monoclonal antibody measuring total eIF2 α was kindly provided by Dr. Scott Kimball (Pennsylvania State University College of Medicine, Hershey, PA). Immunoblots were developed either using chemiluminescence with X-ray film or LI-COR Odyssey (LI-COR Biosciences) imaging.

2.4 mRNA measurements by qPCR

RNA was isolated from MEF cells, MSPCs, and polysome fractions using TRIzol reagent (Invitrogen) and single-strand cDNA synthesis was performed using TaqMan reverse transcriptase kit (Applied Biosystems) according to the manufacturer's instructions. Transcript levels were measured by qPCR using SYBR Green (Applied

Biosystems) on a Realplex2 Master Cycler (Eppendorf). $\Delta\Delta\text{CT}$ values were calculated for each transcript in which β -actin levels were used for normalization. Averages and S.D. between biological replicates for each genotype and treatment group were then normalized to the average $\Delta\Delta\text{CT}$ value calculated for either the WT MEF or *Nmp4*^{+/+} MSPC no treatment group. Data are represented as mRNA levels relative to the WT MEF or *Nmp4*^{+/+} MSPC no treatment group. Primers used for measuring transcripts include: *Gadd34* forward 5'-AGGACCCCGAGATTCCTCT-3', *Gadd34* reverse 5'-CCTGGAATCAGGGGTAAGGT-3', *Crep* forward 5'-GGCTACAGTGGCCTTCTCTG-3', *Crep* reverse 5'-CATCCATCCCTTGCAAATTC-3', *Chop* forward 5'-CGGAACCTGAGGAGAGAG-3', *Chop* reverse 5'-CGTTTCCTGGGGATGAGATA-3', *Atf5* forward 5'-GGCTGGCTCGTAGACTATGG-3', *Atf5* reverse 5'-CCAGAGGAACCAGAGCTGTG-3', *Bim* forward 5'-TTTGACACAGACAGGAGCCC-3', *Bim* reverse 5'-CAGCTCCTGTGCAATCCGTA-3', *Atf4* forward 5'-GCCGGTTTAAGTTGTGTGCT-3', *Atf4* reverse 5'-CTGGATTCGAGGAATGTGCT-3', *Eprs* forward 5'-TGTGGGGAAATTGACTGTGA-3', *Eprs* reverse 5'-AACTCCGACCAAACAAGGTG-3', *c-Myc* forward 5'-GAAAACGACAAGAGGCGGAC-3', *c-Myc* reverse 5'-AATGGACAGGATGTAGGCGG-3', *45S rRNA* forward 5'-TTTTTGGGGAGGTGGAGAGTC-3', *45S rRNA* reverse 5'-CTGATACGGGCAGACACAGAA-3', *Rpl11* forward 5'-CCTCAATATCTGCGTCGGGG-3', *Rpl11* reverse 5'-TTCCGCAACTCATACTCCCG-3', *Rps6* forward 5'-CAGGACCAAAGCACCCAAGA-3', *Rps6* reverse 5'-CAGTGAGGACAGCCTACGTC-3', β -actin forward 5'-TGTTACCAACTGGGACGACA-3', β -actin reverse 5'-GGGGTGTGTAAGGTCTCAA-3', *Firefly luciferase* forward 5'-CCAGGGATTTTCAGTCGATGT-3', and *Firefly luciferase* reverse 5'-AATCTCACGCAGGCAGTTCT-3'.

2.5 Total RNA and DNA measurements

RNA and DNA were isolated from MSPCs using TRIzol reagent (Invitrogen) following the manufacturer's instructions. Quantification of RNA and DNA was determined by absorbance measurement at 260 and 280 nm by nanodrop.

2.6 Polysome profiling and sucrose gradient ultracentrifugation

MEF cells were left untreated or treated with either 1 μ M thapsigargin or 25 nM halofuginone for 6 hours. Additionally, MSPCs were treated with 2 μ M tunicamycin or 10 μ M salubrinal for 6 hours or left untreated. Cells were incubated in culture media containing 50 μ g/mL cycloheximide just prior to lysate collection. Lysates were collected, sheared, and layered on top of 10-50% sucrose gradients followed by ultracentrifugation as previously described (5,68). Sucrose gradients were fractionated and whole-cell lysate polysome profiles were collected using a Piston Gradient Fractionator (BioComp) and a 254 nm UV monitor with Data Quest Software.

Following fractionation, 10 ng/mL firefly luciferase control RNA (Promega) was spiked into each pooled sample to generate polysome shifts for specific transcripts normalized to an exogenous RNA control (5,68). Samples were mixed with 750 μ L TRIzol, and RNA isolation and cDNA generation was performed as described above. Calculations for % total gene transcript and % transcript shifts are as described previously (5). Whole-cell lysate polysome profiles and mRNA polysome shifts are representative of three independent biological experiments.

2.7 Plasmid constructions and luciferase assays

A 5'-Rapid Amplification of cDNA Ends (5'-RACE; FirstChoice Ambion) was performed using RNA lysates collected from WT MEF cells treated with 1 μ M thapsigargin for 6 hours, or left untreated, to determine the transcriptional start sites for

Gadd34 and *Crep*. The cDNA segments encoding the 5'-leader of *Gadd34* and *Crep* were inserted between HindIII and NcoI between the TK-promoter and firefly luciferase CDS in a derivative of plasmid pGL3 (13). The resulting *P_{TK}-Gadd34-Luc* and *P_{TK}-Crep-Luc* contain the mouse *Gadd34* and *Crep* 5'-leaders and the start codon for each CDS fused to a luciferase reporter. Site-directed mutagenesis and subcloning of synthesized cDNAs were used to generate mutant *P_{TK}-Gadd34-Luc* and *P_{TK}-Crep-Luc* constructs that were sequenced to verify nucleotide substitutions. *P_{TK}-Gadd34-Luc* and *P_{TK}-Crep-Luc* constructs were transiently co-transfected with a *Renilla* reporter plasmid into WT or A/A MEF cells for 24 hours followed by a treatment with 0.1 μ M thapsigargin for 6 hours. Lysates were collected and Firefly and *Renilla* luciferase activities were measured as described previously (13). At least three independent biological experiments were conducted for each luciferase measurement, and relative values are represented with S.D. indicated. The average and S.D. of the biological replicates for each construct and treatment group was calculated and values are represented relative to the no treatment group for either the WT *P_{TK}-Gadd34-Luc* or WT *P_{TK}-Crep-Luc* constructs with the positive S.D. indicated.

The T7 promoter of sequence, TAATACGACTCACTATAGGGAGA, and a DNA segment encoding the 5'-leader of the *Gadd34* mRNA that contains the start codon for the *Gadd34* CDS were inserted between HindIII and NcoI in the pGL3 basic luciferase vector (Promega) for generation of *P_{T7}-Gadd34-Luc* constructs for *in vitro* translation assays. Sequencing was used to verify nucleotide substitutions and *in vitro* assays were conducted as described below.

The cDNA segment encoding the 5'-leader of the *Chop* mRNA was inserted between HindIII and NcoI restriction sites situated between the TK-promoter and firefly luciferase CDS in a derivative of plasmid pGL3 for generation of *Chop-Luc* (13). The resulting reporter plasmid *Chop-Luc* contains a DNA segment encoding the mouse 5'-

leader of the *Chop* mRNA and the start codon for the *Chop* CDS fused to a luciferase reporter. Site-directed mutagenesis or DNA directly synthesized with desired *Chop* 5'-leader sequences were used to generate the mutant versions of *Chop-Luc*. Each of the reporter plasmids were sequenced to verify the desired nucleotide substitutions.

The full-length *Chop* uORF was fused in-frame to the luciferase CDS, which was transcriptionally expressed from the TK-promoter, generating *uORF-Luc*. Site-directed mutagenesis was performed following the manufacturer's instructions (Stratagene) and all mutant *uORF-Luc* constructs were sequenced to verify the desired nucleotide residue substitutions. *Chop-Luc* and *Chop uORF-Luc* constructs were transiently co-transfected with a *Renilla* reporter plasmid into WT MEF cells for 24 hours followed by either no treatment or exposure to 0.1 μ M thapsigargin for 6 hours. Lysates were collected and firefly and *Renilla* luciferase activities were measured as described previously (13). At least three independent biological experiments were conducted for each luciferase measurement. The average and S.D. of the biological replicates for each construct and treatment group was calculated and values are represented relative to the no treatment group for either the WT *Chop-Luc* or WT *Chop uORF-Luc* constructs with the positive S.D. indicated.

A three-part CDS fusion construct was generated that featured the *Renilla* luciferase CDS fused in-frame to the last 30 nucleotides of the *Chop* uORF, followed by the firefly luciferase CDS. To begin this plasmid construction, DNA encoding the *Renilla* CDS was inserted between HindIII and NcoI restriction sites that were downstream of a TK promoter and upstream of the firefly CDS in a derivative of plasmid pGL3. Annealed oligo cloning was then used to insert WT and mutant versions of the *Chop* uORF sequences into the AatII and NarI sites situated between the *Renilla* and firefly luciferase CDS. All constructs were characterized by restriction mapping and sequenced to verify the desired recombinant DNA ligations and nucleotide substitutions. *Renilla-uORF-Luc*

constructs were transiently transfected into WT MEF cells for 24 hours, followed by either no treatment or a 6 hour exposure to 0.1 μ M thapsigargin. Lysates were collected and firefly and Renilla luciferase activities were measured as described previously (13). At least three independent biological experiments were conducted for each luciferase measurement. The average and S.D. of the biological replicates for each construct and treatment group was calculated and values are represented relative to the no treatment group for the WT *Renilla-uORF-Luc* construct with the positive S.D. indicated.

Plasmids was created for expression of mRNAs in toeprint assays following a previously described strategy (69). For expression of the fusion transcript *α -globin-Chop-Luc*, the T7 promoter containing sequence TAATACGACTCACTATAGGGAGA was inserted between SacI and MluI restriction sites in the pGL3 luciferase vector (Promega). Next the cDNA sequences encoding rabbit *α -globin* fused in-frame to last 30 nucleotides of the *Chop* uORF were inserted between HindIII and NarI sites of the pGL3-derived plasmid. This plasmid yielded a CDS encoding a fusion polypeptide featuring α -globin, the last 10 amino acid residues encoded in the CHOP uORF, followed by firefly luciferase. The *α -globin-Chop-Luc* plasmid was then used for the synthesis of mRNAs for toeprinting assays described below. The WT *Chop* uORF sequence inserted into the *α -globin-Chop-Luc* plasmid was designated p1335. A frameshift mutant of the *Chop* uORF sequence was designated p1336, mutation of the Ile-Phe-Ile codons to Ala-Ala-Ala was p1337, and insertion of a stop codon just following the *Chop* uORF sequence was p1338. Sequencing was used to verify that the plasmid constructs contained the desired base substitutions.

A 5'-Rapid Amplification of cDNA Ends (5'-RACE; FirstChoice Ambion) was performed using RNA lysates collected from WT MEF cells left untreated or treated with 1 μ M thapsigargin for 6 hours to determine the transcriptional start site for *Eprs*. The cDNA fragment encoding the 5'-leader of *Eprs* was inserted between SacI and NcoI

between the TK-promoter and Firefly luciferase CDS in a derivative of plasmid pGL3 (13). The resulting P_{TK} -EPRS-Luc contains the mouse *Eprs* 5'-leader fused to a luciferase reporter. Site-directed mutagenesis and subcloning of synthesized cDNAs was used to generate mutant P_{TK} -*Eprs*-Luc constructs that were sequenced for verification of nucleotide substitutions. P_{TK} -*Eprs*-Luc constructs were transiently co-transfected with a *Renilla* reporter plasmid into WT or A/A MEF cells for 24 hours followed by a 6 hour 0.1 μ M thapsigargin treatment or a 6 hour 50 nM halofuginone treatment. Lysates were collected and Firefly and *Renilla* luciferase activities were measured as described previously (13). Relative values for luciferase measurements are represented for at least three independent biological experiments. The average and S.D. of the biological replicates for each construct and treatment group was calculated and values are represented relative to the no treatment group for the WT P_{TK} -*Eprs*-Luc construct with the positive S.D. indicated.

The full-length *Eprs* uORFs were each individually fused in-frame to the luciferase CDS and were transcriptionally expressed from a TK-promoter for generation of P_{TK} -CUG123 uORF-Luc, P_{TK} -UUG1 uORF-Luc, and P_{TK} -UUG2 uORF-Luc. Site-directed mutagenesis and subcloning of synthesized cDNAs was used to generate WT and mutant P_{TK} -uORF-Luc constructs that were sequenced for verification of desired nucleotide substitutions. P_{TK} -uORF-Luc constructs were transiently co-transfected with a *Renilla* reporter plasmid into WT MEF cells for 24 hours. Lysates were collected and Firefly and *Renilla* luciferase activities were measured as described previously (13). Relative values for luciferase measurements are represented for at least three independent biological experiments. The average and S.D. of the biological replicates for each construct was calculated and values are represented relative to the WT P_{TK} -CUG123 with the positive S.D. indicated.

The DNA segments containing 1-kb of the human *Gadd34* and *Crep* promoters were inserted between KpnI and BglII in a pGL3 basic backbone. The *Gadd34* promoter-Luc and *CReP* promoter-Luc constructs were transiently co-transfected with a *Renilla* reporter plasmid into WT or *Nmp4*^{-/-} MSPCs for 24 hours followed by a 6 hour 2 μ M tunicamycin treatment. Lysates were collected and Firefly and *Renilla* luciferase activities were measured as described (13). At least three independent biological experiments were conducted for each luciferase measurement, and relative values are represented with S.D. indicated.

2.8 *In vitro* transcription and translation assays

Capped and polyadenylated RNA was synthesized with T7 RNA polymerase using mMESSAGE mMACHINE T7 Ultra (Ambion) from *P_{T7}-Gadd34-Luc* and *P_{T7}- α -globin-Chop-Luc* constructs. Synthesized *GADD34-Luc* mRNA and *α -globin-Chop-Luc* mRNA was added to rabbit reticulocyte lysate (Promega) per the manufacturers' instructions. For luciferase assays, *in vitro* translation reactions with *Gadd34-Luc* mRNA were carried out for 20 minutes at 30°C, and firefly luciferase activity was measured.

For primer extension inhibition (toeprint) assays using *Gadd34-Luc* mRNA, reticulocyte lysates were treated with cycloheximide upon addition of the *Gadd34-Luc* mRNA to measure initiating ribosomes (time 0) or 5 minutes after addition of the transcript to measure ribosomal localization during steady-state translation (time 5). Toeprint assays were conducted as previously described and using primers: 5'-TGAAGCGCCGGTTCTGGTTG-3' (Figure 8D) and ZW4: 5'-TCCAGGAACCAGGGCGTA-3' (Figure 8E) (70).

For primer extension inhibition assays using *α -globin-Chop-Luc* mRNA, cell-free translation extracts derived from *Neurospora crassa* were prepared as described (71) and treated with cycloheximide upon addition of the *α -globin-Chop-Luc* mRNA to

measure initiating ribosomes (time 0), 15 minutes after addition of the transcript to measure ribosomal localization during steady-state translation (time 15), or left untreated to measure prominent ribosomal stalls. Toeprint assays were conducted using primer ZW4: 5'-TCCAGGAACCAGGGCGTA-3' as previously described (70).

2.9 Cell number and viability assays

For cell proliferation assays featuring *Gadd34* FRT cell lines, *Gadd34*-WT2, *Gadd34*-OPT2, *Gadd34*-AAA2, and *Gadd34*- Δ 2 MEFs were seeded at 5,000 cells/well in a 96 well plate. Cells were fixed (3.7% formalin) and stained (10 μ g/mL Hoechst) immediately following seeding, or 24 hours and 48 hours after seeding, and fluorescence was measured on a Synergy H1 Microplate reader (Bio Tek).

MTT assays for the *Gadd34* FRT cell lines were carried out by seeding cells at 5,000 cells/well in a 96 well plate. Cells were cultured for 24 hours, and MTT activity was measured using CellTiter 96 Well Non-Radioactive Cell Proliferation Assay (Promega). For measurements of MTT activity after ER stress treatment, cells were seeded, allowed to grow for 24 hours, and treated with 0.4 μ M thapsigargin with or without 1 μ M guanabenz as indicated, or left untreated for an additional 24 hours.

MTT and caspase 3/7 assays featuring the *Chop* FRT cell lines were carried out by seeding cells at 5,000 cells/well in a 96 well plate. Cells were cultured for 24 hours, treated with either 25 nM thapsigargin or 0.5 mM tunicamycin for up to an additional 24 hours, and MTT and caspase 3/7 activity was measured using CellTiter 96 Well Non-Radioactive Cell Proliferation Assay and Caspase-Glo 3/7 Assay System (Promega).

For MTT assays featuring *Gcn2*^{+/+} and *Gcn2*^{-/-} MEFs, cells were seeded in 96-well culture plates at 5,000 cells/well 24 hours prior to treatment. MEFs were treated with 12.5, 25, or 50 nM halofuginone for 6 hours, followed by recovery in fresh media for 18 hours. Viability was measured using a CellTiter 96 Well Non-Radioactive Cell

Proliferation Assay (Promega). Treatment values were normalized to untreated groups for each respective cell line.

MTT and Caspase 3/7 assays utilizing MSPCs were conducted by seeding cells at 5,000 cells/well in a 96-well plate. For MTT time course analysis, cells were cultured for 24 hours followed by up to 24 hours of treatment with 2 μ M tunicamycin alone or in combination with either 10 μ M salubrinal or 250 nM torin for an additional 24 hours, and MTT activity was measured using CellTiter 96 Well Non-Radioactive Cell Proliferation assay (Promega). For Caspase 3/7 assays, cells were seeded, cultured for 24 hours, and treated in the presence or absence of 2 μ M tunicamycin for an additional 24 hours and Caspase 3/7 activity was measured using the Caspase-Glo 3/7 Assay System (Promega).

2.10 Statistical analyses

Values indicate the mean +/- standard deviation and represent at least three independent experiments. Statistical significance was calculated using the two-tailed student's t-test. Differences between multiple groups were analyzed using a two-way analysis of variance (ANOVA) followed by a post hoc Tukey HSD test. For the statistical analyses, genotype and treatment were set as fixed factors and StatPlus software was used to calculate significance. P values less than 0.05 were considered statistically significant with differences between treatment groups indicated by “*”, and differences between genotypes indicated by a “#” sign.

CHAPTER 3. RESULTS: RIBOSOME REINITIATION DIRECTS GENE-SPECIFIC TRANSLATION AND REGULATES THE INTEGRATED STRESS RESPONSE

3.1 eIF2 α ~P is required for *Gadd34* transcription and translation, but *Crep* expression occurs independent of eIF2 α ~P

A major focus of this thesis is the nature of uORFs that facilitate preferential translation in response to eIF2 α ~P. Translation of *Gadd34* mRNA is enhanced in response to eIF2 α ~P and serves a central role for feedback regulation of the ISR (30,40), whereas the related CReP (PPP1R15B) is suggested to be expressed independent of eIF2 α ~P and functions to target PP1c for dephosphorylation of eIF2 α ~P under basal conditions (11,72). To further explore the role that eIF2 α ~P and translational control play in the differential expression of *Gadd34* and *Crep*, changes in their mRNA and protein levels were measured in wild-type (WT) mouse embryonic fibroblast (MEF) cells and mutant MEF cells (A/A) expressing eIF2 α -S51A that cannot be phosphorylated. eIF2 α ~P was induced only in WT cells by treatment with thapsigargin, a potent trigger of endoplasmic reticulum (ER) stress (Figure 5A). Both *Gadd34* mRNA and protein levels were increased in WT MEF cells, whereas there was no change in *Gadd34* mRNA and minimal protein expression in A/A cells (Figure 5A and B). By contrast, there was no change in the amount of *Crep* mRNA and protein in WT cells upon ER stress. Of interest, while the levels of *Crep* mRNAs were similar between WT and A/A cells, there was reduced CReP protein in A/A cells during ER stress (Figure 5A and B).

To explore the role of translational control in the differential expression of *Gadd34* and *Crep*, WT MEF cells were subjected to thapsigargin treatment, and lysates were prepared and analyzed by polysome profiling using sucrose density ultracentrifugation. As expected, polysome profiling revealed that ER stress led to reduced global translation initiation as viewed by a decrease in polysomes coincident

with increased monosomes (Figure 5C). *Gadd34* and *Crep* mRNAs, along with *Chop* mRNA that is known to be subject to preferential translation, were then measured by qPCR in the polysome fractions. Both *Gadd34* and *Chop* transcripts were predominantly associated with monosomes and disomes in the absence of stress. However upon thapsigargin treatment and eIF2 α -P, there was a significant shift of the *Gadd34* and *Chop* transcripts to heavy polysomes (Figure 5D). By contrast, *Crep* mRNA was associated with heavy polysomes in both thapsigargin treated cells and those not subjected to stress. Together these results suggest that in addition to transcriptional induction, *Gadd34* is preferentially translated upon stress and eIF2 α -P, whereas *Crep* is largely translated independent of the stress conditions. These results are consistent with earlier reports that indicated that expression of *Gadd34* is induced upon stress as part of a feedback control of the ISR and *Crep* is constitutively present (40,72).

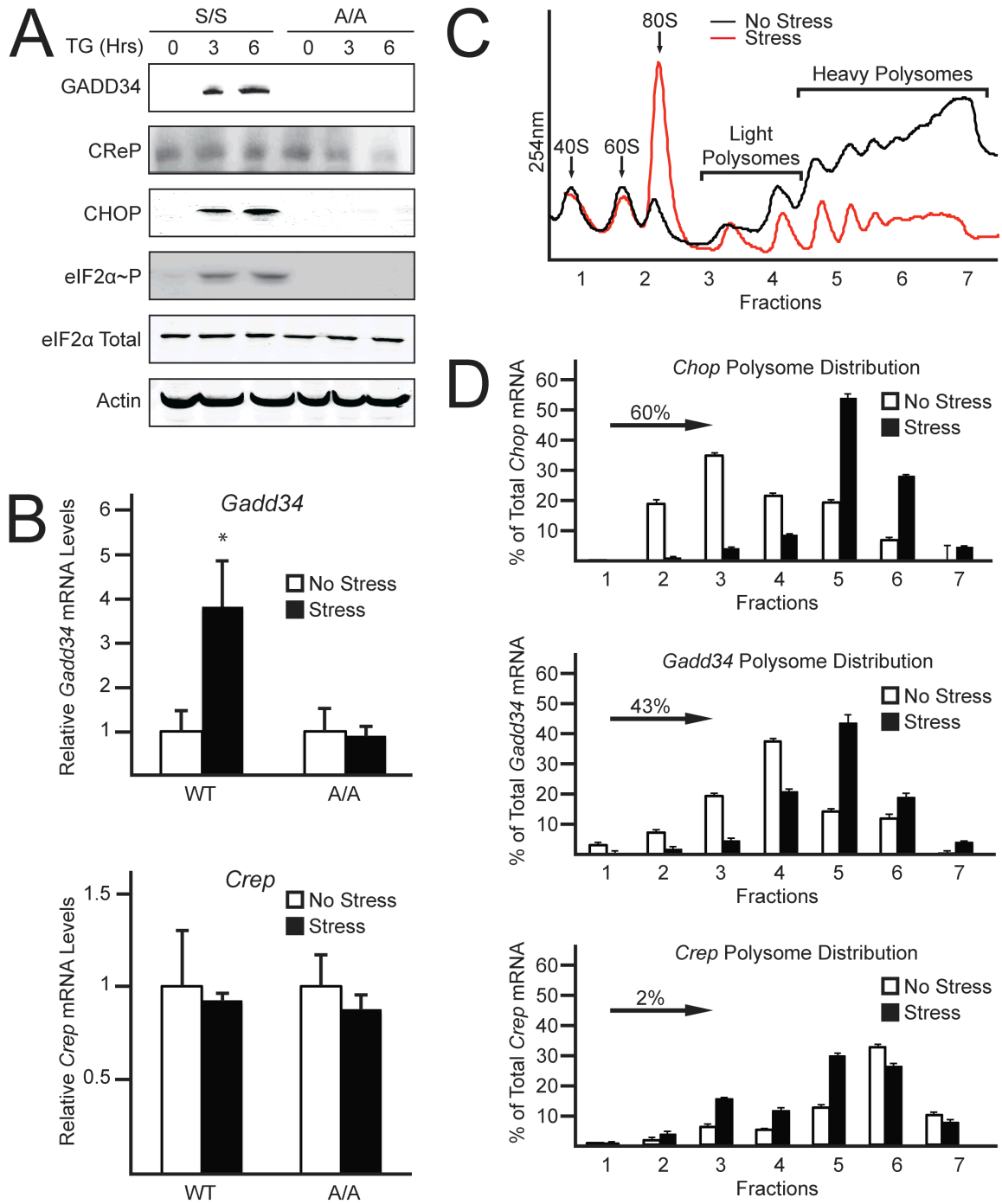


Figure 5. eIF2 α ~P is required for induced *Gadd34* translation, but *Crep* expression occurs independent of eIF2 α ~P. A, WT and A/A MEF cells were treated with thapsigargin, for up to 6 hours or left untreated. Lysates were processed and levels of GADD34, CReP, CHOP, eIF2 α ~P, eIF2 α total, and β -actin were measured by

immunoblot. B, total RNA was collected from WT and A/A MEFs treated with thapsigargin for 6 hours or left untreated and relative levels of *Gadd34* and *Crep* mRNA were measured by qRT-PCR. C, WT MEF cells were treated with thapsigargin for 6 hours or left untreated. Lysates were collected and layered on top of 10-50% sucrose gradients, followed by centrifugation and analysis of whole-lysate polysome profiles at 254 nm. D, Total RNA was isolated from sucrose fractions and the percentage of total *Chop*, *Gadd34*, and *Crep* mRNAs was determined by qRT-PCR. Panels C and D are representative of three independent biological experiments.

3.2 Preferential translation of *Gadd34* features an inhibitory uORF

Next we carried out a 5'-RACE to define the transcriptional start site in mouse of the *Gadd34* gene (Figure 6A). A cDNA segment encoding the 228-nucleotide sequence of the 5'-leader of *Gadd34* was then inserted between a minimal TK promoter and the firefly luciferase reporter CDS, generating *P_{TK}-Gadd34-Luc*. This luciferase reporter featured the initiation codon of the *Gadd34* CDS fused in-frame to the luciferase CDS. Expression of *Gadd34-Luc* was increased 3-fold in WT MEF cells treated with thapsigargin as compared to no change in luciferase activity in A/A cells (Figure 6B). In these reporter measurements, and subsequent ones discussed below, there was no significant change in the luciferase mRNA. These results indicate that the 5'-leader of *Gadd34* directs preferential translation in response to eIF2 α -P.

To determine if enhanced *Gadd34* translation occurs via ribosome scanning, a palindromic sequence with a predicted free energy of $\Delta G = -41$ kcal/mol was inserted 10 nucleotides downstream of the 5' cap of the *Gadd34-Luc* mRNA (Figure 6A). Addition of this stem-loop to the *Gadd34-Luc* transcript significantly decreased luciferase activity independent of stress, indicating that preferential translation mediated by the 5'-leader of *Gadd34* occurs by ribosome scanning (Figure 6C). Ribosomes scanning the 5'-leader of *Gadd34* encounter two uORFs before reaching the start codon for the *Gadd34* CDS. To determine the contribution of the two uORFs to *Gadd34* translation regulation, the uORF start codons were mutated from ATG to an AGG or ATA, as indicated by the Δ ATG in Figure 6C. Deletion of uORF1 alone led to a small increase, albeit significant, in the basal luciferase expression, with an induction upon ER stress that was similar to the reporter with the WT version of the *Gadd34* 5'-leader. This result suggests that uORF1 serves to modestly dampen downstream translation regardless of stress. By comparison, deletion of uORF2 led to a 30-fold increase in luciferase activity independent of ER stress, indicating that uORF2 is inhibitory to downstream translation

and is the dominant regulatory uORF in the *Gadd34* 5'-leader, a finding consistent with Lee et al. (30). Combined deletion of uORF1 and uORF2 led to an additional increase in luciferase activity, further supporting the roles of uORF2 and uORF1 as repressing elements in *Gadd34* translational expression (Figure 6C).

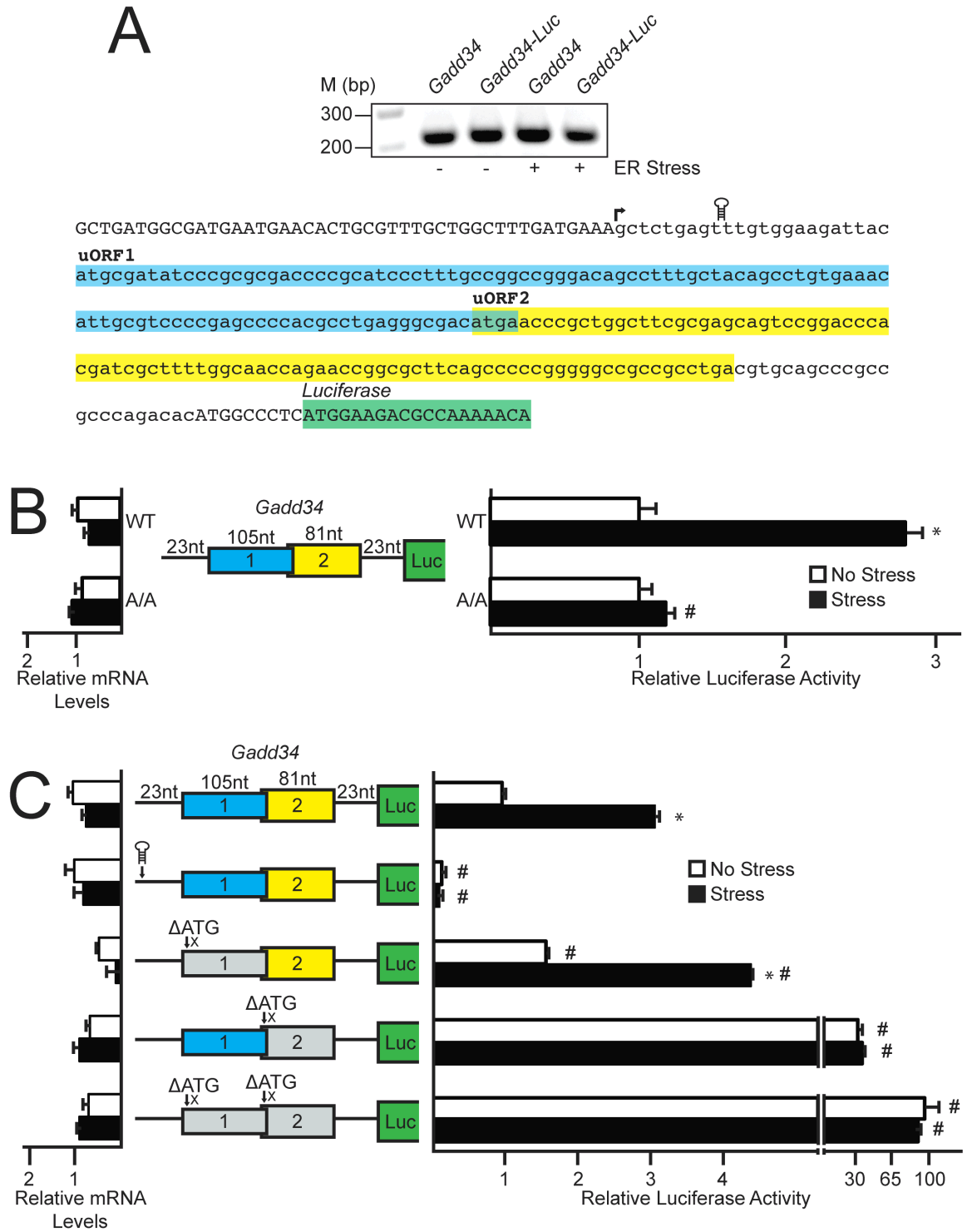


Figure 6. Preferential translation of *Gadd34* features an inhibitory uORF. A, top panel, 5'-RACE was carried out for *Gadd34* using WT MEFs treated with thapsigargin for 6 hours or left untreated; total RNA was prepared and DNA products were separated by

gel electrophoresis, with markers of the indicated base pair sizes illustrated on the left.

A, bottom panel, Representation of *Gadd34* 5'-leader in lowercase letters, with uppercase letters representing the 5'-linker added during the 5'-RACE procedure and the beginning of the CDS of the *Gadd34-Luc* fusion. Colored boxes represent the *Gadd34* uORFs and the coding region of the *Gadd34-Luc* fusion. The transcription start site is indicated with an arrow, and the location of stem loop insertion is illustrated.

B, The P_{TK} -*Gadd34-Luc* construct and a *Renilla* luciferase reporter were co-transfected into WT or A/A MEF cells and treated for 6 hours with thapsigargin or left untreated. *Gadd34* translation control was measured via Dual-Luciferase assay and corresponding *Gadd34-Luc* mRNA was measured by qRT-PCR. The P_{TK} -*Gadd34-Luc* construct contains the cDNA sequence corresponding to the *Gadd34* 5'-leader fused to the luciferase reporter gene with both *Gadd34* uORFs and the CDS of the *Gadd34-Luc* fusion indicated with colored boxes.

C, WT and mutant versions of P_{TK} -*Gadd34-Luc* were transfected into WT MEFs, treated for 6 hours or left untreated, and measured using a Dual-Luciferase assay and qRT-PCR. Mutant versions of P_{TK} -*Gadd34-Luc* include a stem loop insertion and mutation of the initiation codons for uORFs individually or together, as represented by Δ ATG. Relative values are represented as histograms for each with the positive S.D. indicated.

3.3 *Gadd34* translation control involves bypass of an inhibitory uORF

The initiation codon context for the *Gadd34* uORF2 (GGCGACAUGU) is less than optimal compared to the Kozak consensus sequence (GCC(A/G)CCAUGG), a feature similar to the single uORF present in the *Chop* mRNA that is subject to the Bypass model of translational control (12). To determine if context of the start codon plays a role in uORF2-mediated regulation of *Gadd34* translation, the poor start codon context of uORF2 was mutated to the optimal Kozak consensus. Mutation of uORF2 to the strong Kozak context reduced luciferase expression basally and decreased stress-induced luciferase activity to 2.7-fold as compared to a 3.3-fold induction for the WT *Gadd34-Luc* reporter (Figure 7A). This finding suggests that uORF2 can be bypassed during eIF2 α -P in part due to its poor initiation codon context, thereby enhancing translation of the downstream *Gadd34* CDS.

Translation initiation downstream of uORFs can also be dependent on translation reinitiation (16,19). To determine the contribution of post-uORF2 translation reinitiation in *Gadd34* translation regulation, the stop codon of uORF2 was mutated from TGA to GGA, resulting in an uORF that overlaps out-of-frame with the luciferase CDS (Figure 7A). There was no statistically significant difference between the WT *P_{TK}-Gadd34-Luc* and the reporter with the uORF2 overlapping the CDS. This finding argues against significant ribosome reinitiation at the *Gadd34* CDS following synthesis of the uORF2 polypeptide, and instead supports the idea that preferential translation of *Gadd34* CDS relies on ribosomal bypass of the inhibitory uORF2.

3.4 The inhibitory function of *Gadd34* uORF2 is reliant on Pro-Pro-Gly juxtaposed to the uORF2 stop codon

Many features of uORFs, including length and coding sequences, can promote the repressing functions of uORFs. To investigate the inhibitory nature of the *Gadd34* uORF2, in-frame-deletions from codons 5-25 and 15-25 were analyzed in the *Gadd34-Luc* reporter. Both deletions in the uORF2 coding sequence increased luciferase expression independent of stress, suggesting that the repressing function of uORF2 lies at least in part within its coding sequence (Figure 7C).

To address whether the RNA sequence in uORF2 *per se* contributes to the repressing functions of this uORF, a single nucleotide was deleted just after the ATG start codon in uORF2 and a single nucleotide was inserted just prior to the TGA termination codon. The resulting frameshift thus maintains the uORF2 nucleotide sequence and length, but the uORF now encodes a different polypeptide. Luciferase activity of this frameshift reporter was increased in the presence or absence of stress, consistent with the hypothesis that the encoded uORF2 polypeptide sequence is responsible for the inhibitory function of uORF2 in translational control (Figure 7C).

A comparison of the uORF2-encoding polypeptide sequences among mammals revealed several conserved segments, including a carboxy-terminal Pro-Pro-Gly sequence (Figure 7B). Contiguous prolines and Pro-Pro-Gly sequences have been suggested to be problematic for translation elongation and require eIF5A for efficient protein synthesis (73). Substitution of the uORF2 codons encoding the Pro-Pro-Gly sequence with codons encoding Ala-Ala-Ala resulted in a 5-fold increase in luciferase activity basally, while retaining a modest induction during ER stress (Figure 7C). Alteration of the uORF2 start codon to an optimal Kozak sequence in the presence of the Pro-Pro-Gly to Ala-Ala-Ala substitution also led to elevated luciferase activity in absence of stress, along with a modest increase (1.3-fold) upon thapsigargin treatment.

These results suggest that bypass of the uORF2 during stress is required for maximal induction of *Gadd34* translation, because translation of the codons encoding the uORF2 Pro-Pro-Gly residues precludes the ribosome from efficiently reinitiating at the downstream CDS. Insertion of three alanine residues between the Pro-Pro-Gly sequence and the uORF2 termination codon also led to similar increases in luciferase activity in the presence or absence of stress (Figure 7C), indicating that the ability of the Pro-Pro-Gly sequence in uORF2 to inhibit translation reinitiation involves its juxtaposition to a termination codon.

As will be discussed in detail in Chapter 4, translation of the *Chop* inhibitory uORF is suggested to trigger an elongation pause that is responsible for lowering downstream translation reinitiation (12). This can be visualized by low expression of an in-frame fusion of the *Chop* uORF with the luciferase CDS. Luciferase activity of the CHOP uORF–Luc fusion protein is significantly enhanced upon deletion of its critical inhibitory sequences and alleviation of the elongation pause (Figure 8A). To determine if the Pro-Pro-Gly sequence in *Gadd34* uORF2 results in an elongation pause a similar in-frame fusion between *Gadd34* uORF2 and the luciferase CDS was made. There was elevated expression of the GADD34 uORF-Luc fusion, suggesting that the *Gadd34* Pro-Pro-Gly sequence does not facilitate a pause in ribosomal elongation (Figure 8A).

To analyze the effects of selected *Gadd34* uORF2 mutations for translational expression, a T7 RNA polymerase was used to synthesize *Gadd34-Luc* mRNAs that were introduced into an *in vitro* translation assays using rabbit reticulocyte lysates. Consistent with the analysis of MEF cells, mutations of the initiation codon of uORF2 led to elevated luciferase activity, which was further enhanced by combined loss of uORF1 (Figure 8B). Substitution of the Pro-Pro-Gly codons to Ala-Ala-Ala in uORF2 also led to significantly enhanced luciferase expression compared to WT. Finally, introduction of an optimized Kozak context for the initiation codon of uORF2 sharply lowered luciferase

activity (Figure 8B). Together these results support the idea that the Pro-Pro-Gly codons are important for the uORF2 inhibition of downstream CDS translation.

As the *Gadd34* uORF2 fusion construct from Figure 8A does not take into account the dependence of the Pro-Pro-Gly sequence on juxtaposition to a termination codon for its inhibitory nature, toeprinting experiments using two different primers were used to map the positions of ribosomes along the 5'-leader of *Gadd34* transcripts during *in vitro* translation (Figure 8C). Reticulocyte lysates were treated with cycloheximide (CHX) upon addition of the *Gadd34-Luc* mRNA to measure where ribosomes first initiate translation (time 0). Alternatively, cycloheximide was added 5 minutes after addition of the transcript to measure ribosome positions during steady state translation and active polypeptide synthesis (time 5). At time 0 there were toeprints measuring the ribosomes positioned at the initiation codons of uORF1 (blue star) and uORF2 (yellow star) and the luciferase CDS (green star) (Figure 8D and E). Mutation of the initiation codon of uORF2 individually or in combination with uORF1 resulted in lowered toeprint signals at the uORF2, with a similar corresponding increase in initiation at the luciferase CDS (Figure 8D and E). Initiation at the luciferase CDS is also observed at time 5 for these mutant transcripts, indicating that translation initiation at the dominant uORF2 precludes ribosome reinitiation at the downstream CDS during steady state translation (Figure 8E).

Introduction of an optimized Kozak context for the initiation codon of uORF2 significantly reduced translation initiation at the CDS at both time 0 and time 5, indicating increased ribosomal preference for the more 5' optimized start codon of uORF2 largely precludes translation at the downstream CDS (Figure 8E). A modest toeprint at the uORF2 termination codon is also observed (red hexagon) for both the WT and optimized uORF2 mRNAs at time 5. Substitution of the Pro-Pro-Gly codons to Ala-Ala-Ala resulted in a 32% reduction in the toeprint signal at the uORF2 termination codon as compared to the WT mRNA. Collectively these results indicate that there is not an extended

ribosome pause at uORF2, but the Pro-Pro-Gly sequence can promote inefficient ribosome termination (Figure 8E).

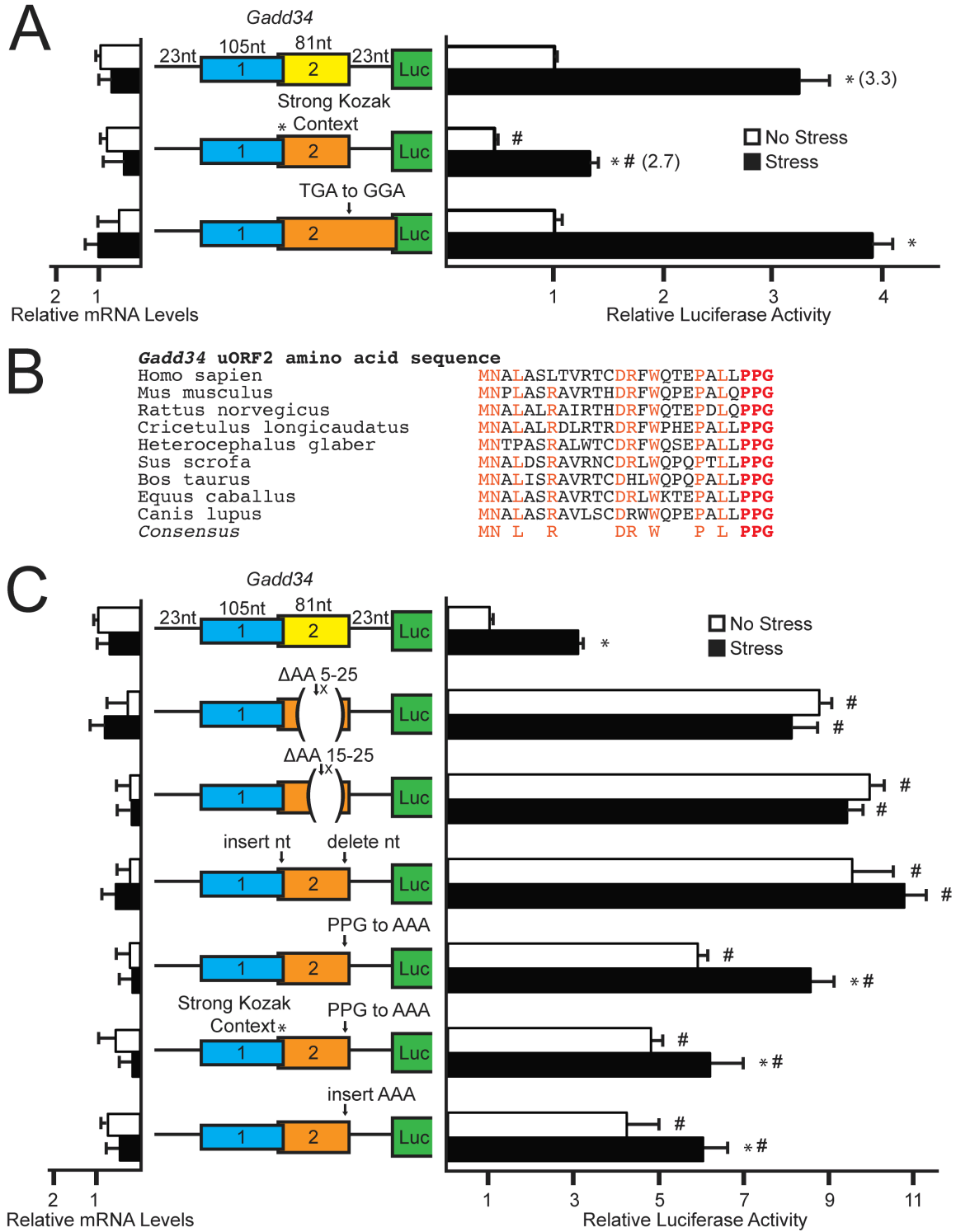


Figure 7. *Gadd34* translation control involves bypass of an inhibitory uORF that relies on a Pro-Pro-Gly juxtaposed to the uORF2 stop codon. A, WT and mutant versions of *P_{TK}-Gadd34-Luc* were transfected into WT MEFs, treated for 6 hours or left

untreated, and measured using a Dual-Luciferase assay and qRT-PCR. Mutant versions of *P_{TK}-Gadd34-Luc* include mutation of the *Gadd34* uORF2 poor start codon context to “* Strong Kozak Context,” and mutation of the stop codon of uORF2 to generate an overlapping out-of-frame uORF (TGA to GGA). Relative values are represented as histograms for each with the S.D. indicated. B, Polypeptide sequence encoded by *Gadd34* uORF2 from different vertebrates. The uORF2 polypeptide sequences were from cDNAs derived from *Gadd34* orthologs, including human (GenBank accession number NM_014330), mouse (NM_008654), rat (NM_133546), hamster (L28147), naked mole-rat (XM_004889808), pig (XM_003127275), cow (NM_001046178), horse (XM_001489532), and dog (XM_533626). Residues conserved between the uORF sequences are listed in the consensus and are highlighted. C, WT and mutant versions of *P_{TK}-Gadd34-Luc* were transfected into WT MEFs, treated for 6 hours or left untreated, and measured using a Dual-Luciferase assay and qRT-PCR. Mutant versions of *P_{TK}-Gadd34-Luc* include deletion of codons 5-25 or 15-25 (Δ AA 5-25 or Δ AA 15-25) and a frameshift construct in which a nucleotide was inserted just following the uORF2 ATG start codon and just prior to the uORF2 stop codon. Additional constructs included mutation of the codons encoding Pro-Pro-Gly to codons for Ala-Ala-Ala (PPG to AAA), simultaneous mutation of the uORF2 start codon to Kozak consensus sequence with the Pro-Pro-Gly to Ala-Ala-Ala mutation (* Strong Kozak Context, PPG to AAA), and insertion of codons encoding Ala-Ala-Ala just prior to the uORF2 stop codon (insert AAA). Relative values are represented as histograms for each with the S.D. indicated.

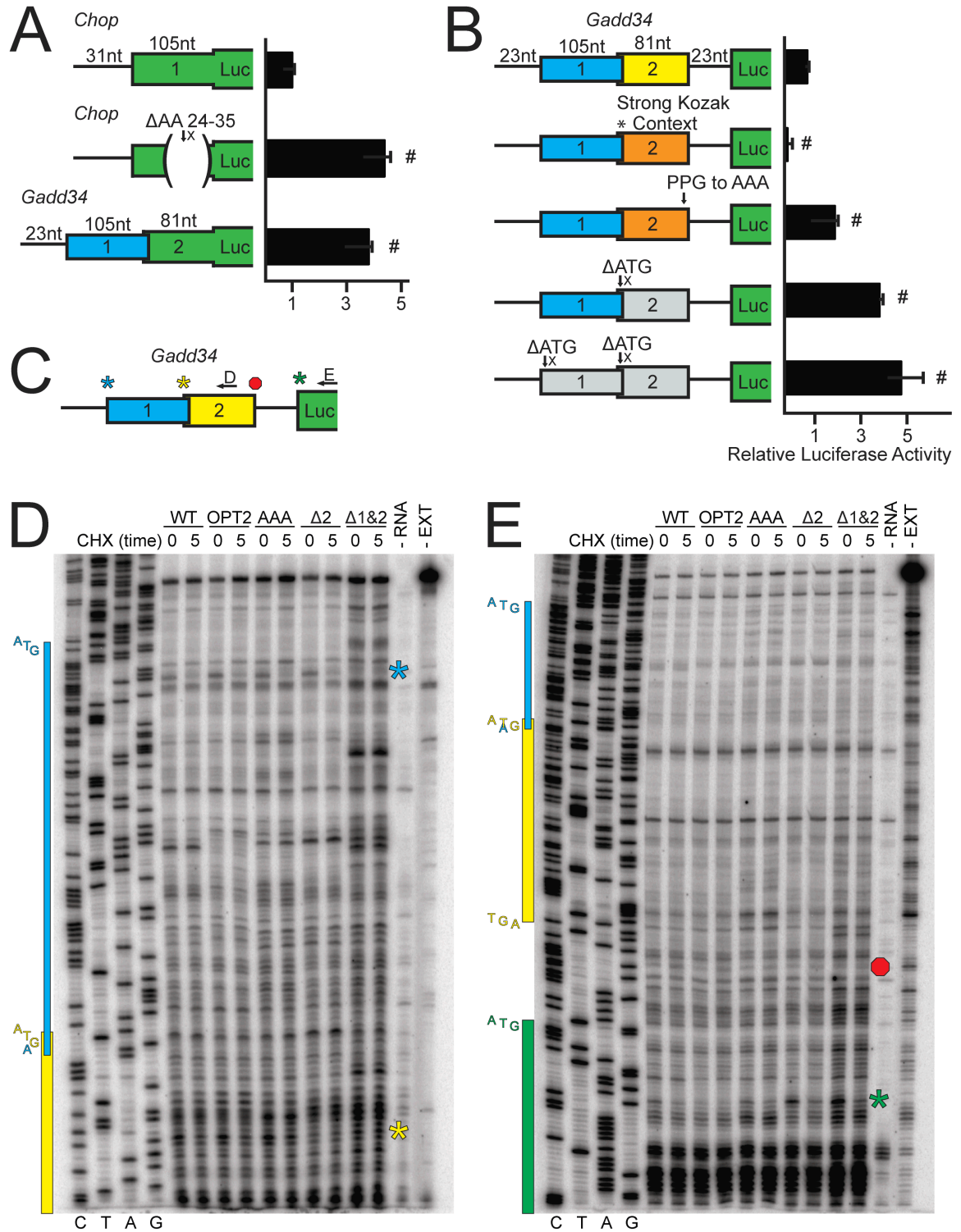


Figure 8. *Gadd34* translation control involves bypass of an inhibitory uORF. A, In-frame fusions between firefly luciferase reporter with the WT *Chop* uORF, *Chop* uORF deleted for codons 24-35, or *Gadd34* uORF2 and firefly luciferase, were transfected into

WT MEF cells, treated for 6 hours or left untreated, and measured using a Dual-Luciferase assay. Relative values are represented as histograms for each with the S.D. indicated. B, WT and mutant versions of *Gadd34-Luc* mRNAs were added to *in vitro* translation reactions and expression was measured using a Luciferase assay. Mutant versions of *P_{T7}-Gadd34-Luc* included uORF2 start codon context mutated to the Kozak consensus sequence (* Strong Kozak Context), substitution of the codons for Pro-Pro-Gly to codons for Ala-Ala-Ala (PPG to AAA), and deletion of uORF2 or uORF1&2 (Δ ATG). Data are representative of three independent biological experiments. C, Depiction of the toeprint design using the WT version of *Gadd34-Luc* mRNA. Black arrows represent the location of primers used in panels D and E. Toeprints corresponding to initiation at uORF1, uORF2, or the luciferase CDS are indicated by a blue, yellow, or green star respectively. Termination at uORF2 is indicated by a red octagon. D and E, Reticulocyte lysates were treated with cycloheximide upon addition of WT or mutant versions of *Gadd34-Luc* mRNA to measure initiating ribosomes (time 0), or 5 minutes after addition of the transcript to measure ribosome localization during steady state translation (time 5). Toeprint assays were conducted for each sample and sequencing reactions can be read 5' to 3' from top to bottom. The nucleotide complementary to the dideoxynucleotide added to each sequencing reactions is listed on the left, below the first four lanes. The products from control primer extension assays in the absence of RNA (-RNA) or in the absence of rabbit reticulocyte lysate translation mixture (-EXT) are indicated on the right. The green star represents the toeprint corresponding to initiation at the luciferase coding region and the yellow star and red octagon represent the toeprint corresponding to initiation and termination of the *Gadd34* uORF2, respectively. Initiation at uORF1 is indicated by a blue star. The blue, yellow, and green colored boxes on the left span the sequences to corresponding to uORF1, uORF2, and the luciferase CDS respectively and are comparable to *Gadd34* 5'-leader

schematic in panel C. The start and stop codons for each ORF are represented to the left of their corresponding colored box. Mutant constructs utilized are the same as listed in panel B and data are representative of three independent biological experiments.

3.5 *Crep* translation is dampened by an inhibitory uORF in an eIF2 α ~P independent manner

Crep has two uORFs with similar spatial arrangements to the 5'-leader of *Gadd34* mRNA, yet CReP expression appears to be unchanged in WT cells upon eIF2 α ~P and stress. A 5'-RACE was carried out to define the transcriptional start site for mouse *Crep*, and determined that the 5'-leader of the *Crep* mRNA is 421 nucleotides in length (Figure 9A). The cDNA encoding the 5'-leader of the *Crep* transcript was inserted between the TK promoter and luciferase reporter gene, generating *P_{TK}-Crep-Luc*. Transfection of *P_{TK}-Crep-Luc* into WT and A/A MEF cells resulted in similar levels of luciferase activity independent of stress treatment and eIF2 α ~P (Figure 9B). Levels of *Crep-Luc* mRNA in these assays, as well as those described below, were similar, indicating that luciferase activity is a measure of translational expression. These results further support the idea that *Crep* mRNA is efficiently translated independent of eIF2 α ~P.

To determine whether *Crep* translation occurs by ribosome scanning, a stem-loop was inserted 10 nucleotides downstream of the 5'-end of the *Crep* mRNA (Figure 9C). Insertion of the stem-loop structure sharply reduced luciferase activity in the presence or absence of ER stress, consistent with the requirement for ribosome scanning for *Crep* translation. As ribosomes scanning the 5'-leader of *Crep* would encounter two uORFs, the uORF start codons were changed from ATG to AGG individually or in combination, as indicated by the Δ ATG in Figure 9C. Deletion of uORF1 led to a modest reduction in luciferase activity in the presence or absence of

stress (Figure 9C). By contrast, deletion of uORF2 led to a 7-fold increase in luciferase activity independent of stress, suggesting that uORF2 is the dominant repressing uORF in *Crep* translation, a feature shared with *Gadd34*. Deletion of both uORF1 and uORF2 led to a further increase in luciferase activity.

To address the ability of ribosomes to reinitiate downstream after translation of uORF2, the *Crep* uORF2 stop codon was mutated from a TGA to a GGA, generating an extended uORF that overlaps out-of-frame with the *Crep* CDS. The overlapping uORF2 resulted in a 5-fold reduction in basal luciferase activity, which was increased 2-fold upon ER stress (Figure 10A). These results suggest that whereas a small portion of the scanning ribosomes can bypass *Crep* uORF2 and initiate downstream translation, the majority of ribosomes that initiate at the downstream *Crep* CDS are reinitiating ribosomes that have previously translated uORF2.

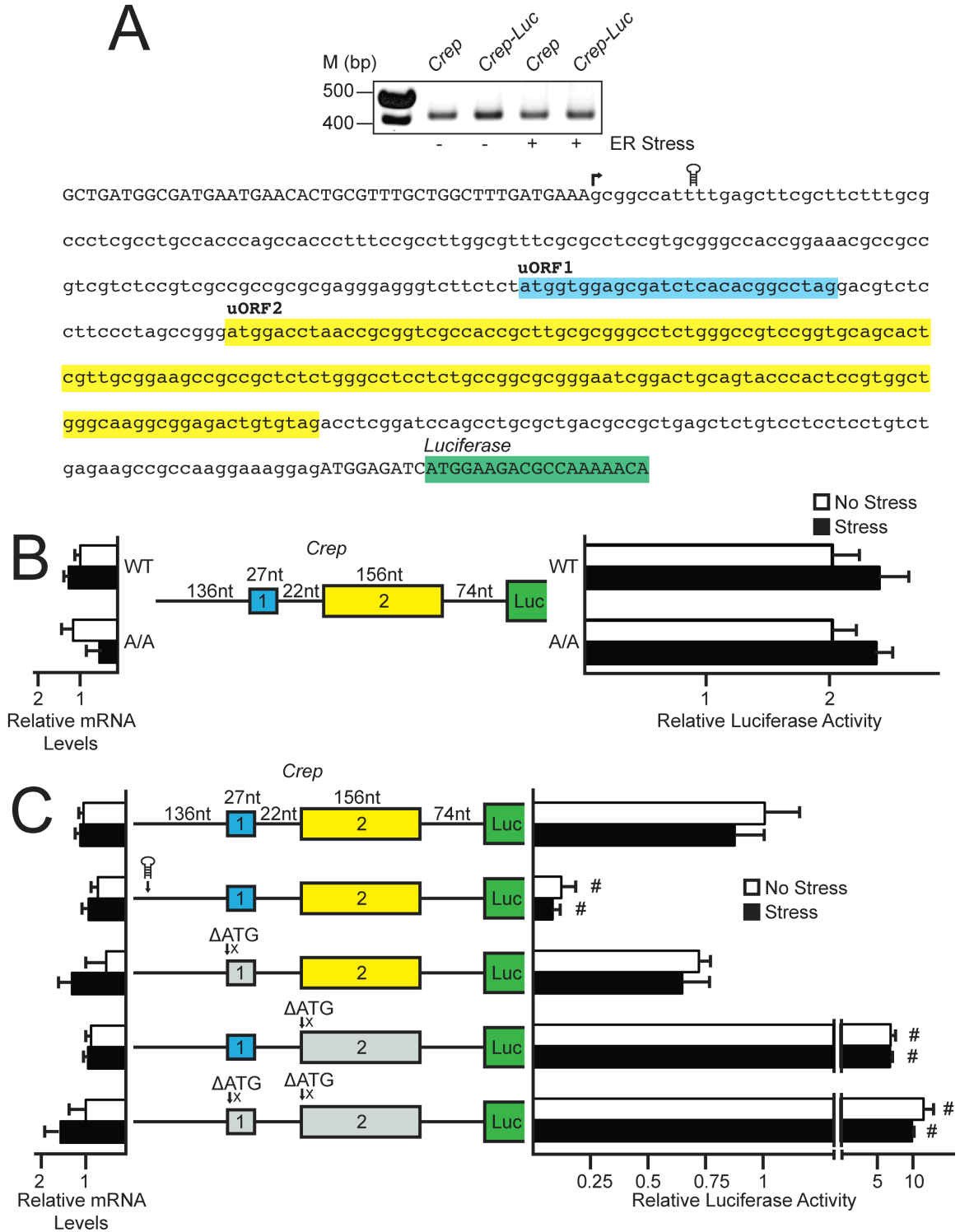


Figure 9. Crep translation is dampened by an inhibitory uORF in an eIF2 α -P independent manner. A, top panel, A 5'-RACE was carried out for Crep using WT MEF cells either transfected with P_{TK} -Crep-Luc or left untransfected. MEFs were treated with

thapsigargin for 6 hours or left untreated and total RNA was prepared. DNA products were separated by gel electrophoresis and a DNA ladder with markers of the indicated base pair sizes is illustrated on the left. A, bottom panel, The DNA sequence encoding the 5'-leader of the *Crep* mRNA is represented in lowercase letters with upper case letters representing the 5'-linker added during the 5'-RACE procedure and the coding region of the *Crep-Luc* fusion. Colored boxes represent the two *Crep* uORFs and the coding region of the *Crep-Luc* fusion. The transcription start site is indicated by an arrow and the location of stem loop insertion is also illustrated. B and C, WT and mutant versions of P_{TK} -*Crep-Luc* and a *Renilla* luciferase reporter were co-transfected into WT or A/A MEF cells, as indicated, and treated with thapsigargin for 6 hours or left untreated. *Crep* translation control was measured Dual-Luciferase assay and corresponding *Crep-Luc* mRNA was measured by qRT-PCR. The P_{TK} -*Crep-Luc* construct contains the cDNA sequence corresponding to the *Crep* 5'-leader fused to the luciferase reporter gene with both *Crep* uORFs and the CDS of the *Crep-Luc* fusion indicated with colored boxes. Relative values are represented as histograms for each with the S.D. indicated. Mutant versions of P_{TK} -*Crep-Luc* include a stem loop insertion and deletion of both uORFs individually or together, as represented by Δ ATG.

3.6 Regulatory properties of *Gadd34* uORF2 are transferable to a heterologous 5'-leader derived from *Crep*

To determine if the regulatory properties of *Gadd34* uORF2 could be transferred to a heterologous 5'-leader derived from *Crep*, the *Crep* uORF2 was replaced with the coding sequence of *Gadd34* uORF2 (Figure 10A). The proximity of the *Gadd34* uORF2 in the context of the *Crep* uORF1 and CDS was also the same as that of WT *Crep*. Introduction of the *Gadd34* uORF2 into the *Crep-Luc* reporter led to a significant reduction in luciferase activity in the absence of stress, which was induced 3.3-fold upon ER stress (Figure 10A). This result indicates that uORF2 of *Gadd34* is a transferable element that can direct preferential translation of a heterologous mRNA.

To define the critical portions of the *Gadd34* uORF2 that confer translational control, smaller portions of the *Gadd34* uORF2 were introduced into the *Crep-Luc* reporter (Figure 10A). Exchange of 21 nucleotides centered on the initiation codon of the *Gadd34* uORF2 for the corresponding sequences in *Crep* resulted in no significant differences from the WT *Crep-Luc* reporter (Figure 10A). This finding is interpreted to suggest that the enhanced ability of *Crep* uORF2 to allow for reinitiation at the downstream CDS diminishes in part the translational control that can be imparted by bypass of the substituted *Gadd34* start codon.

Exchange of a 21 nucleotide sequence that includes the Pro-Pro-Gly and *Gadd34* uORF2 stop codon for the corresponding sequences in *Crep-Luc* resulted in a large decrease in luciferase activity in non-stressed conditions that was enhanced over 4-fold upon ER stress (Figure 10A). This result indicates that the 3'-portion of the *Gadd34* uORF2 is sufficient to confer significant preferential translation to *Crep* upon stress.

To delineate further the contribution of this 21 nucleotide sequence for preferential translation, only the 9 nucleotides encoding the Pro-Pro-Gly residues were

exchanged from *Gadd34* uORF2 for the corresponding sequences in the *Crep* uORF2 in the *Crep-Luc* reporter (Figure 10A). Introduction of the nucleotides encoding the Pro-Pro-Gly sequence led to a decrease in basal luciferase activity that was stress-inducible, similar to that observed for exchange of the entire *Gadd34* uORF2 in *Crep*. This result suggests that the *Gadd34* uORF2 Pro-Pro-Gly sequence can serve to block translation reinitiation in the heterologous *Crep* 5'-leader.

The exchange of the 9 nucleotide segment following the termination codon of the *Gadd34* uORF2 for the corresponding region of the *Crep* 5'-leader resulted in luciferase activities similar to WT *Crep-Luc*, although there was some induction upon ER stress. These results suggest that the Pro-Pro-Gly sequence encoded in *Gadd34* uORF2 is the dominant regulator of downstream translation reinitiation and is central to preferential translation, with the 9 nucleotides following *Gadd34*'s uORF playing a modest role in this regulation. Additionally, the proximity of the uORF to the CDS of the transcript does not appear to be a key feature of the regulation imparted by the *Gadd34* Pro-Pro-Gly sequence due to its ability to regulate expression predictably in the *Crep* 5'-leader, even though *Crep* uORF2 is nearly 3 times further from the CDS as is found for *Gadd34* uORF2. Figure 29 illustrates the models for *Gadd34* and *Crep*, highlighting the differential abilities of the uORF2 from each to allow for translation reinitiation. The translation models for *Gadd34* and *Crep* and their broader implications will be further highlighted in the Chapter 7 Discussion.

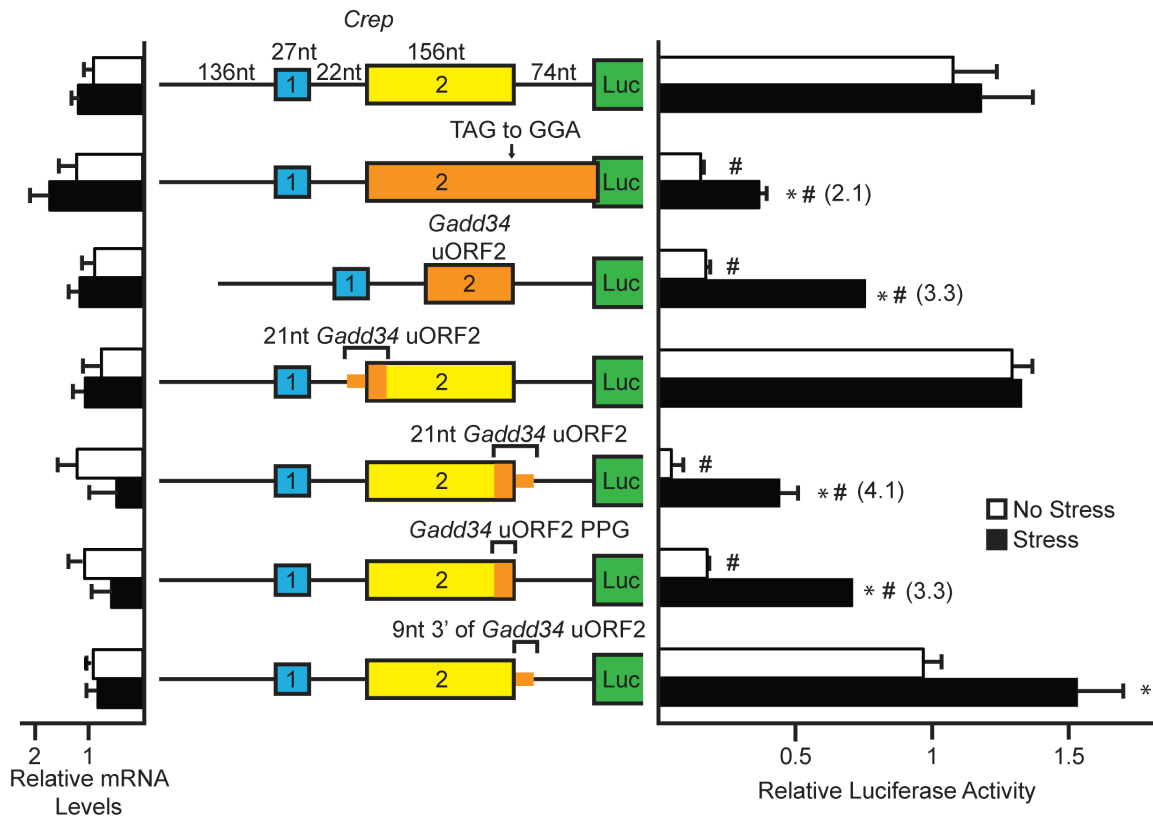


Figure 10. Regulatory properties of *Gadd34* uORF2 are transferable to a heterologous 5'-leader derived from *Crep*. WT and mutant versions of *P_{TK}-Crep-Luc* were transfected into WT MEFs, treated for 6 hours or left untreated, and measured using a Dual-Luciferase assay and qRT-PCR. Mutant versions of *P_{TK}-Crep-Luc* include mutation of uORF2 stop codon from TAG to GGA to generate an overlapping out-of-frame uORF (TAG to GGA), insertion of *Gadd34* uORF2 in place of *Crep* uORF2 (*Gadd34* uORF2), insertion of the 21 nucleotides surrounding *Gadd34* uORF2 start codon in place of the corresponding *Crep* uORF2 sequence (21nt *Gadd34* uORF2), insertion of the 21 nucleotides surrounding *Gadd34* uORF2 stop codon in place of the corresponding *Crep* uORF2 sequence (21nt *Gadd34* uORF2), insertion of the codons encoding *Gadd34* uORF2 Pro-Pro-Gly sequence in place of the corresponding *Crep* uORF2 sequence, and insertion of the 9 nucleotides 3' of *Gadd34* uORF2 in place of the

corresponding *Crep* sequence. Relative values are represented as histograms for each with the S.D. indicated.

3.7 Alterations in the regulatory features of *Gadd34* uORF2 affect cell viability during ER stress

GADD34 is central for determining the appropriate levels of eIF2 α -P in the ISR during transitions from basal to stress conditions, and vice versa. In turn, the amounts of eIF2 α -P can dictate the levels of global and gene-specific translation that determine protein homeostasis and the health of the cell. To determine the role that *Gadd34* translational control by the uORF2 has on eIF2 α -P and cellular adaptation to ER stress, MEF cells were engineered such that they stably expressed *Gadd34* with WT or selected mutant versions of uORF2. Initially, a Flp Recombination Target (FRT) site was integrated in a single location in the genome of GADD34 functional knockout MEF cells (*Gadd34* ^{Δ C/ Δ C}). Integration of the FRT site was then followed by the insertion and clonal isolation of cells expressing full-length *Gadd34* cDNAs under the control of 1-kb of the *Gadd34* promoter, which ensures its proper transcriptional induction in response to ER stress (55).

Four different versions of the GADD34 expressing cells were generated using the FRT-strategy, including MEF cells expressing *Gadd34* with a WT uORF2 (WT2), an uORF2 with a mutant initiation codon (Δ 2), an uORF2 with an initiation codon with optimal Kozak consensus (OPT2), or an uORF2 with Pro-Pro-Gly substituted to Ala-Ala-Ala (AAA2). This isogenic collection of *Gadd34*-expressing cells was then cultured in the presence or absence of thapsigargin, a potent inducer of ER stress. Measurements of GADD34 protein revealed the predicted pattern of expression based on the earlier analyses of endogenous *Gadd34* and *Gadd34-Luc* reporters (Figure 11A). For each, there was a significant increase in *Gadd34* mRNA upon ER stress, indicating that the transcription induction was retained for each version of *Gadd34* (Figure 11B). Cells expressing the *Gadd34*- Δ 2 displayed sharply elevated GADD34 protein in the absence of stress, which was induced 57-fold upon thapsigargin treatment as compared to

Gadd34-WT2 (Figure 11A). The *Gadd34*-AAA2 cells presented with GADD34 protein that was expressed independent of stress, which were much lower than that measured in *Gadd34*- Δ 2 cells, but greater than that expressed in cells with *Gadd34*-WT2. Finally, the *Gadd34*-OPT2 displayed minimal detectable GADD34 protein even during ER stress.

Expression of these *Gadd34* uORF variants led to significant changes in the levels of eIF2 α ~P during stress treatment. Of note, the sharply elevated GADD34 expression in *Gadd34*- Δ 2 cells led to a decrease in eIF2 α ~P in response to ER stress as compared to cells containing the *Gadd34*-WT2 (Figure 11A). *Gadd34*-AAA2 cells presented with a partial lowering of induced eIF2 α ~P. Polysome analyses of cells expressing *Gadd34*-WT2 or *Gadd34*- Δ 2 supported the translational control effects predicted from the patterns of induced eIF2 α ~P (Figure 11C). In both non-stressed and ER stress conditions, the *Gadd34*- Δ 2 cells displayed increased polysome levels compared to *Gadd34*-WT2. These results suggest that *Gadd34* expression is tightly regulated through uORF2-mediated translational control to allow for the optimal amounts of eIF2 α ~P during stress. It is also noted that while *Crep* mRNA and protein levels are considered to be constitutively expressed independent of ER stress, that there were significant differences in *Crep* expression among the cells containing the selected uORF2 versions of *Gadd34*. The most dramatic changes were found in cells expressing *Gadd34*- Δ 2, where coincident with increased GADD34 protein levels there was a sharp reduction in *Crep* mRNA and protein levels upon ER stress (Figure 11A and B). Furthermore, in *Gadd34*-OPT2 cells there was a 2-fold increase in *Crep* mRNA upon thapsigargin, although the CREP protein levels appeared to be unchanged. These results suggest that *Crep* mRNA levels can be modulated depending on the nature of *Gadd34* translational expression.

To determine how the status of *Gadd34* translational control by uORF2 affects cell homeostasis, cell nuclei were stained with Hoechst fluorescent dye and MTT activity was measured to assess cell number and vitality. Both measures were significantly increased in *Gadd34-Δ2* and *Gadd34-AAA2* expressing cells compared to *Gadd34-WT2* (Figure 11D and E). *Gadd34-OPT2* cells were significantly reduced for MTT activity, and trended lower for Hoeschst staining, although without significance. These results suggest that the status of *Gadd34* translational expression can affect cell homeostasis.

Next the collection of *Gadd34*-expressing cells were treated with thapsigargin to determine how the status of the uORF2 and *Gadd34* translational expression can affect their ability to adapt to ER stress. While each of the cells showed reduced MTT activity upon ER stress, the *Gadd34-Δ2* that expressed the highest levels of GADD34 fared the most poorly, whereas the *Gadd34-OPT2* with the lowest levels of GADD34 protein expression showed the most resistance (Figure 11F). These results suggest that enhanced GADD34 expression can render cells more sensitive to stress. Supporting this idea, the addition of guanabenz, a potent inhibitor of GADD34-targeting of PP1c dephosphorylation of eIF2α~P (74) to the *Gadd34-Δ2* cells substantially alleviated its sensitivity to thapsigargin treatment (Figure 11G).

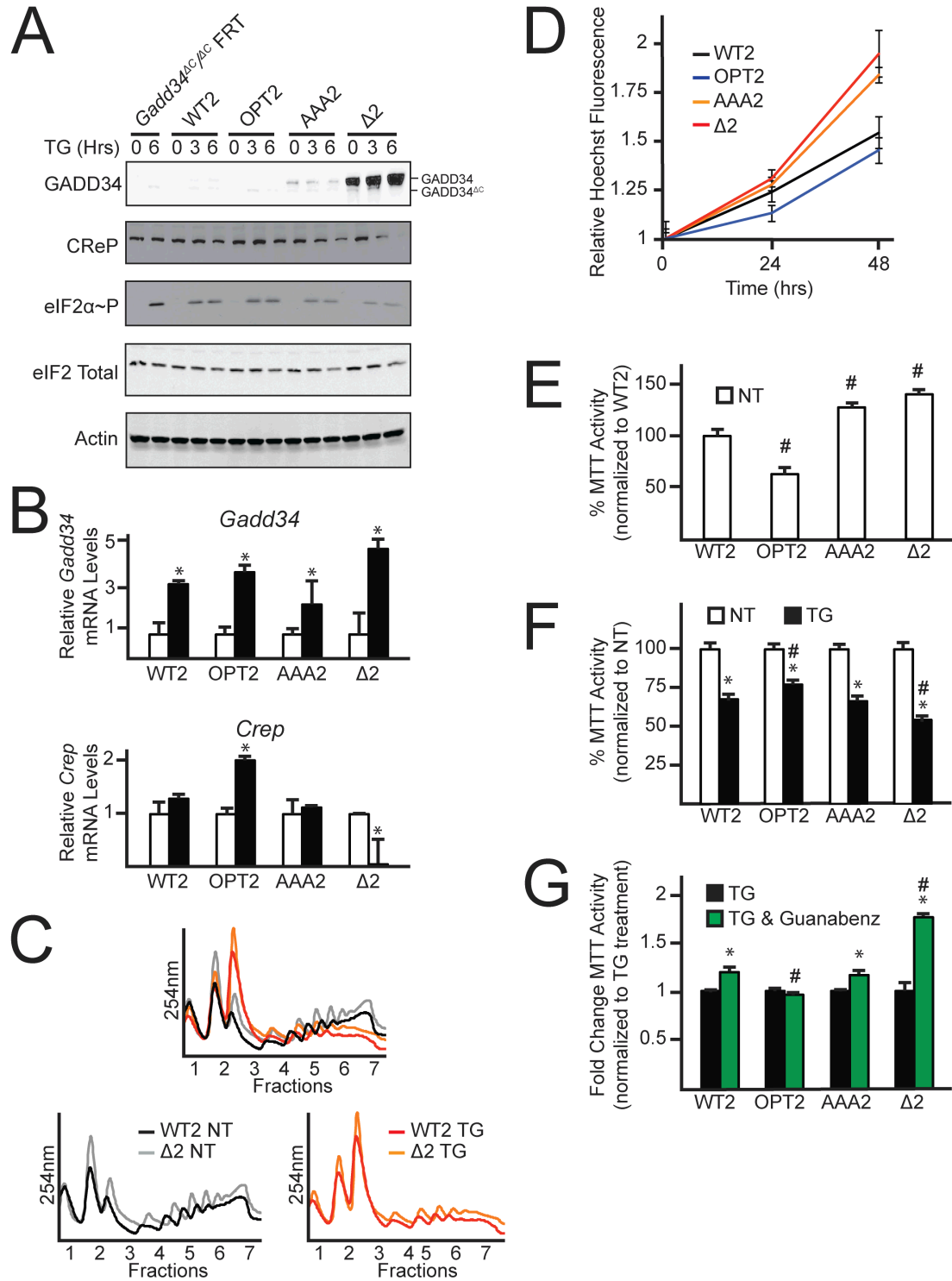


Figure 11. Alterations in the regulatory features of *Gadd34* uORF2 affect cell viability during ER stress. A, MEF cells functionally deleted for *Gadd34* via deletion of the GADD34 C-terminal PP1c interacting domain were stably selected to express WT

Gadd34 (WT2), *Gadd34* with an optimized uORF2 (OPT2), *Gadd34* with uORF2 codons encoding Pro-Pro-Gly mutated to Ala-Ala-Ala (AAA2), and *Gadd34* with uORF2 deleted (Δ 2) and treated with ER stress agent, thapsigargin, for up to 6 hours or left untreated. Full-length GADD34 is labeled as GADD34. Truncated GADD34 lacking the C-terminal PP1c interacting domain is labeled as GADD34 ^{Δ C}. Lysates were processed and levels of GADD34, CReP, eIF2 α -P, eIF2 α total, and β -actin were measured by immunoblot. B, Total RNA was collected from WT2, OPT2, AAA2, and Δ 2 MEF cells cultured in the presence or absence of thapsigargin and relative levels of *Gadd34* and *Crep* mRNA were measured by qRT-PCR. C, WT2 and Δ 2 MEF cells were treated with thapsigargin for 6 hours or left untreated. Lysates were collected and layered on top of 10-50% sucrose gradients, followed by centrifugation and analysis of whole-lysate polysome profiles at 254 nm. D, Equal numbers of WT2, OPT2, AAA2, and Δ 2 MEF cells were seeded in 96-well plates, cultured for 0, 24, or 48 hours, and then fixed using 3.7% formalin with Hoechst stain. Relative values for Hoechst fluorescence are represented with the S.D. indicated. E, Equal numbers of WT2, OPT2, AAA2, and Δ 2 MEF cells were seeded in 96-well plates, cultured for and allowed to grow for 24 hours, and then MTT activity was measured. Relative values are represented as histograms for each with the S.D. indicated. F, The WT and mutant *Gadd34* cells were seeded in 96-well plates, cultured for 24 hours, followed by treatment with or without thapsigargin for an additional 24 hours. MTT activity was measured by the conversion of tetrazolium to formazan. G, The collection of *Gadd34* MEF cells were seeded in 96-well plates, cultured for 24 hours, followed by treatment with thapsigargin with or without guanabenz for an additional 24 hours. MTT activity was measured by the conversion of tetrazolium to formazan.

CHAPTER 4. RESULTS: RIBOSOME ELONGATION STALL DIRECTS GENE-SPECIFIC TRANSLATION CONTROL IN THE INTEGRATED STRESS RESPONSE

4.1 The inhibitory function of *Chop* uORF is reliant upon an Ile-Phe-Ile sequence

In addition to *Gadd34*, other mRNAs that are preferentially translated during cellular stress are also regulated through bypass of an inhibitory uORF. The original observation for preferential translation via ribosomal bypass of an uORF was characterized for the pro-apoptotic transcription factor CHOP (12). The inhibitory nature of the *Chop* uORF was not well understood, however, and is the focus of the research in this thesis chapter. The uORF in the *Chop* mRNA serves as a barrier that prevents downstream translation at the *Chop* coding region during basal conditions. However, upon stress and increased eIF2 α -P, the inhibitory effects of the uORF can be bypassed to increase translation of the *Chop* CDS. This bypass is recapitulated by using luciferase reporter assays, where a cDNA segment encoding the 168-nucleotide sequence of the 5'-leader of *Chop* was inserted between a minimal TK promoter and the firefly luciferase reporter CDS, generating *Chop-Luc*. This luciferase reporter contains the initiation codon of the *Chop* CDS fused in-frame to the luciferase CDS. Expression of *Chop-Luc* was increased almost 3-fold in MEF cells treated with 6 hours of thapsigargin (Figure 12A). Deletion of the uORF by mutation of two ATG start codons at positions 1 and 4 in the uORF to AGG led to constitutively high levels of luciferase activity, which emphasizes the inhibitory function of the uORF. Furthermore, mutation of the stop codon of the uORF from TGA to GGA extended the uORF so that it now overlapped out-of-frame with the CDS (Figure 12A). In this case, there was a similar induction of *Chop-Luc* as observed for the WT version of the uORF, consistent with the idea that eIF2 α -P facilitates bypass of the uORF as opposed to changing translation reinitiation. Finally, substitution of the initiation codon context for both start codons in the uORF to an optimal Kozak consensus sequence lowered luciferase expression and

induction upon ER stress (Figure 12A). This finding indicates that a less than optimal initiation context contributes in part to the ribosomal bypass of the inhibitory uORF upon eIF2 α -P. Normalization of luciferase activity to *Chop-Luc* mRNA levels among these reporter constructs resulted in similar trends as luciferase activity alone, supporting the idea that the observed changes in luciferase activity are the result of translational control (Figure 12A). Together these results support the key tenets of the bypass model described for *Chop* translational control (12,37).

The coding sequence of the *Chop* uORF shares many conserved features among vertebrates (Figure 12B). To explore the basis of the inhibitory nature of the *Chop* uORF sequences during basal conditions, an in-frame fusion of the *Chop* uORF with the firefly luciferase CDS downstream of a minimal TK promoter was generated to create *uORF-Luc* (Figure 13). This reporter lacks the luciferase CDS start codon, ensuring that any measurable luciferase activity is a product of the uORF-luciferase fusion polypeptide. Basal expression of *uORF-Luc* (construct 1) was minimal in MEF cells, suggesting that the *Chop* uORF coding sequence reduced translation of the uORF-luciferase fusion polypeptide (Figure 13A and B). In this reporter construct and those that follow, there was no significant difference in the *uORF-Luc* mRNA and normalization of luciferase activity to *uORF-Luc* mRNA levels resulted in similar trends as luciferase activity alone, supporting the idea that the observed changes in luciferase activity are the result of translation control.

To determine which portion of the *Chop* uORF is critical for its inhibition of downstream translation, in-frame deletions of codons 14-34 and 2-23 were next analyzed in the *uORF-Luc* (Figure 13B, constructs 2 and 3). Deletion of codons 2-23 led to no change in luciferase activity compared to the WT construct, whereas deletion of codons 14-34 increased luciferase expression 6-fold, suggesting that the repressing function of *Chop* uORF lies within the carboxy-terminal coding sequence. To investigate

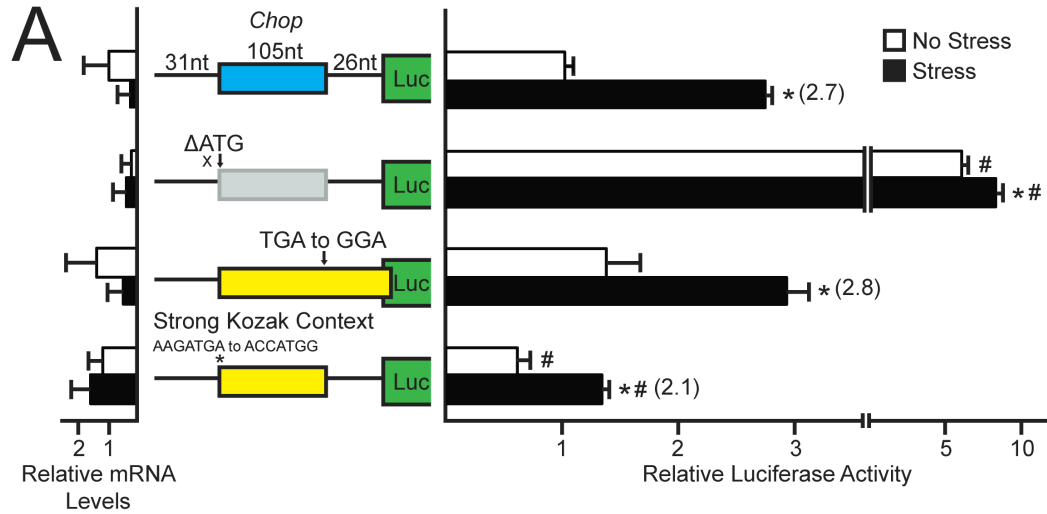
whether the *Chop* uORF RNA sequence contributes to the inhibitory function of this uORF, a single nucleotide was deleted just after codon 23 and a single nucleotide was inserted following codon 34. The resulting frameshift thereby largely retains the uORF nucleotide sequence, but the uORF now encodes a polypeptide of different sequence for the last 10 amino acids in the C-terminal region of the *Chop* uORF (Figure 13A and Figure 13B, construct 4). Luciferase activity for this *Chop uORF-Luc* frameshift reporter was increased to the same extent as deletion of codons 14-34, suggesting that the encoded carboxy-terminal polypeptide sequence is responsible for the inhibitory nature of the *Chop* uORF.

Phylogenetic analysis of the *Chop* uORF polypeptide sequence among vertebrates indicates that there are several conserved amino acid residues in the C-terminal region of the *Chop* uORF (Figure 12B). Single amino acid substitutions, including Cys-27, Ile-28, Phe-29, and Ile-30, to alanine resulted in no significant change in luciferase activity (Figure 13B, constructs 8, 9, 10, and 11). Furthermore, substitution of consecutive residues His-His-His to Ala-Ala-Ala resulted in no change in luciferase activity. By comparison, Ala substitutions for the consecutive Arg-Arg-Lys and Ile-Phe-Ile sequences resulted in a 2.4 and 4.9-fold increase in luciferase activity, respectively (Figure 13B, constructs 5, 6, and 7). In fact the fold induction observed for the Ile-Phe-Ile substitution (construct 6) was similar to that measured for the C-terminal *uORF-Luc* amino acid frameshift reporter (construct 4), suggesting that the Ile-Phe-Ile sequence plays a dominant role in the repressive function of the *Chop* uORF.

Also of importance is whether the activity of the inhibitory amino acid sequences identified in the uORF-luciferase fusion is conserved in translational control directed by the endogenous *Chop* 5'-leader. As noted earlier, there was almost a 3-fold induction of *Chop-Luc* expression in the reporter that features the full *Chop* 5'-leader inserted between a minimal TK promoter and the firefly luciferase CDS (Fig 12A and 14). In this

reporter and those that follow, there was no significant difference in the *Chop-Luc* mRNA upon stress treatment, supporting the idea that the observed changes in luciferase activity are the result of translation control. The Arg-24 codon (encoded by AGA) was mutated to a TGA stop codon in *Chop-Luc*, generating a *Chop* uORF that lacks the last 10 amino acid residues (Figure 14). Removal of these C-terminal residues from the *Chop* uORF resulted in a 4-fold increase in basal luciferase activity, which was further induced upon thapsigargin treatment. Combined mutation of the initiation codon context for each start codon in the uORF to the Kozak consensus sequence and stop codon insertion at codon 24 resulted in a similar basal level of luciferase activity as the stop codon insertion construct alone, but was even less inducible (1.2-fold). These results indicate that the 10 amino acid residues in the carboxy-terminus of the *Chop* uORF thwart reinitiation of ribosomes at the downstream CDS and are thus critical for its inhibition of translation of the downstream CDS during basal conditions. Furthermore, bypass of the *Chop* uORF is required for maximal *Chop* expression during cellular stress.

Next Ile-Phe-Ile and His-His-His sequences were each substituted to Ala-Ala-Ala in the *Chop-Luc* reporter. Substitution of the Ile-Phe-Ile sequence resulted in a basal increase in luciferase activity that was further induced with thapsigargin treatment, whereas mutation of the His-His-His sequence resulted in no significant difference in expression from the WT *Chop-Luc* (Figure 14). These results further support the idea that the carboxy-terminal Ile-Phe-Ile residues are a major reason for the repressing function of the *Chop* uORF and are critical for maintaining low levels of *Chop* expression during basal conditions.



B Chop uORF amino acid sequence

Homo sapien	MLKMSG-----WQRQSQNSWNLRRECSRRKCFIFHHHT
Mus musculus	MLKMSG-----WQRQSQNNSRNLRRECSRRKCFIFHHHT
Tursiops truncatus	MLKMSG-----WQRQSQNQSRNLRRECSRRKCFIFHHHT
Sus scrofa	MLKM SR-----WQRQSQNQSRNLRRECSRRKCFIFHHHT
Ursus maritimus	MLKMSG-----WQPQSQNQSRNLRRECSRRKCFIFHHHT
Bos taurus	MLKMSG-----WQRQSQNQSRNLRRECSRRKCFIFHHHT
Capra hircus	---MSG-----WQRQSQNQSWNLRRECSRRKCFIFHHHT
Canis lupus	MLKMSG-----WQPQSHSQSRNLRRECSRRKCFIFHHHT
Felis catus	MLKMSG-----WQQQSQNQSRNLRRECSRRKCFIFHHHT
Myotis lucifugus	MLKMSG-----WQRQSQNQSRNLRRECSRRKCFIFHHHT
Xenopus tropicalis	MFNMSPSQLNVQPQTSSRCRFICQKRTDPTWRKCRRKCFIFHHHT
Consensus	MS R C R R K I F I H H H T

Figure 12. Chop translation control involves bypass of an inhibitory uORF due in part to poor start codon context. A, WT and mutant versions of *Chop-Luc* and a *Renilla* luciferase reporter were co-transfected into MEF cells and treated for 6 hours with thapsigargin, or left untreated. *Chop* translation control was measured via a Dual-Luciferase assay and corresponding *Chop-Luc* mRNA was measured by qRT-PCR. The *Chop-Luc* construct contains the cDNA sequence corresponding to the *Chop* 5'-leader fused to the luciferase reporter gene with the *Chop* uORF and CDS of the *Chop-Luc* fusion indicated with colored boxes. Mutant versions of *Chop-Luc* include substitution of the *Chop* uORF ATG start codons to AGG, mutation of the *Chop* uORF stop codon from TGA to GGA, and optimization of the *Chop* uORF start codons to the Kozak consensus sequence. Relative values are represented as histograms for each, with the S.D. indicated. The following values represent firefly luciferase activity normalized for mRNAs expressed from the indicated WT and mutant versions of *Chop-Luc* reporters.

These values feature the no stress, stress, and in parentheses induction ratios: WT 1, 10.2 (10.2); ATG to AGG 32.4, 24.1 (0.75); TGA to GGA 0.9, 5.6 (6); and strong Kozak consensus 0.5, 0.8 (1.6). B, Polypeptide sequence encoded by the *Chop* uORF from different vertebrates. The uORF polypeptide sequences were from cDNAs derived from *Chop* orthologs, including Homo sapien (BC003637), Mus musculus (BC013718), Tursiops truncatus (XM_004316348), Sus scrofa (AK346731), Ursus maritimus (GW278660), Bos taurus (BC122721), Capra hircus (NM_001287231), Canis lupus (DN431044), Felis catus (XM_006933848), Myotis lucifugus (XM_006093575), and Xenopus tropicalis (BC153679). Residues conserved between the uORF sequences are listed in the consensus and are highlighted.

A CHOP uORF peptide sequence (1): ¹ML²KMSGWQRQSQNNSRNLRRECSRRK¹⁴**IF**HHHT²³²⁷282930...³⁴
 CHOP uORF frameshift peptide sequence (4): MLKMSGWQRQSQNNSRNLRRECS²³**EGSASSY**TTTP³⁴
↑ delete nt ↑ insert nt

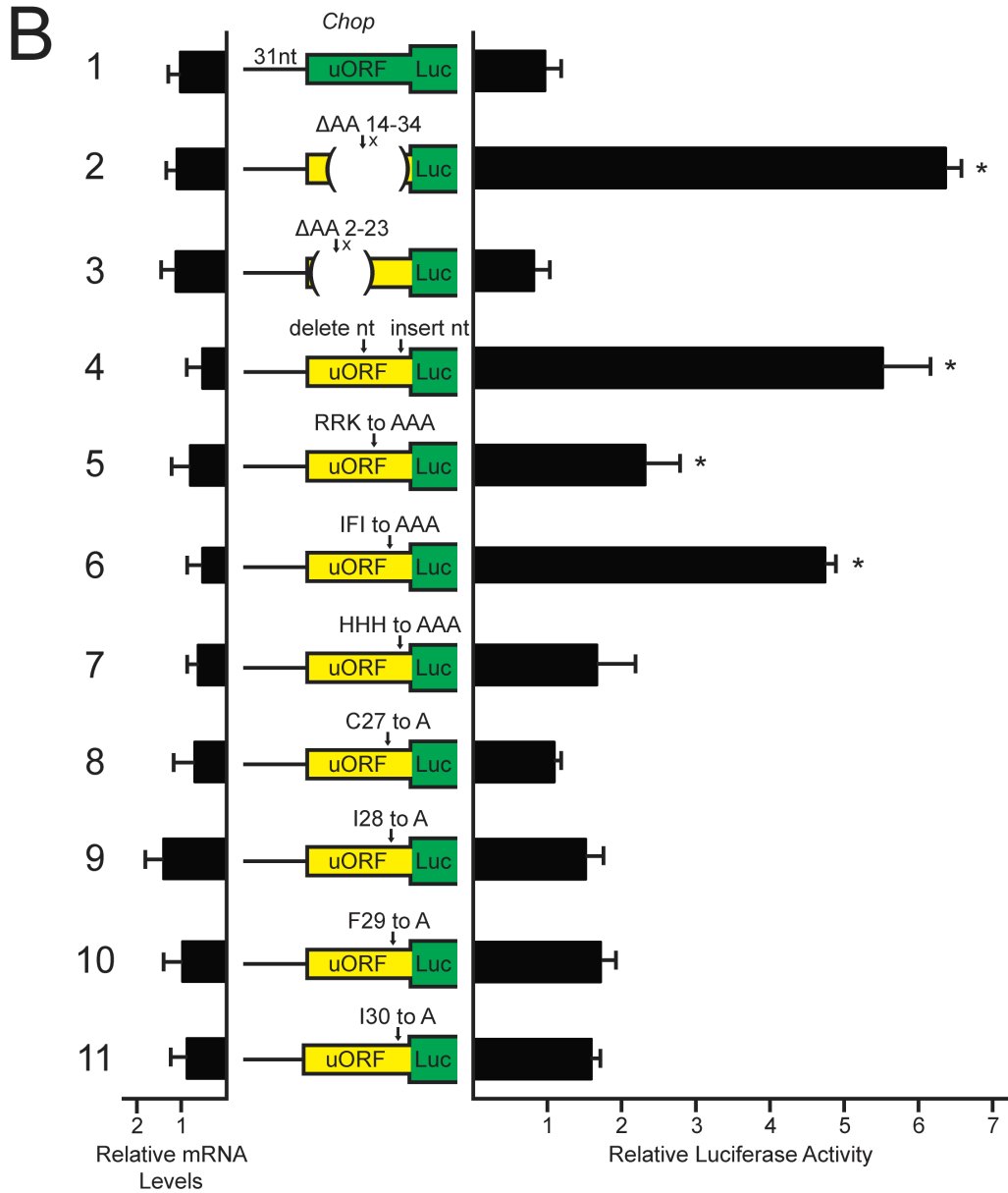


Figure 13. Chop translation control involves an inhibitory uORF that relies on an encoded Ile-Phe-Ile sequence. A, Representation of the *Chop* uORF amino acid sequence in the wild-type context (construct 1) and the frameshift polypeptide sequence in which a nucleotide was deleted just after amino acid 23 and inserted following amino acid 34 (construct 4). The amino acid sequences in the uORF polypeptide are listed,

with corresponding positions. The inhibitory Ile-Phe-Ile sequence is highlighted in red in the WT *Chop* uORF peptide sequence. The last 10 amino acid residues in the *Chop* uORF were altered as a consequence of the uORF frameshift construct and are highlighted in blue. B, The WT and mutant versions of the uORF-Luc constructs and a *Renilla* luciferase reporter were co-transfected into MEF cells. Twenty-four hours later, *Chop* uORF translation control was measured via Dual-Luciferase assay and corresponding *Chop-Luc* mRNAs were measured by qRT-PCR. The uORF-Luc constructs contain the *Chop* uORF fused in-frame to the luciferase reporter gene, with the ATG start codon of luciferase deleted. The *Chop* uORF sequence and luciferase CDS are indicated by the colored boxes. The green *Chop* uORF box represents the wild-type *Chop* uORF sequence. Yellow *Chop* uORF boxes represent mutant constructs in which a change was made to the *Chop* uORF sequence. Mutant versions of uORF-Luc include an in-frame deletion of uORF codons 14-34 or 2-23, frameshift in the last 10 *Chop* uORF codons, substitution of *Chop* uORF codons Arg-Arg-Lys to Ala-Ala-Ala, change of Ile-Phe-Ile to Ala-Ala-Ala, mutation of His-His-His to Ala-Ala-Ala, and alanine substitutions for Cys-27, Ile-28, Phe-29, and Ile-30. Relative values are represented as histograms for each, with the S.D. indicated. The following values represent firefly luciferase activity normalized for mRNA for the WT and mutant versions of the uORF-Luc reporters. These values feature the construct number in parentheses followed by the luciferase activity to mRNA ratios: (1) 1; (2) 6.1; (3) 0.8; (4) 10.9; (5) 3; (6) 9.3; (7) 2.8; (8) 1.6; (9) 1.1; (10) 1.8; (11) 1.9.

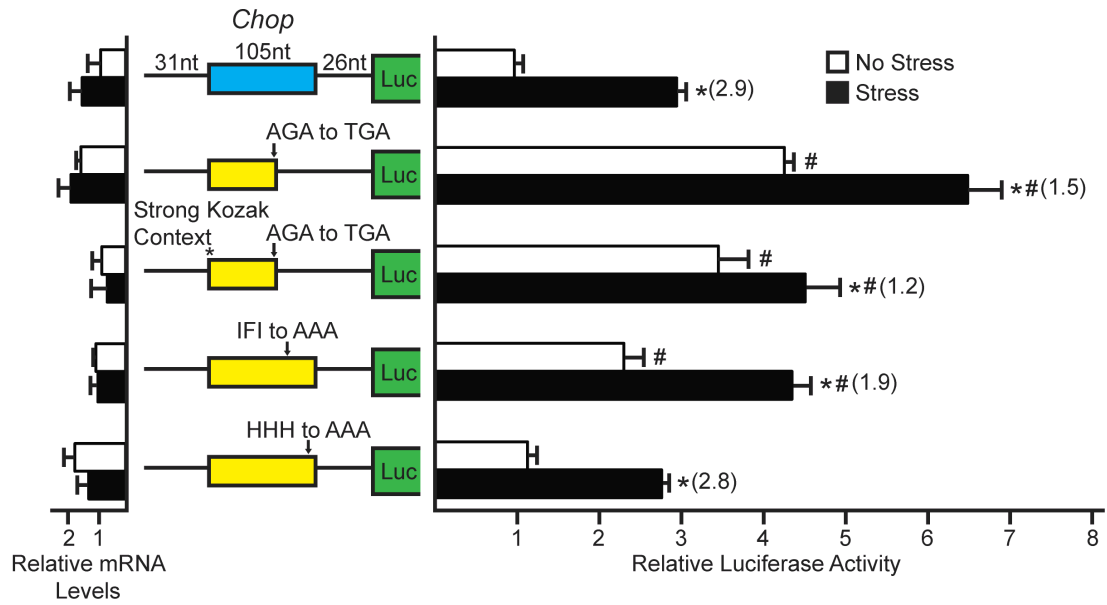


Figure 14. *Chop* translation control involves bypass of an inhibitory uORF. WT and mutant versions of *Chop-Luc* and a *Renilla* luciferase reporter were co-transfected into MEF cells and treated for 6 hours with thapsigargin, or left untreated. *Chop* translation control was measured via a Dual-Luciferase assay and corresponding *Chop-Luc* mRNA was measured by qRT-PCR. The *Chop-Luc* construct contains the cDNA sequence corresponding to the *Chop* 5'-leader fused to the luciferase reporter gene with the *Chop* uORF and CDS of the *Chop-Luc* fusion indicated with colored boxes. Mutant versions of *Chop-Luc* include mutation of the AGA codon of Arg-24 to TGA, simultaneous mutation of the *Chop* uORF start codon to Kozak consensus sequence with the AGA to TGA mutation, change of the Ile-Phe-Ile codons to those encoding Ala-Ala-Ala, and mutation of the His-His-His codons to those encoding Ala-Ala-Ala. Relative values are represented as histograms for each, with the S.D. indicated. The following values represent firefly luciferase activity normalized for mRNA from the WT and mutant versions of *Chop-Luc* reporters. These values feature the no stress, stress, and in parentheses induction ratios: WT 1, 1.8 (1.8); AGA to TGA 2.5, 3.1 (1.2); optimized

Kozak context with AGA to TGA 3.8, 6.5 (1.7); IFI to AAA 2.1, 4.1 (2); and HHH to AAA 0.6, 2 (3.4).

4.2 Translation of an Ile-Phe-Ile sequence in the *Chop* uORF results in an elongation stall

An *in vitro* translation assay using selected *Chop* uORF mutants followed by toeprinting analysis was carried out to map the position of ribosomes potentially stalled at the inhibitory *Chop* uORF sequence. The *Chop* uORF C-terminal sequence was fused in-frame between a rabbit α -globin domain and the firefly luciferase CDS to determine if the inhibitory uORF amino acid sequence could regulate translation when placed internally as a part of a polypeptide of heterologous sequence (Figure 15A) (69). The α -globin-*Chop*-Luc reporters were constructed with a WT portion of the *Chop* uORF (WT), a frameshift version with single nucleotide deleted after codon 23 and an inserted nucleotide following codon 34 (FS), a substitution of Ala residues for Ile-Phe-Ile (IFI), and a version containing a stop codon following the inserted *Chop* uORF sequence (STOP). T7 RNA polymerase was used to synthesize the WT and mutant versions of the α -globin-*Chop*-Luc mRNAs, which were then introduced into cell-free translation extracts for toeprint mapping of translating ribosomes. Cell-free translation extracts were treated with cycloheximide (CHX) simultaneous to addition of α -globin-*Chop*-Luc mRNA to measure translation initiation events (time 0) or 15 minutes after introduction of α -globin-*Chop*-Luc mRNA to map the position of ribosomes during steady-state translation and polypeptide synthesis (time 15). Alternatively, cycloheximide was not added to the *in vitro* translation reactions after addition of α -globin-*Chop*-Luc mRNA to map any ribosome stalls strong enough to result in detectable toeprint signals without the addition of an elongation inhibitor (time -).

Initiation at the AUG start codon was observed for the α -globin-*Chop*-Luc mRNA (green star) without cycloheximide treatment and at time 15, but was strongest at time 0, indicative of efficient translation initiation at this codon (Figure 15B). Toeprints were also observed with the second Ile codon of the repressing Ile-Phe-Ile sequence in the

ribosomal P site both without cycloheximide addition and with greater intensity at time 15 (yellow star), but not at time 0. Modest toeprints were additionally present at the Phe codon of the same amino acid sequence in the ribosomal P site, suggesting that the repressing capability of the *Chop* uORF is due to an elongation stall at the encoded Ile-Phe-Ile sequence of the *Chop* uORF. Importantly these toeprint patterns suggest that this *Chop* uORF sequence can sustain the same capacity for translation inhibition when transferred to an internal position of a coding sequence in a heterologous polypeptide.

Introduction of a single nucleotide just prior to the *Chop* portion of the α -globin-*Chop-Luc* mRNA and deletion of a single nucleotide just after the *Chop* sequence significantly reduced the toeprint signals for stalled ribosomes at the *Chop* uORF sequence. This finding provides additional evidence that the inhibitory nature of the *Chop* uORF is predominantly caused by a specific encoded amino acid sequence rather than RNA sequence *per se*. Alanine substitutions for the Ile-Phe-Ile *Chop* uORF sequence resulted in a similar reduction in toeprint signals for a stalled elongating ribosome, suggesting that Ile-Phe-Ile in the *Chop* uORF can serve as a barrier to downstream translation. Finally, introduction of a TGA stop codon just following the *Chop* portion of the α -globin-*Chop-Luc* mRNA resulted in a strong toeprint signal at both the termination codon (red octagon) and the Ile-Phe-Ile sequence (now shifted up three nucleotides in the sequencing gel; blue star). These results indicate that the Ile-Phe-Ile sequence has the capacity to stall elongating ribosomes in the *Chop* uORF (Figure 15A and B).

To address if the capacity of the Ile-Phe-Ile sequence to stall elongating ribosomes is regulated in a stress dependent manner, an in-frame-fusion of the *Chop* uORF C-terminal sequence in between the *Renilla* CDS and the firefly luciferase CDS was generated (Figure 15C). This luciferase reporter lacks the firefly luciferase start codon, ensuring that any measurable luciferase activity is a product of the *Renilla*-uORF-

Luc fusion polypeptide. Basal firefly luciferase activity from *Renilla*-uORF-Luc was minimal in MEF cells, consistent with reduced translation of the fusion polypeptide due to the placement of the *Chop* uORF coding sequence between the *Renilla* and firefly luciferase CDSs (Figure 15C). Thapsigargin treatment resulted in no difference in luciferase activity as compared to no stress, indicating that the inhibitory nature of the *Chop* uORF is not regulated in stress dependent manner. In this reporter and those that follow, there was no significant difference in the *Renilla-uORF-Luc* mRNA upon stress treatment, supporting the idea that the observed changes in luciferase activity are the result of translation control.

Next a single nucleotide was deleted just after codon 23 and a single nucleotide was inserted following codon 34 of the *Chop* uORF, generating a *Renilla*-uORF-Luc fusion polypeptide of different sequence encoded in the *Chop* uORF region. Introduction of the frameshift resulted in almost a 3-fold increase in luciferase activity independent of stress, emphasizing that the encoded carboxy-terminal polypeptide sequence is responsible for the inhibitory nature of the *Chop* uORF (Figure 15C). Mutation of the nucleotides encoding Ile-Phe-Ile to those for Ala-Ala-Ala also led to a 2-fold increase luciferase activity in both stress and non-stressed conditions, illustrating that the Ile-Phe-Ile sequence is critical for the ribosomal elongation stall. Finally, addition of a stop codon just following the *Chop* uORF sequence resulted in almost no luciferase activity as expected for a termination event prior to the firefly luciferase CDS. These results further support the idea that the carboxy-terminal Ile-Phe-Ile residues are a major reason for the repressing function of the *Chop* uORF and that the nature of the inhibitory activity of the Ile-Phe-Ile is not regulated in a stress-dependent manner. A model for *Chop* translational control and its broader implications will be highlighted in the Chapter 7 Discussion.

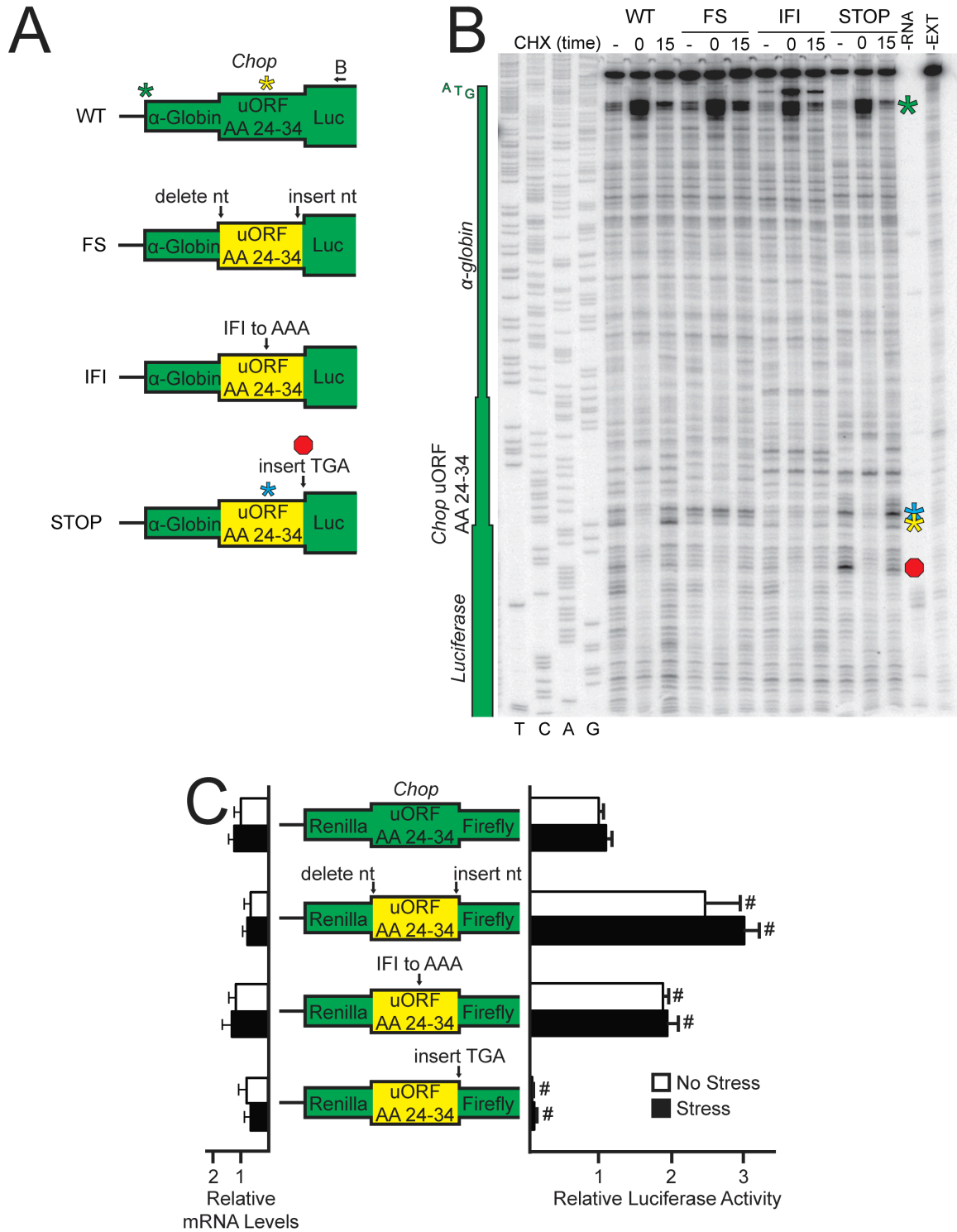


Figure 15. Translation of the *Chop* uORF results in a ribosome elongation stall that is dependent on an Ile-Phe-Ile sequence. A, Depiction of toehold design using the last 30 nucleotides of the *Chop* uORF inserted in-frame between the rabbit α -globin

and luciferase coding sequences to generate *α-globin-Chop-Luc* fusion mRNA. Mutant versions of *α-globin-Chop-Luc* mRNA include frameshift of the 30 nucleotides corresponding to the *Chop* uORF (FS), mutation of the Ile-Phe-Ile codons to those encoding Ala-Ala-Ala (IFI), and insertion of a TGA stop codon just following the 30 *Chop* uORF nucleotides (STOP). The black arrow depicted above the WT *α-globin-Chop-Luc* mRNA represents the location of the primer used in panel B. Toeprints corresponding to ribosome initiation at the start codon for the WT and mutant *α-globin-Chop-Luc* mRNAs are represented by a green star. Toeprints corresponding to a ribosome elongation stall for the WT, FS, and IFI mRNAs are represented by a yellow star. Toeprints corresponding to an elongation stall and ribosome termination for the STOP mRNA are represented by a blue star and a red octagon respectively. B, Cell-free translation extracts were treated with cycloheximide upon addition of WT or mutant versions of the *α-globin-Chop-Luc* mRNA to measure initiating ribosomes (time 0), 15 minutes after addition of the transcript to measure ribosome localization during steady state translation (time 15), or left untreated to measure prolonged ribosomal stalls that present without the use of an elongation inhibitor (time -). Toeprint assays were conducted for each sample and sequencing reactions can be read 5'- to 3'- from top to bottom. The nucleotide complementary to the dideoxynucleotide residue added to each sequencing reaction is listed on the left, below the first four lanes. The products from control primer extension assays in the absence of RNA (-RNA) or in the absence of cell-free translation extracts are indicated on the right. The green star represents the toeprint corresponding to initiation at the *α-globin-Chop-Luc* fusion, the yellow and blue stars represent prominent ribosome elongation stalls, and the red octagon represents the toeprint corresponding to termination at the introduced stop codon. The green boxes on the left span the sequences corresponding to the *α-globin*, *Chop* uORF, and luciferase CDS and are comparable to the *α-globin-Chop-Luc* schematic in panel A. Mutant constructs are

the same listed in panel A and data are representative of three independent biological experiments. C, WT and mutant versions of *Renilla-uORF-Luc* were transfected into MEF cells and treated for 6 hours with thapsigargin, or left untreated. *Chop* translation control was measured via a Dual-Luciferase assay and corresponding *Renilla-uORF-Luc* mRNA was measured by qRT-PCR. The *Renilla-uORF-Luc* construct includes the last 30 nucleotide residues of the *Chop* uORF inserted in-frame between the *Renilla* and firefly luciferase coding sequences. Mutant versions of *Renilla-uORF-Luc* include frameshift of the 30 nucleotide segment corresponding to the *Chop* uORF, mutation of the Ile-Phe-Ile codons to those encoding Ala-Ala-Ala, and insertion of a TGA stop codon just following the 30 nucleotide *Chop* uORF segment. Relative values are represented as histograms for each, with the S.D. indicated. The following values represent firefly luciferase activity normalized for mRNA from the WT and mutant versions of *Renilla-uORF-Luc* reporters. These values feature the no stress, stress, and in parentheses induction ratios: WT 1, 0.9 (0.9); Frameshift 4, 4.1 (1); IFI to AAA 1.6, 1.5 (0.9); and TGA insertion 0.1, 0.1 (1).

4.3 Alterations in *Chop* uORF translation control change the dynamics of CHOP expression

Based on the data presented here, increased translation of *Chop* during eIF2 α ~P is central for determining expression of CHOP and its downstream transcriptional activity, which are suggested to be critical for stress-induced apoptosis when ISR signaling is insufficient to alleviate stress damage and restore cellular homeostasis (49,50,75). To address this idea, *Chop*^{-/-} MEF cells were engineered to stably express *Chop* with either the WT uORF or an uORF with mutant initiation codons (Δ uORF *Chop*) (Figure 16A). To generate these *Chop* expressing cell lines, a FRT site was integrated in the genome of *Chop*^{-/-} cells in a single location (*Chop*^{-/-} FRT), followed by clonal isolation. Integration of the FRT site was followed by insertion of full-length *Chop* cDNAs including the WT or Δ uORF *Chop* 5'-leader under control of 1-kb of the *Chop* promoter to ensure its proper transcriptional regulation in response to ER stress (50,76). These isogenic *Chop*-expressing cells were then assayed for changes in *Chop* expression and cell viability in the presence or absence of thapsigargin. Measurements of CHOP protein levels showed the expected pattern of CHOP expression in WT uORF *Chop* MEF cells with low basal levels of CHOP expression that increased in response to thapsigargin treatment (Figure 16A). Δ uORF *Chop* MEF cells presented with sharply elevated levels of CHOP protein in the absence of stress that was increased further after 1 and 3 hours of stress, and reduced by 6 hours. The reduction of CHOP protein levels in the Δ uORF *Chop* cells after 3 hours of stress could be a consequence of feedback regulation, and this feature of CHOP expression is addressed below. Phosphorylation of eIF2 α after thapsigargin treatment followed similar patterns, peaking at 3 hours of treatment, with the highest levels of eIF2 α ~P being observed in the Δ uORF *Chop* cells. In each of the *Chop*-derived cells, eIF2 α ~P was reduced by 6 hours, which is consistent with the ISR feedback control directed by GADD34 (40).

Polysomes analysis of cells expressing either WT uORF or Δ uORF *Chop* supported the translation control changes predicted based on the earlier analysis of endogenous *Chop* and *Chop-Luc* reporters (Figures 12A and 16B) (12). For this analysis, lysates were prepared from WT and Δ uORF *Chop* cells that were subjected to thapsigargin or no ER stress. These lysates were then separated by sucrose gradient ultracentrifugation (Figure 16B, top panels). Consistent with lowered global translation initiation in response to stress and eIF2 α -P, both cell lines displayed lowered polysome levels coincident with increased monosomes after thapsigargin treatment. To assess the efficiency of translation of *Chop* mRNA, *Chop* transcript levels were next measured among the sucrose fractions. In the WT uORF *Chop* cell line, *Chop* mRNA was largely associated with light polysomes in the absence of stress, with a 58% shift of transcript to heavy polysomes with thapsigargin treatment (Figure 16B). This is consistent with preferential translation in response to eIF2 α -P. In the Δ uORF *Chop* cells, *Chop* transcripts were associated with increased polysome levels compared to the WT uORF *Chop* cells in both non-stressed and ER stress conditions. Overall this suggests that *Chop* transcript is robustly translated for both the WT and Δ uORF *Chop* cells after 6 hours of thapsigargin treatment, the recovery phase of eIF2 α -P. Furthermore, deletion of the *Chop* uORF is suggested to result in resistance to translation repression in the presence of eIF2 α -P, resulting in a constitutively translated transcript. These results suggest that CHOP protein abundance is tightly regulated through an uORF-mediated mechanism of translational control.

It is also known that *Chop* expression is regulated by transcription through the activity of ISR-induced ATF4 and C/EBP β (76,77). Time course analysis of *Chop* mRNA levels for up to 12 hours after thapsigargin treatment of the *Chop*-expressing cells lines revealed that *Chop* mRNA expression is substantially reduced both basally and with thapsigargin treatment in Δ uORF *Chop* as compared to WT uORF *Chop* (Figure 16C).

Transfection of the WT uORF and Δ uORF *Chop* cell lines with a luciferase reporter under the control of 1-kb of the *Chop* promoter ($P_{CHOP-Luc}$) and measurement of luciferase activity resulted in a similar trend in expression as observed for the endogenous *Chop* mRNA levels, with low levels of luciferase activity in the Δ uORF *Chop* cell line (Figure 16D). Combined, these results suggest that *Chop* transcriptional regulation is altered in the Δ uORF *Chop* cell line resulting in lowered *Chop* mRNA levels.

To determine if changes in *Chop* mRNA turnover also contribute to the differences observed in *Chop* transcript abundance, WT uORF and Δ uORF *Chop* cells were subjected to thapsigargin treatment or no stress treatment for 3 hours, followed by actinomycin D treatment for up to an additional 3 hours. *Chop* mRNAs from the WT uORF cells presented with a half-life of ~2 hours, consistent with an earlier report (50). Interestingly, deletion of the *Chop* uORF increased the half-life of *Chop* transcript to ~4.5 hours. *Chop* was previously identified in a genome-wide screen as a target of the nonsense mediated mRNA decay pathway (78) and these findings suggest that deletion of the *Chop* uORF thwarts the decay machinery to detect and lower the abundance of *Chop* mRNA. Given that levels of the more stable Δ uORF *Chop* mRNA were significantly less than WT, these results emphasize that decreased abundance of the Δ uORF *Chop* is due to substantial reductions in *Chop* transcription. Despite the lowered *Chop* mRNA in the Δ uORF *Chop* cells, there was a marked increase in basal and induced CHOP protein (Figure 16A), which reinforces the idea that translational expression of *Chop* is a major feature in its regulated expression. As will be highlighted further in the Chapter 7 Discussion, a likely mechanism contributing to this difference in *Chop* mRNA expression is direct or indirect feedback regulation by CHOP (79,80).

CHOP is a short-lived protein with a half-life of less than four hours (50). To determine if CHOP protein turnover was differentially regulated in the WT uORF and Δ uORF *Chop* cells, both *Chop*-expressing cells lines were pretreated with thapsigargin

for 3 hours followed by either no cycloheximide treatment or cycloheximide treatment for up to 5 hours (Figure 16E). WT uORF *Chop* cells presented with a CHOP protein half-life of about 3 hours, similar to endogenous CHOP in WT MEF cells (50). However, CHOP protein half-life in the Δ uORF *Chop* cells was decreased to about 1 hour. This protein destabilization correlates with the sharp reduction in CHOP protein expression that is observed after 6 hours of thapsigargin treatment in the Δ uORF *Chop* cells. Overall, these results suggest that increased CHOP synthesis resulting from altered translation regulation elicits multiple compensating mechanisms targeted to lower CHOP protein expression.

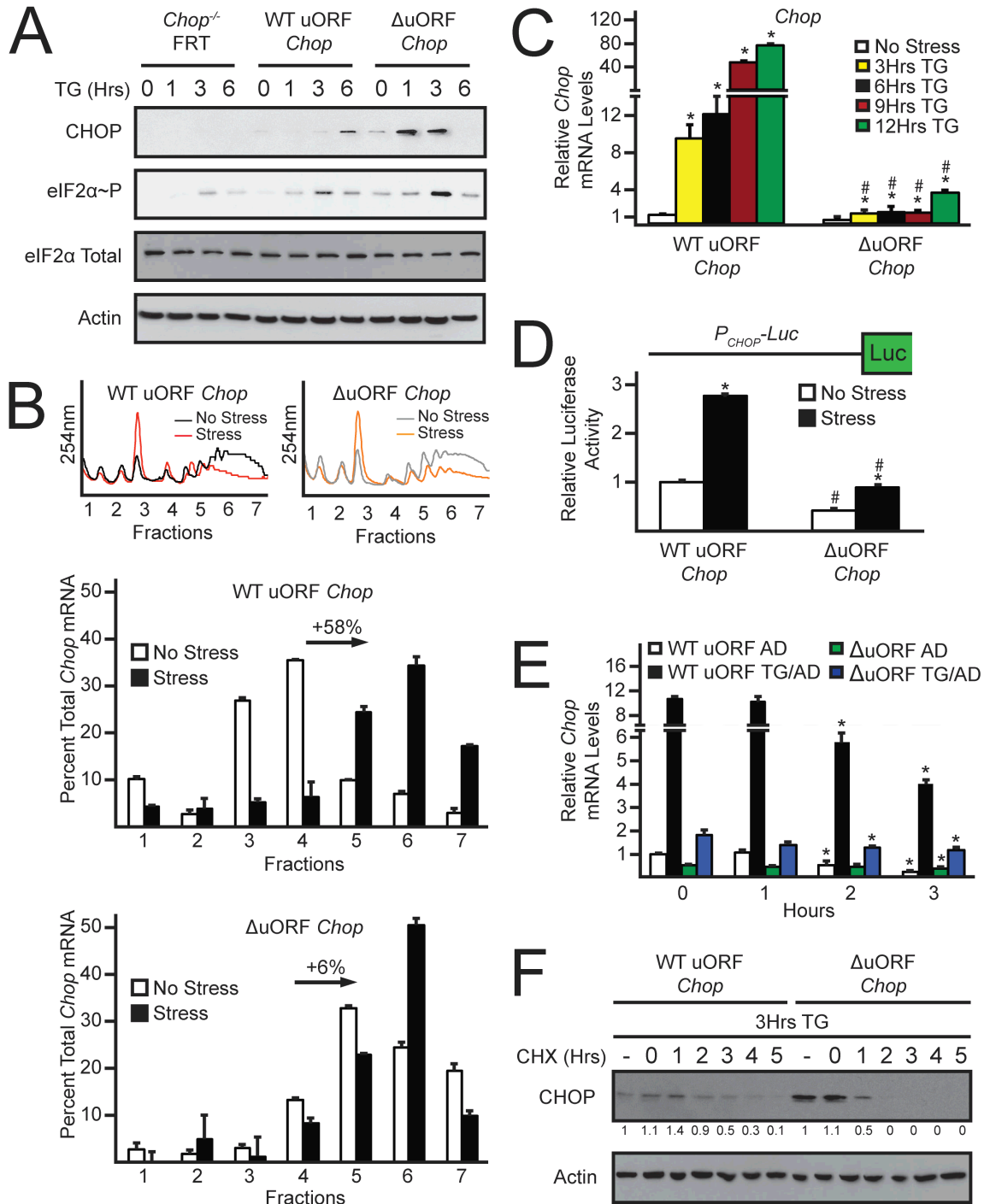


Figure 16. Alterations in *Chop* uORF translation control change the dynamics of *Chop* expression. A, MEF cells deleted for *Chop* were stably selected to express WT *Chop* (WT uORF *Chop*) and *Chop* with its uORF deleted (Δ uORF *Chop*) and treated with the ER stress agent, thapsigargin, for up to 6 hours or left untreated. The levels of

CHOP, eIF2 α -P, eIF2 α total, and β -actin in these cultured cells were measured by immunoblot analyses. B, WT uORF *Chop* and Δ uORF *Chop* cells were treated with thapsigargin for 6 hours or left untreated. Lysates were collected and layered on top of 10-50% sucrose gradients, followed by ultracentrifugation, and analysis of whole-lysate polysome profiles at 254 nm. Sucrose gradients were fractionated simultaneous to analysis of polysome profiles at 254 nm. Total RNA was isolated from sucrose fractions and the percentage of total *Chop* mRNA was determined by qRT-PCR. Panel B is representative of three independent biological experiments. C, Total RNA was collected from WT uORF *Chop* and Δ uORF *Chop* cells cultured in the presence or absence of thapsigargin and relative levels of *Chop* mRNA were measured by qRT-PCR. D, Fusion of 1-kb of the *Chop* promoter (P_{CHOP} -Luc) and a *Renilla* luciferase reporter were co-transfected into MEF cells, treated for 6 hours or left untreated, and measured using a Dual-Luciferase assay. Relative values are represented as histograms and the S.D. is indicated. E, Total RNA was collected from WT uORF *Chop* and Δ uORF *Chop* cells cultured in the presence or absence of thapsigargin for 3 hours followed by 0, 1, 2, or 3 hours of treatment with actinomycin D. Relative levels of *Chop* mRNA were measured by qRT-PCR. F, WT uORF *Chop* and Δ uORF *Chop* cells were treated with thapsigargin for 3 hours, washed and lysed (CHX -) or washed and treated with cycloheximide for up to 5 hours (CHX 0, 1, 2, 3, 4, 5). Levels of CHOP and β -actin in the cultured cells were measured by immunoblot analyses. Quantification of changes in CHOP protein expression are depicted under the CHOP immunoblot panel and are normalized to the no cycloheximide treatment for both WT uORF *Chop* and Δ uORF *Chop* cells.

4.4 Alterations in *Chop* uORF translation control affect cell viability

CHOP regulates the transcription of multiple genes controlling apoptosis via CHOP homodimerization and heterodimerization with additional factors (80,81). Two of the pro-apoptotic genes that are known to be transcriptionally upregulated through CHOP activity are *Atf5* and *Bim* (67,82). Analysis of *Atf5* and *Bim* mRNAs in both *Chop*^{-/-} and WT *Chop* FRT cell lines revealed that CHOP serves to enhance expression of these two genes in response to ER stress (Figure 17A). Of importance, basal and stress-induced levels of both *Atf5* and *Bim* mRNAs were sharply increased in the Δ uORF *Chop* cells, coincident with the enhanced CHOP protein expression (Figures 16A and 17A). These results suggest that disruption of *Chop* translation control results in a CHOP-dependent increase in *Atf5* and *Bim* transcripts that requires stress for maximal expression.

Next the consequences of the Δ uORF and enhanced CHOP protein levels on cell viability were determined. The WT and Δ uORF *Chop*-expressing cells were treated with thapsigargin or tunicamycin for up to 12 hours and MTT activity was measured. Tunicamycin blocks N-glycosylation and is also a potent inducer of ER stress. In both ER stress conditions, Δ uORF *Chop* cells presented with decreased MTT activity compared to the cells expressing WT uORF *Chop* (Figure 17B). There was a 15% decrease in MTT activity in *Chop* Δ uORF cells after 18 hours of treatment with thapsigargin and nearly 20% lowered MTT activity in response to tunicamycin. Caspase 3/7 activity was also significantly increased in the Δ uORF cells following up to 24 hours exposure to thapsigargin (Figure 17C), suggesting that increased apoptosis occurs in response to ER stress with the sharply enhanced CHOP protein levels. Collectively, these results suggest that disruption of *Chop* uORF-mediated translation regulation decreases cell viability upon exposure to ER stress.

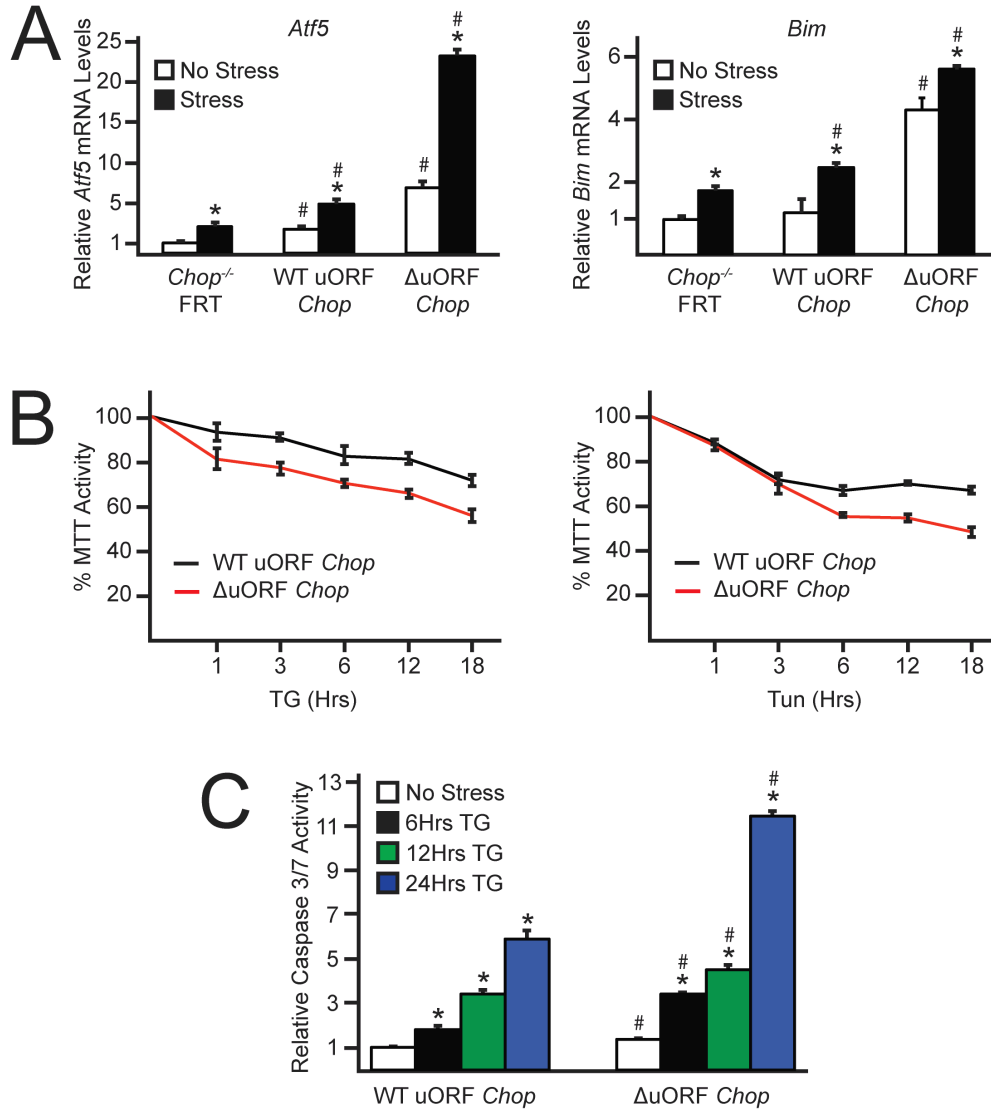


Figure 17. Alterations in *Chop* uORF translation control lower cell viability during stress. A, Total RNA was collected from WT uORF *Chop* and Δ uORF *Chop* cells cultured in the presence or absence of thapsigargin. Relative levels of *Atf5* and *Bim* mRNAs were measured in the cultured cells by qRT-PCR. B, Equal numbers of WT uORF *Chop* and Δ uORF *Chop* cells were seeded in 96-well plates, cultured for 24 hours, followed by treatment with thapsigargin or tunicamycin, as indicated, for up to an additional 18 hours. MTT activity was measured by conversion of tetrazolium to formazan. C, Equal numbers of WT uORF *Chop* and Δ uORF *Chop* cells were seeded in 96-well plates, cultured for 24 hours, followed by treatment with or without thapsigargin

for up to an additional 24 hours. Caspase 3/7 activity was measured by cleavage of a proluminescent caspase-3/7 DEVD-aminoluciferin substrate.

CHAPTER 5. RESULTS: TRANSLATION REGULATION OF THE GLUTAMYL-PROLYL tRNA SYNTHETASE GENE *EPRS* THROUGH BYPASS OF μ ORFS WITH NON-CANONICAL INITIATION CODONS

5.1 *Eprs* expression is increased in response to $eIF2\alpha\sim P$ through enhanced translation

The glutamyl-prolyl-tRNA synthetase gene *Eprs* was previously identified in a genome-wide analysis of changes in translation as a transcript that has enhanced expression in response to $eIF2\alpha\sim P$ (5). To further explore the role that $eIF2\alpha\sim P$ and translation control play in the expression of *Eprs*, WT MEF cells were treated with thapsigargin and analyzed for changes in translation by sucrose gradient ultracentrifugation. Polysome profiles of cells subjected to ER stress indicated reduced global translation initiation as ascertained by a decrease in heavy polysomes coincident with increased monosomes (Figure 18A). *Eprs* and *Atf4*, a transcript known to be subject to preferential translation (13), were measured for changes in translation by qPCR analysis of polysome fractions. Both *Eprs* and *Atf4* transcripts were predominantly associated with monosomes and light polysomes in the absence of stress. However, upon ER stress induction, *Eprs* and *Atf4* mRNAs significantly shifted to association with heavy polysomes (Figure 18A). These results suggest that *Eprs* is preferentially translated in response to ER stress.

To determine the role that $eIF2\alpha\sim P$ plays in the expression of *Eprs*, changes in EPRS protein levels were measured in WT MEF cells and mutant A/A MEF cells. As expected, $eIF2\alpha\sim P$ was detectable only in WT cells treated with thapsigargin. EPRS protein expression was increased 3-fold by 6 hours of thapsigargin treatment in WT MEFs, whereas A/A MEFs presented with reduced and delayed induction in EPRS expression (Figure 18B). *Eprs* mRNA expression did not significantly change in

response to ER stress (Figure 18C), suggesting that *Eprs* is not subject to transcriptional regulation, but is preferentially translated upon ER stress and eIF2 α ~P.

5.2 Preferential translation of *Eprs* features two uORFs with non-canonical initiation codons

The advent of ribosome profiling has resulted in the genome-wide identification of previously uncharacterized translation initiation sites including those for amino-terminal protein extensions, protein truncations, and uORFs with non-canonical (non-AUG) initiation codons (4,6,83). Intriguingly, the 5'-leader of *Eprs* contains three putative uORFs with five non-canonical initiation codons, two of which have been identified in ribosome profiling studies as functional initiation codons (Figure 18D) (6).

Multiple mechanisms of preferential translation rely on uORF mediated translation control (12,13,15). To determine the role of the 5'-leader of the *Eprs* mRNA in preferential translation of this tRNA synthetase, a 5'-RACE was conducted to define the transcriptional start site of the mouse *Eprs* gene (Figure 19A). A cDNA segment encoding the 155-nucleotide *Eprs* 5'-leader was cloned in between a minimal TK-promoter and the firefly luciferase CDS, producing *P_{TK}-Eprs-Luc*. This construct and the subsequent ones that follow feature in-frame replacement of the firefly luciferase initiation codon with the initiation codon of the *Eprs* CDS. Luciferase activity from *P_{TK}-Eprs-Luc* was induced 2-fold in WT MEF cells treated with thapsigargin compared to minimal induction in A/A cells (Figure 19B). In both these and the following reporter measurements, there was no significant change in *Eprs-Luc* mRNA levels, suggesting that the changes in luciferase activity are the result of translation control. These results suggest that the *Eprs* 5'-leader is sufficient to direct preferential translation of *Eprs* in response to eIF2 α ~P.

To determine which, if any, of the five non-canonical initiation codons can serve as functional sites of translation initiation, in-frame fusions of each uORF with the firefly luciferase CDS were constructed. These constructs featured deletion of the luciferase AUG, ensuring that any measurable luciferase activity was the product of translation initiation at the in-frame uORF. Fusion of the first uORF resulted in the in-frame fusion of three CUG initiation codons, here denoted CUG1, 2, and 3. Fusion of uORF1 with the firefly luciferase CDS had measurable luciferase activity, indicative of at least one functional initiation codon (Figure 20). Individual deletion of CUG1 and CUG3 each resulted in slight decrease in luciferase activity, whereas deletion of CUG2 resulted in a 75% decrease in luciferase activity. This finding indicates that while all three CUGs can serve as functional initiation codons, CUG2 is the dominant site of translation initiation in uORF1. Optimization of CUG2 to an AUG with strong Kozak context (ACCAUGG) resulted in a 24-fold increase in luciferase activity as compared to fusion of uORF1 with all three CUG initiation codons intact. Together, these results indicate that CUG2 is the dominant initiation codon in uORF1 and that optimization of CUG2 to an AUG with strong Kozak context can further facilitate translation initiation at this site.

Fusion of the second uORF that contains a UUG initiation codon resulted in a 1.5-fold increase in luciferase activity as compared to fusion of uORF1 (Figure 20). Deletion of the UUG initiation codon, denoted UUG1, by mutating it to AAA resulted in no appreciable luciferase activity due to the lack of any additional initiation codons in the uORF2 fusion. Mutation of the UUG1 initiation codon to an AUG in optimal context (ACCAUGG) resulted in nearly a 14-fold increase in luciferase activity as compared to the WT UUG1 fusion. These results suggest that UUG1 serves as the functional site of translation initiation in uORF2 and that translation initiation at this site can be further increased with the introduction of an AUG initiation codon in Kozak context.

Fusion of the third uORF also with a UUG initiation codon, denoted UUG2, did not result in any appreciable luciferase activity (Figure 20). Furthermore, deletion of UUG2 by mutation to AAA did not result in any change in luciferase activity, indicating that there are no functional initiation sites in the uORF3 fusion. Consistent with a previous ribosome profiling study, these combined results suggest that CUG2 and UUG1 can both serve as functional sites of translation initiation in the *Eprs* 5'-leader (Figure 18D) (6) and that the 5'-leader of *Eprs* mRNA can direct *Eprs* preferential translation in response to eIF2 α ~P.

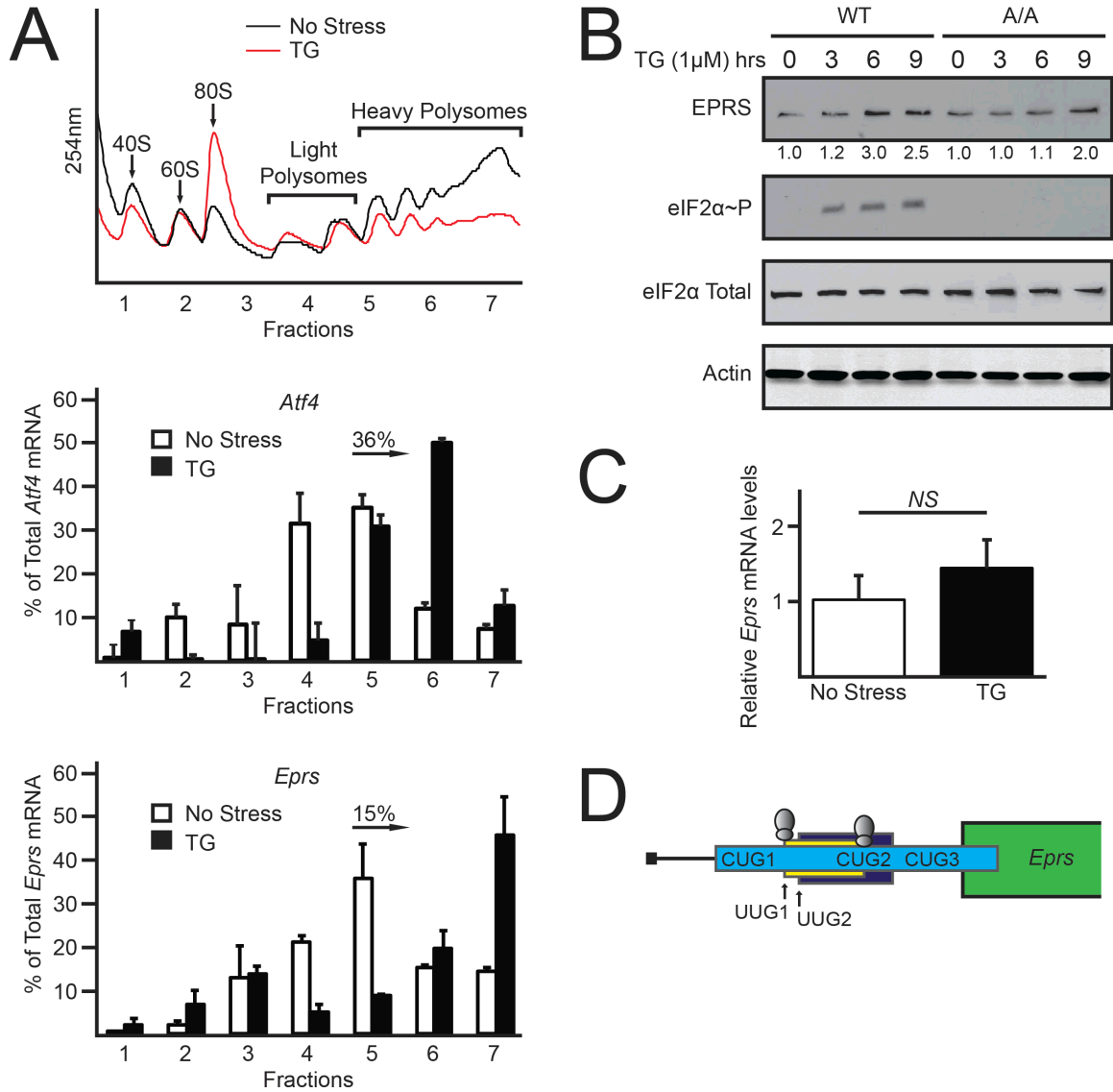


Figure 18. *Eprs* translational expression is increased in response to eIF2 α -P. A, WT MEF cells were treated with thapsigargin for 6 hours or left untreated. Lysates were collected separated by sucrose gradient centrifugation, followed by analysis of polysome profiles at 254 nm. Total RNA was isolated from sucrose fractions and the percentage of total *Atf4* and *Eprs* mRNA was determined by qRT-PCR. Profiles and *Atf4* and *Eprs* mRNA polysome shifts are representative of at least three independent biological experiments. B, WT and A/A MEF cells were treated with thapsigargin for up to 9 hours, or left untreated. Protein lysates were processed and levels of EPRS, eIF2 α -P, eIF2 α

total, and β -actin were measured by immunoblot. C, Total RNA was collected from WT and A/A MEF cells treated with thapsigargin for 6 hours or left untreated and relative levels of *Eprs* mRNA were measured using qRT-PCR. D, Representation of *Eprs* 5'-leader. The uORFs in the 5'-end of the *Eprs* mRNA are illustrated by the colored boxes, with the initiation codon(s) for each uORF listed. The green box indicates the CDS for *Eprs*. Ribosomes above UUG1 and CUG2 indicate those start codons that have been suggested to facilitate translation initiation in previous ribosome profiling studies (6,83).

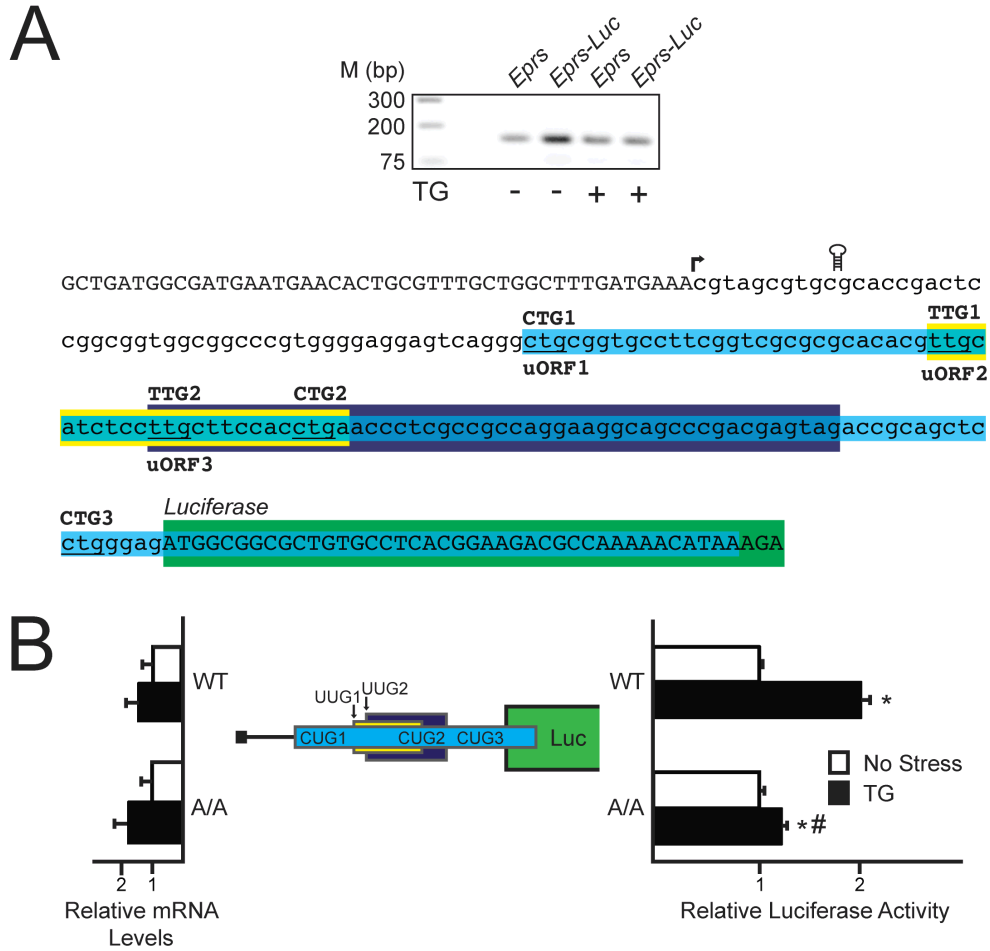


Figure 19. The 5'-leader of the *Eprs* mRNA directs preferential translation. A, top panel, A 5'-RACE was conducted for *Eprs* using WT MEFs treated with thapsigargin for 6 hours or left untreated. Total RNA and cDNA was prepared and DNA products were separated by gel electrophoresis, with markers for the indicated base pair sizes listed on the left. A, bottom panel, Nucleotide representation of the *Eprs* 5'-leader in lowercase letters, with upper case letters representing the 5'-linker added during the 5'-RACE procedure and the beginning of the CDS of the *Eprs-Luc* fusion. Colored boxes represent the *Eprs* uORFs, with uORF1 in blue, uORF2 in yellow, and uORF3 in purple. Start codons for each uORF are indicated above the colored boxes. The coding region of the *Eprs-Luc* fusion is illustrated by the green box. The transcription start site is indicated with an arrow, and the location of the stem loop insertion is illustrated. B, The

P_{TK}-Eprs-Luc construct and a *Renilla* luciferase reporter were co-transfected into WT or A/A MEFs and treated with thapsigargin for 6 hours or left untreated. Translational control involving the 5'-leader of *Eprs* mRNA was measured via Dual-Luciferase assay and corresponding *Eprs-Luc* mRNA was measured by qRT-PCR. The *P_{TK}-Eprs-Luc* construct contains the cDNA sequence corresponding to the *Eprs* 5'-leader fused to the luciferase reporter gene, with both the *Eprs* uORFs and the CDS of the *Eprs-Luc* fusion indicated by colored boxes that are the analogues to those indicated in Figure 19A.

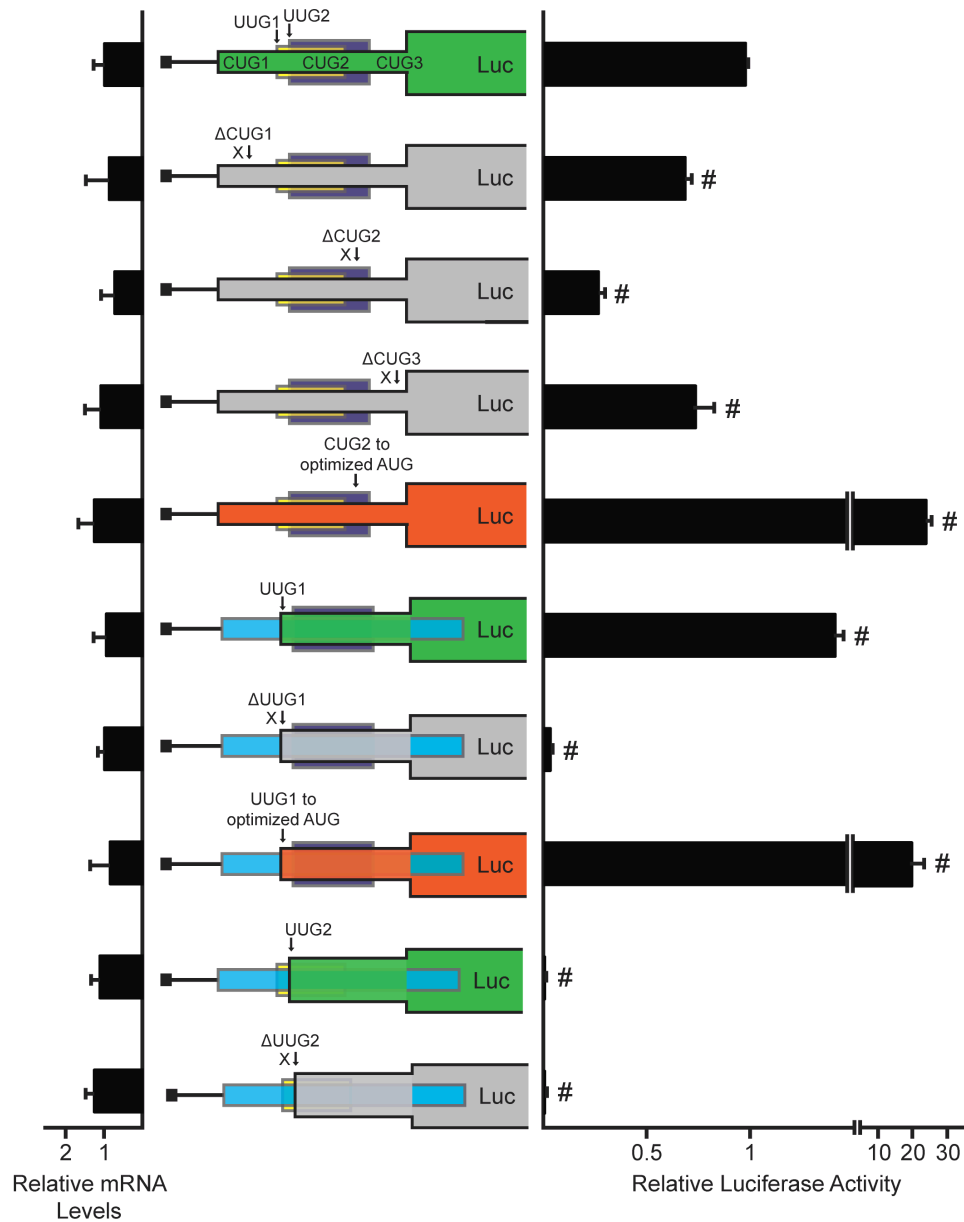


Figure 20. Preferential translation of *Eprs* features two uORFs with non-canonical initiation codons. The full-length *Eprs* uORFs were each individually fused in-frame to the luciferase CDS and were transcriptionally expressed from a TK-promoter for generation of P_{TK} -CUG123 uORF-Luc, P_{TK} -UUG1 uORF-Luc, and P_{TK} -UUG2 uORF-Luc. WT and mutant versions of the uORF-Luc fusions were transfected into WT MEF cells and uORF translation control was measured by Dual-Luciferase assay and

corresponding *CUG123 uORF-Luc*, *UUG1 uORF-Luc*, and *UUG2 uORF-Luc* mRNA levels were measured by qRT-PCR. WT versions of each luciferase fusion are illustrated by the green boxes. Mutant versions of *P_{TK}-CUG123 uORF-Luc* include mutations of the CUG initiation codons, as represented by Δ CUG1, Δ CUG2, and Δ CUG3, and optimization of the start codon for CUG2 to an AUG in strong Kozak consensus sequence (ACCAAUGG), as represented by CUG2 to optimized AUG. Mutant versions of *P_{TK}-UUG1 uORF-Luc* include mutation of the UUG initiation codon, as represented by Δ UUG1, and optimization of the UUG start codon to an AUG in strong Kozak consensus sequence (ACCAAUGG), as represented by UUG1 to optimized AUG. Mutation of *P_{TK}-UUG2 uORF-Luc* includes mutation of the UUG initiation codon, as represented by Δ UUG2. Loss of the indicated initiation codon in the *uORF-Luc* fusion is illustrated by the gray boxes, and the optimized initiation codon in the *uORF-Luc* fusion is illustrated in orange. Relative values are represented as histograms for each with the S.D. indicated.

5.3 *Eprs* translational control involves bypass of two uORFs with non-canonical initiation codons

To determine if preferential translation of *Eprs* occurs through ribosome scanning, a stem loop structure with a predicted free energy of $\Delta G = -41$ kcal/mol was inserted 10 nucleotides downstream of the 5' cap of the *Eprs-Luc* transcript (Figure 19A and 21 construct 2). Introduction of this palindromic sequence to the *Eprs-Luc* mRNA significantly reduced luciferase activity independent of stress, suggesting that *Eprs* preferential translation is mediated by ribosome scanning beginning from the 5'-end of the *Eprs* transcript.

Ribosomes scanning the *Eprs* mRNA would encounter the three uORFs located in the *Eprs* 5'-leader (Figure 19A). To determine the contribution of each uORF and non-canonical initiation codon to the preferential translation of the *Eprs* CDS, the three CUG initiation codons located in uORF1 were mutated to AAA, as indicated by Δ CUG in the figure (Figure 21). Deletion of CUG1 and CUG3 individually resulted in no significant difference in basal luciferase activity and were induced 2-fold with ER stress treatment, a similar result as the WT P_{TK} -*Eprs-Luc* construct (Figure 21, constructs 1, 3, and 5). Combined deletion of CUG1 and CUG3 resulted in a slight increase in luciferase activity both basally and with ER stress treatment (Figure 21, construct 6). This result is consistent with the observation that CUG1 and CUG3 incur low amounts of translation initiation (Figure 20) and serve as mild dampeners of downstream translation. Deletion of CUG2, however, resulted in an almost 2.5-fold increase in basal luciferase activity that was stress inducible (Figure 21, construct 4). Furthermore, deletion of all three CUGs resulted in similar luciferase activity as deletion of CUG2 alone, supporting the role of CUG2 as the dominant regulatory initiation codon in uORF1 (Figure 21, constructs 4 and 7).

Multiple preferentially translated mRNAs rely on ribosome bypass of uORFs with poor start codon context for optimal expression during cellular stress (12). To determine if non-canonical initiation codons function in a similar manner by allowing for ribosome bypass, CUG2 was next mutated to an AUG with the optimal Kozak consensus sequence (ACCAAUGG). Introduction of the optimized AUG reduced luciferase activity over 60% (Figure 21, construct 8). Since, uORF1 overlaps out-of-frame with the *Eprs* CDS, the observed decrease in luciferase activity after substitution of the AUG for CUG2 suggests that while CUG2 serves as the dominant site of initiation in uORF1, it can be bypassed, in part due to a non-canonical initiation codon, to facilitate translation at the downstream *Eprs* CDS.

To determine the contribution of the remaining two uORFs, the UUG initiation codon for uORF2 was next mutated to AAA, as indicated by Δ UUG1 (Figure 22, construct 2). Deletion of UUG1 resulted in lower basal luciferase activity as compared to WT *P_{TK}-Eprs-Luc* and a decreased induction ratio upon thapsigargin treatment, suggesting that UUG1 can act as a positive element that facilitates initiation at the downstream CDS. Deletion of the third uORF by substituting the UUG initiation codon for AAA, denoted Δ UUG2, resulted in no difference in luciferase activity as compared to the WT *P_{TK}-Eprs-Luc* construct (Figure 22, constructs 1 and 3). This finding is consistent with the low levels of luciferase activity observed for the UUG2 in-frame fusion (Figure 20), and indicates that the uORF3 does not serve a regulatory role in *Eprs* translation.

To further dissect the role of uORF2 in *Eprs* translation control, the UUG initiation codon was mutated to an AUG in optimal context, as indicated by UUG1 to optimized AUG in the figure (Figure 22, construct 4). Mutation of UUG1 to an optimized AUG resulted in a decrease in both the basal luciferase activity and the luciferase induction

ratio upon ER stress treatment. This result suggests that the ability of uORF2 to allow for initiation at the downstream CDS relies upon its non-canonical UUG initiation codon.

In addition to bypass of uORFs, downstream translation initiation can also be regulated by ribosome reinitiation (13,15,19). To determine the contribution of ribosome reinitiation after uORF2 translation, the uORF2 stop codon was mutated from TGA to TGG to generate an overlapping out-of-frame uORF. Mutation of the uORF2 stop codon resulted in a 25% decrease in basal luciferase activity that was still induced 2-fold upon thapsigargin treatment. The basal reduction in luciferase activity suggests that after translation initiation at uORF2s UUG1 in the WT *P_{TK}-Eprs-Luc* construct, a certain amount of translating ribosomes terminate and later reinitiate at the *Eprs* CDS. UUG1 is 5' proximal to CUG2 and likely plays a positive-acting role in the *Eprs* translational control scheme by precluding a small number of scanning ribosomes from initiating translation at the inhibitory, overlapping out-of-frame CUG2. Instead UUG1 would allow for a measurable amount of ribosome reinitiation 3' to the predominant CUG2 initiation codon in the uORF1. Combined mutation of UUG1 to an optimized AUG with the TGA stop codon substituted for TGG resulted in a further decrease in basal luciferase activity that was only induced 1.7-fold upon stress treatment. Overall, these results suggest that while a portion of the ribosomes that translate uORF2 can reinitiate downstream, scanning ribosomes also bypass uORF2 due to its non-canonical UUG1 initiation codon and initiate translation at the downstream CDS.

As CUG2 and UUG1 are suggested to be the dominant initiation codons for uORF1 and uORF2, respectively, in the *Eprs* 5'-leader, their combined deletion was generated by mutating each initiation codon to AAA (Figure 22, construct 7). Combined deletion of both UUG1 and CUG2 resulted in 5-fold increase in luciferase activity independent of stress, further supporting the roles of UUG1 and CUG2 as overall

repressing elements in *Eprs* translation control. A model for *Eprs* translation control and its broader medical implications will be expanded upon in the Discussion.

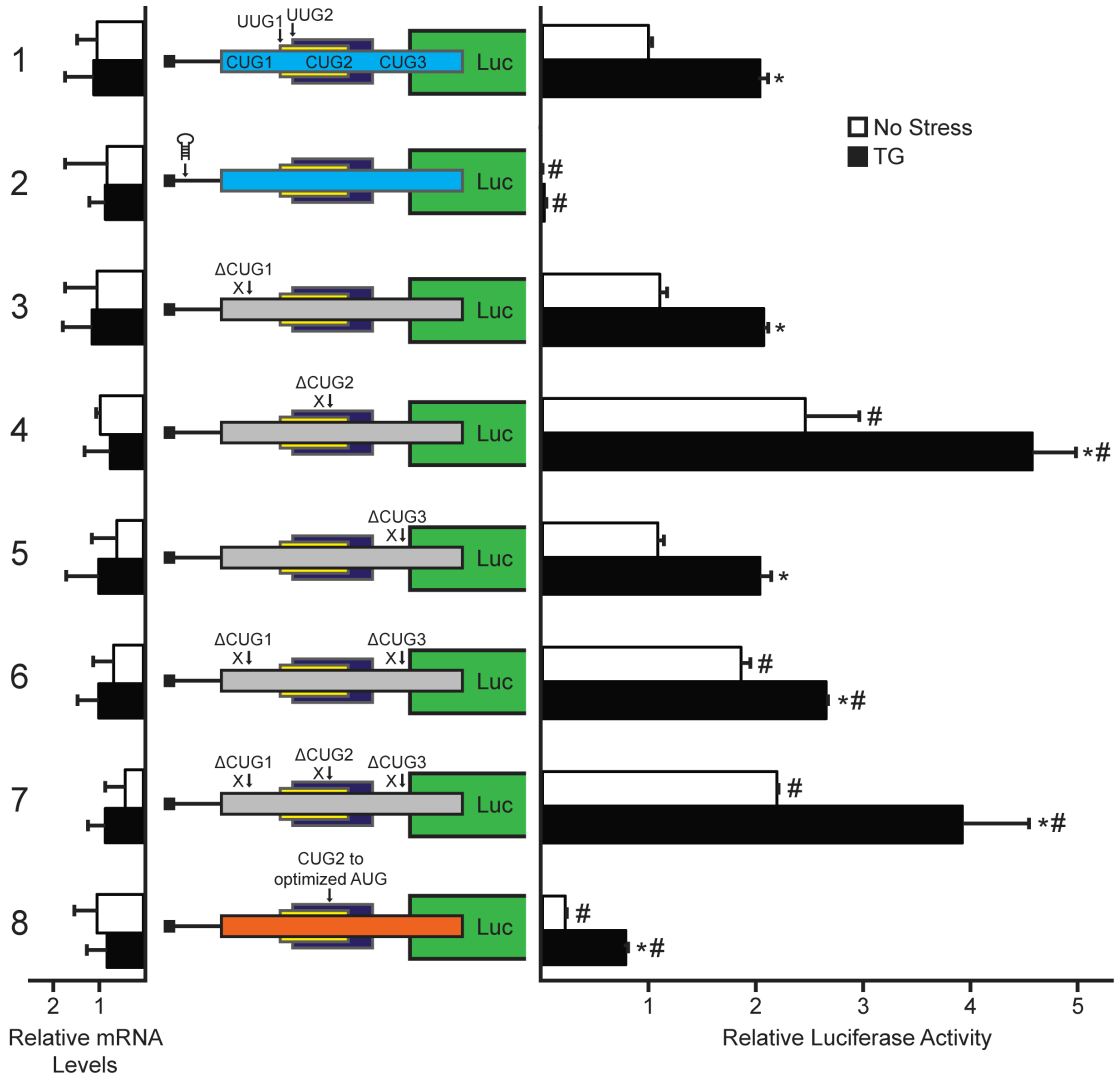


Figure 21. *Eprs* translation control involves bypass of an uORF with a non-canonical CUG initiation codon. WT and mutant versions of P_{TK} -*Eprs-Luc* constructs were transfected into WT MEF cells, treated for 6 hours or left untreated, and measured using a Dual-Luciferase assay and relative levels of the corresponding *Eprs-Luc* mRNAs were measured by qRT-PCR. Mutant versions of P_{TK} -*Eprs-Luc* include a stem loop insertion and mutation of the CUG initiation codons individually or together, as represented by Δ CUG1, Δ CUG2, and Δ CUG3. Loss of the initiation codons CUG1, CUG2, and CUG3, are indicated in the *Eprs-Luc* fusion that is indicated by the gray boxes. Optimization of the CUG2 initiation codon to an AUG in optimal Kozak

consensus sequence (ACCAAUGG) is represented as CUG to optimized AUG (orange box). Relative values are represented as histograms for each with the S.D. indicated.

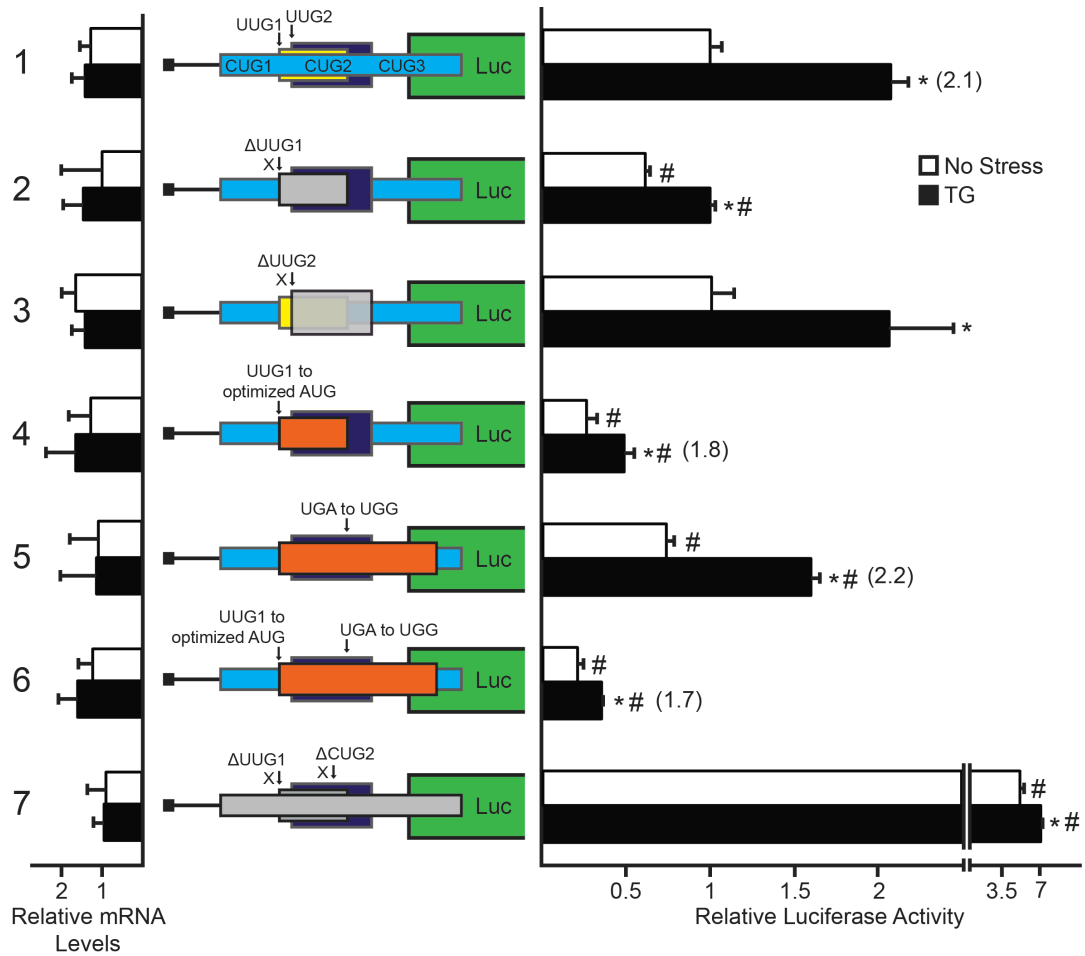


Figure 22. *Eprs* translational control involves bypass of uORFs with non-canonical initiation codons. WT and mutant versions of P_{TK} -*Eprs*-Luc constructs were transfected into WT MEF cells, treated for 6 hours or left untreated, and measured using a Dual-Luciferase assay and corresponding *Eprs*-Luc mRNA levels were measured by qRT-PCR. Mutant versions of P_{TK} -*Eprs*-Luc include mutation of the UUG1 and UUG2 initiation codons (Δ UUG1 and Δ UUG2), optimization of the UUG1 initiation codon to an AUG with optimal Kozak consensus sequence (UUG1 to optimized AUG), mutation of the stop codon of the UUG1 uORF to generate an overlapping out-of-frame uORF (UGA to UGG), combined mutation of UUG1 to an AUG with optimal Kozak consensus sequence (ACCAUGG) with the stop codon mutation (UUG1 to optimized AUG and UGA to UGG), and combined mutation of the initiation codons for UUG1 and CUG2 (Δ UUG1

and Δ CUG2). Loss of the indicated initiation codon in the *Eprs-Luc* fusion is illustrated by the gray boxes, and those involving optimization of the initiation codon or extension of the uORF are indicated by orange boxes. Relative values are represented as histograms for each with the S.D. indicated.

5.4 Translation control of *Eprs* during treatment with the drug halofuginone

Halofuginone, a drug currently in phase II clinical trials for the treatment of fibrotic disease and solid tumors (identified: NCT00064142), was shown to confer surgical stress resistance in an animal model by a mechanism requiring the eIF2 α kinase GCN2 (84). Halofuginone competes with proline for the active site of EPRS, leading to an accumulation of uncharged tRNA^{Pro} and activation of the GCN2/eIF2 α ~P pathway (84-86). Dietary restriction has been associated with an improved clinical outcome prior to an ischemic event in both animal and clinical models. The pharmacological induction of the GCN2/eIF2 α ~P pathway by halofuginone offers the exciting potential of conferring pre-surgical stress resistance using a pharmaceutical. Our results indicate that *Eprs* mRNA is preferentially associated with heavy polysomes upon ER stress and that the 5'-leader of the *Eprs* gene transcript confers translational control in luciferase reporter constructs, suggesting preferential translation of *Eprs* in response to eIF2 α ~P. As a result, halofuginone treatment is proposed to lead to the enhanced expression of its target substrate EPRS. To first examine the impact of halofuginone treatment on eIF2 α ~P and *Eprs* expression, WT and *Gcn2*^{-/-} MEF cells were treated with increasing concentrations of halofuginone for 6 hours (Figure 23A). As expected, eIF2 α ~P was detectable only in WT cells treated with halofuginone. Levels of EPRS protein increased in a dose-dependent manner with halofuginone treatment in WT MEFs, whereas *Gcn2*^{-/-} MEFs displayed minimal induction in EPRS expression.

To determine the outcome of increased eIF2 α ~P with halofuginone treatment on global translation initiation, WT MEF cells were treated with halofuginone for 6 hours or left untreated. Halofuginone treatment substantially reduced heavy polysomes with an accumulation of the 80S monosome peak, indicative of an eIF2 α ~P induced defect in global translation initiation (Figure 23B). The biological implication of this during preconditioning is that, upon ischemic reperfusion, halofuginone would induce eIF2 α ~P

providing the benefits of target UPR genes important for stress remediation. Coincident with the induction of the UPR, the increase in EPRS protein levels would quickly alleviate the toxicity associated with the drug treatment.

To further address if *Eprs* mRNA is subject to translational control during halofuginone treatment, WT and A/A MEF cells were transfected with the P_{TK} -*Eprs*-Luc reporter followed by either halofuginone treatment or no treatment. Both cell types were also treated with thapsigargin as a positive control for preferential translation of *Eprs* during eIF2 α ~P. In the WT MEF cells, both halofuginone and thapsigargin treatment resulted in a 2.5 fold induction of EPRS-Luc expression (Figure 23C). Importantly, this increase in *Eprs*-Luc mRNA translation was absent in the alanine mutant (Figure 23C). This finding indicates that translation of *Eprs* is enhanced in response to different stress conditions, including that triggered by halofuginone.

To examine the role of the ISR on cell fate, WT and *Gcn2*^{-/-} MEF cells were treated with increasing doses of halofuginone for 6 hours, and then allowed the cells to recover for 18 hours in fresh media prior to measuring viability. From this analysis, a sharp decrease in viability in the *Gcn2*^{-/-} cells was observed compared to their WT counterparts. This difference was most notable at the 12.5 nM treatment, at which an over 20% decrease in viability is observed in the *Gcn2*^{-/-} cells compared to WT (Figure 24A). Collectively, these results suggest that GCN2 and *Eprs* translational control are paramount to cell survival during halofuginone treatment (Figure 24B).

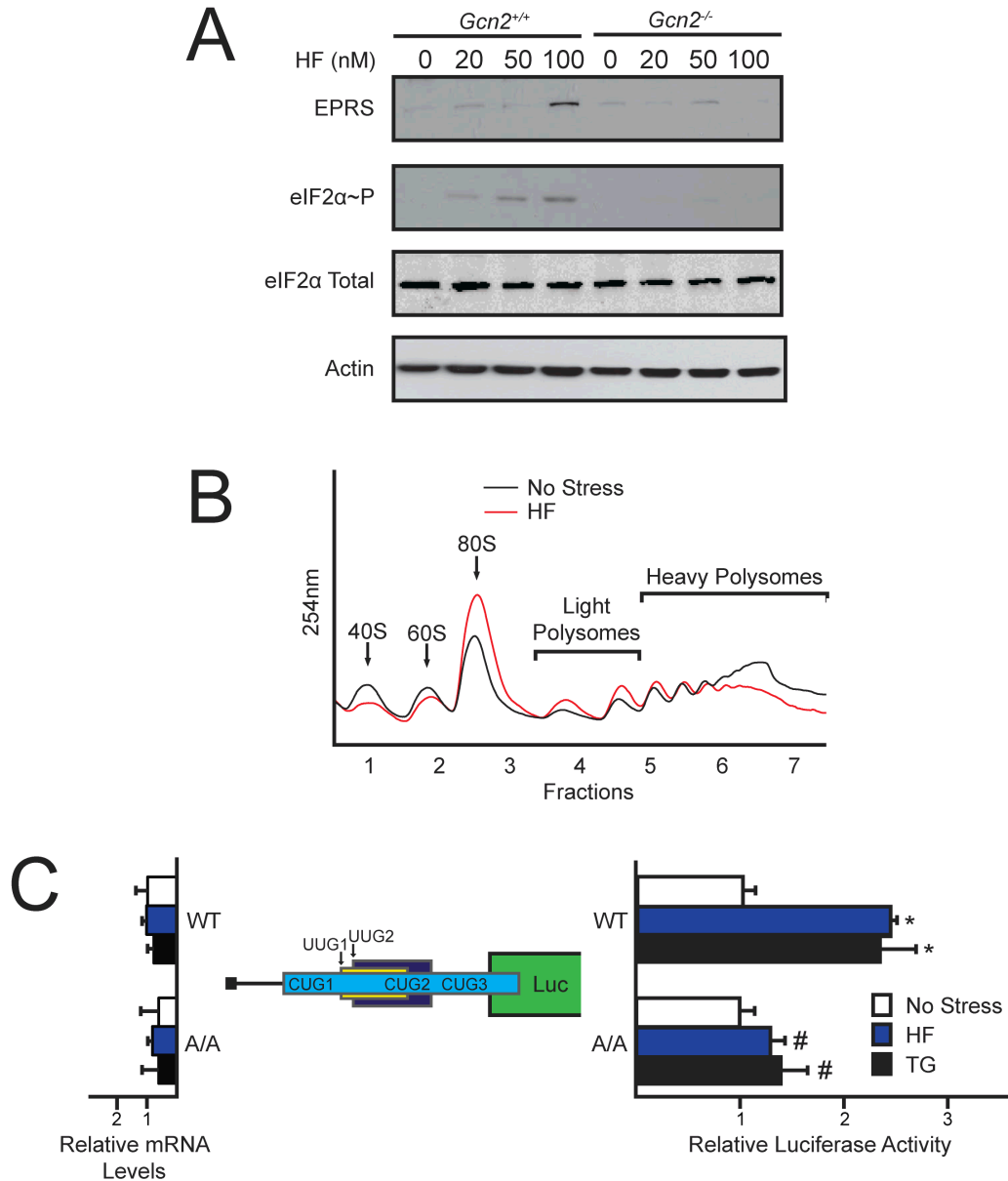


Figure 23. *Eprs* translation control is regulated in response to halofuginone treatment. A, *Gcn2*^{+/+} and *Gcn2*^{-/-} MEF cells were treated with increasing concentrations of halofuginone for 6 hours. Protein lysates were processed and levels of EPRS, eIF2α~P, eIF2α total, and β-actin were measured by immunoblot. B, WT MEF cells were treated with halofuginone for 6 hours or left untreated. Lysates were collected, sheared using a 23-gauge needle, and layered on to 10-50% sucrose gradients followed by ultracentrifugation and analysis of whole-lysate polysome profiles

at 254 nm. C, The P_{TK} -*Eprs-Luc* construct and a *Renilla* luciferase reporter were co-transfected into WT or A/A MEFs and treated with thapsigargin or halofuginone for 6 hours or left untreated. *Eprs* 5'-leader mediated translation control was measured via Dual-Luciferase assay and corresponding *Eprs-Luc* mRNA values were measured by qRT-PCR. Relative values are represented as histograms for each with the S.D. indicated.

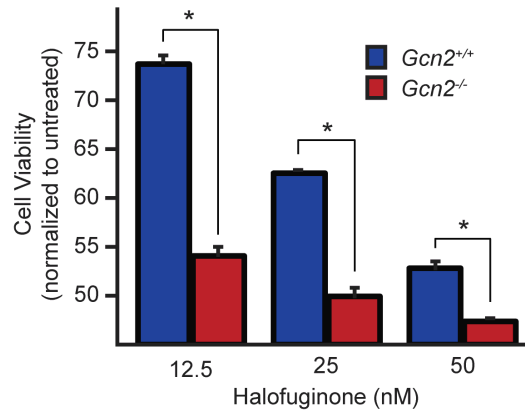


Figure 24. GCN2 confers protection against halofuginone-induced toxicity. Equal numbers of *Gcn2*^{+/+} and *Gcn2*^{-/-} MEFs were seeded in 96-well plates, cultured for 24 hours, and treated with 12.5, 25, or 50 nM halofuginone for 6 hours, followed by recovery in fresh media for 18 hours. MTT activity was measured by the conversion of tetrazolium to formazan.

CHAPTER 6. RESULTS: NMP4 IS A NOVEL REGULATOR OF RIBOSOME BIOGENESIS AND CONTROLS THE UNFOLDED PROTEIN RESPONSE VIA REPRESSION OF *Gadd34*

6.1 Loss of *Nmp4* in MSPCs results in increased expression of *Gadd34*

Many preferentially translated mRNAs are also transcriptionally induced in response to stress, ensuring the availability of mRNAs for enhanced translation. *Gadd34* mRNA, for instance, is induced in response to stress through a mechanism known to involve the direct binding and activity of ATF4 and CHOP (55,87,88). Interestingly, genome-wide analyses of zinc finger transcription factor NMP4 (ZNF384) binding in multiple cell lines, including preosteoblast MC3T3-E1, embryonic cell line ES-E14, B cell lymphoma Ch12, and erythroleukemia MEL cells suggest that NMP4 binds to specific regions in the *Gadd34* promoter and may serve as an additional regulator of *Gadd34* expression (62,65). The reported NMP4 binding site in the *Gadd34* promoter in MC3T3-E1 cells is illustrated in Figure 26A (62). To address the idea that NMP4 alters the transcriptional expression of *Gadd34*, qPCR was used to measure *Gadd34* mRNA in bone marrow, spleen, and liver from wild-type (WT) mice and those containing a whole body deletion of *Nmp4*. In either bone marrow or spleen, loss of *Nmp4* led to over a 2-fold induction in *Gadd34* mRNA, whereas there was a trend towards an increase, although not significant, in the *Nmp4*^{-/-} liver tissues (Figure 26B). These findings suggest that NMP4 can serve as a repressor of *Gadd34* mRNA expression.

Given the diversity of cell types in bone marrow and spleen, mesenchymal stem progenitor cells (MSPCs) were prepared from bone marrow from the WT and *Nmp4*-deleted mice and measured *Gadd34* mRNA in these cultured primary cells. Consistent with the bone marrow measurements, there was almost a 4-fold increase in *Gadd34* mRNA levels in the *Nmp4*-depleted cells compared to WT (Figure 26C). By comparison there was minimal differences between the WT and mutant MSPCs for the amount of

Crep (*Ppp1r15B*) mRNA (Figure 26C), which encodes a constitutively expressed targeting subunit for dephosphorylation of eIF2 α -P (72).

To determine if NMP4 serves to repress transcription of the *Gadd34* gene, luciferase reporter constructs with transcriptional expression directed by the *Gadd34* or *Crep* promoters were transfected into WT and *Nmp4*^{-/-} cells. There was over a 4-fold increase in *Gadd34* promoter activity in the MSPCs deleted for *Nmp4* compared to WT (Figure 26D). ATF4 is known to directly increase the transcriptional expression of the *Gadd34* gene in response to ER stress (55). In both WT and *Nmp4*^{-/-} cells, luciferase activity was sharply increased upon addition of tunicamycin. However, *Nmp4*-deleted cells showed the greatest extent of *Gadd34* promoter activity upon ER stress, with over a 6-fold increase compared to WT (Figure 26D). By comparison, luciferase expressed from the *Crep* promoter showed a 40% decrease in reporter activity compared to WT, and as expected *Crep* promoter activity was not significantly changed upon tunicamycin treatment.

Next GADD34 protein levels were measured in bone marrow, spleen, and liver from WT mice and MSPCs and their *Nmp4* knockout counterparts. Levels of GADD34 protein were increased in *Nmp4*^{-/-} tissues and MSPCs, with the most significant changes observed in bone marrow and MSPCs (Figure 26E). Elevated levels of GADD34 protein would be expected to lead to lowered levels of eIF2 α -P even in conditions not subject to overt stress, and this finding was confirmed in the immunoblot analyses (Figure 26E).

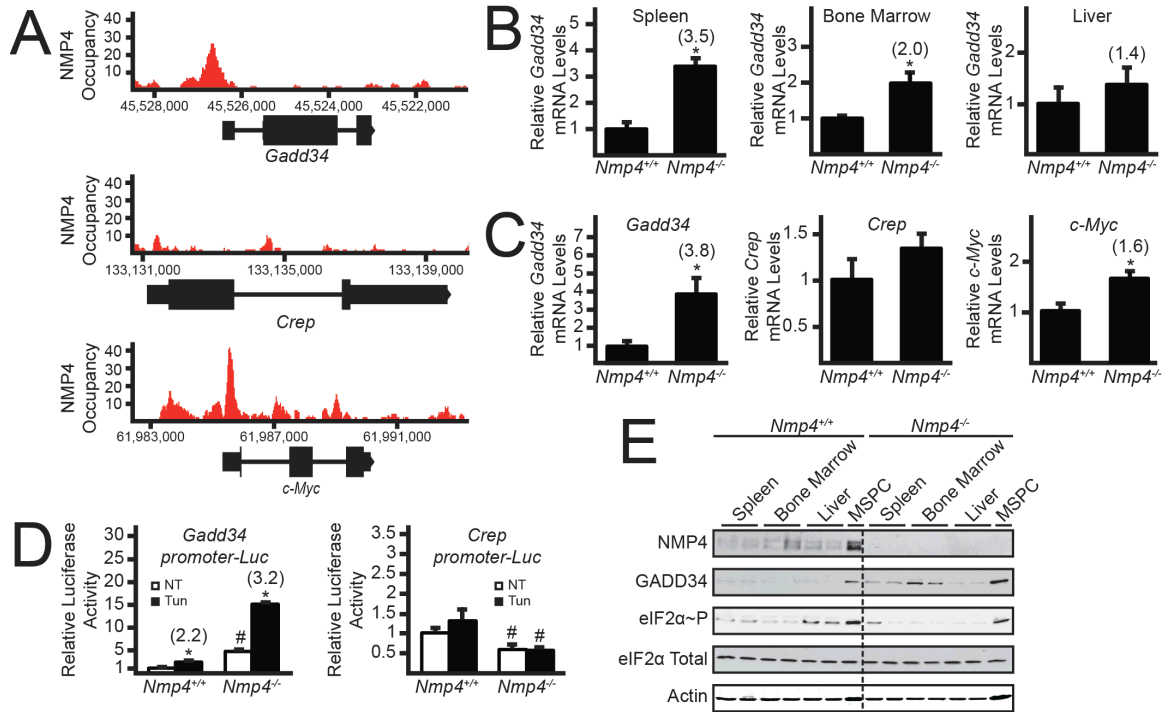


Figure 25. Expression of *Gadd34* is increased upon deletion of *Nmp4*. A, NMP4 occupancy on the genomic loci corresponding to sequences encoding *Gadd34*, *Crep*, and *c-Myc* genes that were reported in the genome-wide ChIP-Seq analysis (62). NMP4 occupancy (read count) is indicated on the y-axis. Boxes indicate exonic sequences encoding *Gadd34*, *Crep*, and *c-Myc* mRNAs and horizontal lines indicate intronic regions. B, Total RNA was collected from spleen, bone marrow, and liver tissues from *Nmp4*^{+/+} and *Nmp4*^{-/-} mice and relative levels of *Gadd34* mRNA were measured by qRT-PCR. C, Levels of *Gadd34*, *Crep*, and *c-Myc* mRNA were also measured in WT and *Nmp4*^{-/-} MSPCs. D, *Gadd34* and *Crep* transcriptional control was measured in WT or *Nmp4*^{-/-} MSPCs in the presence or absence of tunicamycin via Dual-Luciferase assay. E, The indicated proteins were measured in the indicated *Nmp4*^{+/+} and *Nmp4*^{-/-} tissues and MSPCs by immunoblot.

6.2 Loss of *Nmp4* in MSPCs increases protein synthesis

Phosphorylation of eIF2 α represses global translation by lowering the levels of eIF2-GTP available for delivery of aminoacylated initiator tRNA to ribosomes (16). Therefore elevated levels of GADD34 and the consequential reduction of eIF2 α -P would be predicted to enhance global protein synthesis. Lysates prepared from WT and *Nmp4*^{-/-} MSPCs were analyzed by sucrose gradient ultracentrifugation to visual the amounts of translated mRNAs in polysomes (Figure 27A). There was a sharp increase in heavy polysomes upon loss of *Nmp4* in the MSPCs, indicative of much higher levels of protein synthesis. Interestingly there was also an increase in free 40S and 60S ribosomal subunits, and monosomes in the *Nmp4*^{-/-} cells, suggesting that the enhanced translation was also accompanied by an increase the amount of ribosomes.

To test the idea that increased global translation in *Nmp4*^{-/-} cells is a consequence of elevated GADD34 activity, MSPCs were treated with salubrinal, a small molecule inhibitor of GADD34 and CReP-targeted dephosphorylation of eIF2 α -P (89). Treatment of the *Nmp4*-deleted cells led to a marked reduction in heavy polysomes, indicating that the inhibition of GADD34 and CReP lowered global protein synthesis (Figure 27B). By comparison, salubrinal did not appreciably change the polysome profile in WT MSPCs. In conjunction, levels of eIF2 α -P were measured in WT and *Nmp4*^{-/-} MSPCs left untreated, treated individually, or treated in combination with salubrinal or tunicamycin (Figure 27C). Levels of eIF2 α -P in the WT MSPCs remained largely unchanged with salubrinal treatment alone, but were increased with tunicamycin treatment that was further elevated with combined drug treatment. Measurement of eIF2 α -P was largely decreased in the *Nmp4*^{-/-} MSPCs due to increased *Gadd34* expression, however there was a modest increase in eIF2 α -P with either salubrinal or tunicamycin treatment alone that was further exacerbated with the combined drug treatment (quantified in Figure 27C legend). This indicates that elevated *Gadd34*

expression in the *Nmp4*^{-/-} MSPCs contributes to a portion of the observed increase in global protein synthesis.

6.3 Deletion of *Nmp4* in MSPCs increases ribosome biogenesis

Given that more ribosomes are suggested to be present in the *Nmp4*^{-/-} cells, sucrose gradient ultracentrifugation was carried out using lysates depleted for Mg²⁺, a condition that leads to release of ribosomes from mRNAs. There were significant increases in both free 40S and 60S ribosomal subunits in the *Nmp4*^{-/-} cells compared to WT (Figure 27D). Equal amounts of total RNA as determined by absorbance at 260 nm were applied to the sucrose gradients, and it is of note that there was consistently more RNA in the MSPCs deleted for *Nmp4* compared to equal numbers of WT cells. This key finding was confirmed by purifying and measuring total RNA and DNA from equal numbers of the MSPCs. While there were similar amounts of DNA between the *Nmp4*^{-/-} and WT cells, there was 2-fold more total RNA in the *Nmp4*-deleted cells compared to WT (Figure 27E). The majority of total RNA in cells consists of rRNA, and these results support the idea that there is increased ribosome biogenesis in the MSPCs upon deletion of *Nmp4*.

The following experiments were designed to understand the underlying basis for increased ribosomes in the MSPCs deleted for *Nmp4*. mTORC1 and c-MYC are potent inducers of ribosome biogenesis (90,91), and prior ChIP-Seq analyses indicated that NMP4 can bind to the promoter of the *c-Myc* gene (Figure 26A) (62). There were increased levels of *c-Myc* mRNA in the *Nmp4*^{-/-} cells as compared to WT (Figure 26C). Furthermore, there were elevated c-MYC protein levels in the *Nmp4*^{-/-} cells, whereas levels of phosphorylated S6, a measure of mTORC1 activity, were similar between the *Nmp4*-depleted cells and WT (Figure 28B). Of note is that total S6 protein levels were significantly increased in the *Nmp4*^{-/-} cells, consistent with increased ribosome

biogenesis. These results suggest that increased expression of *c-Myc* in the MSPCs deleted for *Nmp4* is an underlying reason for increased ribosomes. To address this idea, qRT-PCR was used to measure expression levels of c-MYC target genes in WT and *Nmp4*-deleted MSPCs. Consistent with the measurements of increased 40S and 60S ribosomal subunits, there was a 1.6-fold increase in expression of 45S rRNA and *Rpl11* mRNA and a 2-fold increase in *Rps6* mRNA. These results support that idea that ribosome biogenesis is increased in MSPCs deleted for *Nmp4* by a mechanism involving c-MYC.

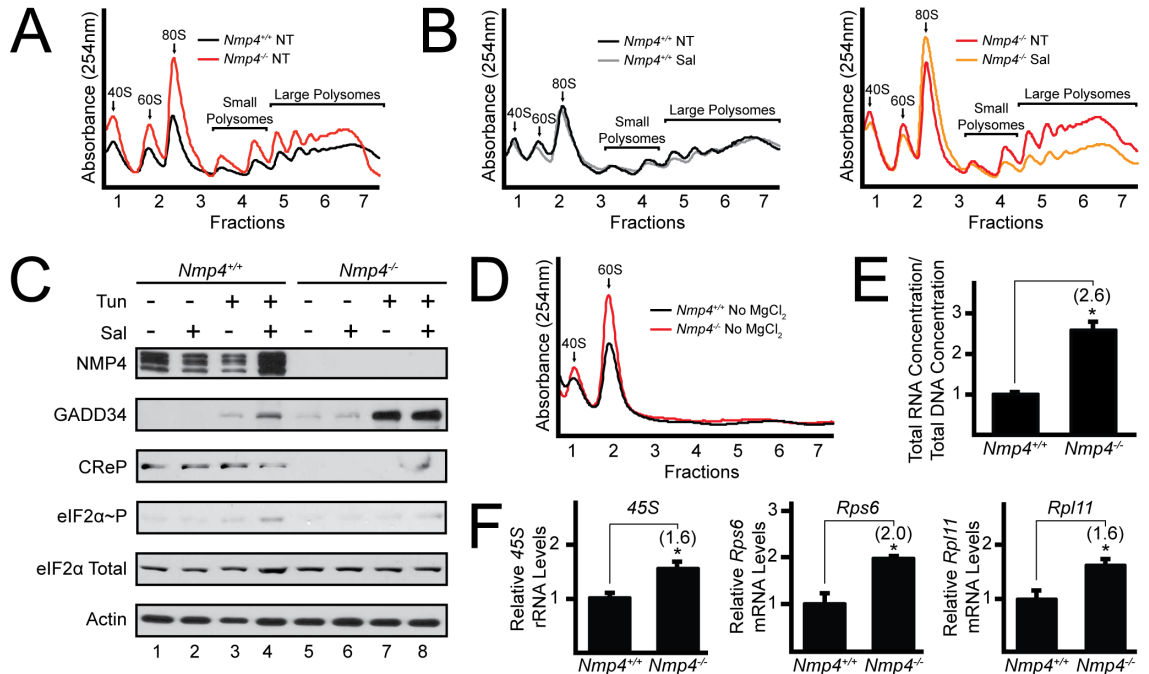


Figure 26. Deletion of *Nmp4* in MSPCs increases ribosome biogenesis and protein synthesis. A, Lysates were collected from WT and *Nmp4*^{-/-} MSPCs and equal amounts of total RNA were layered on top of 10-50% sucrose gradients, followed by ultracentrifugation and analysis of whole-lysate polysome profiles at 254 nm. B, Polysome profiles were conducted as in panel A with the addition of treatment of WT and *Nmp4*^{-/-} cells with salubrinal for 6 hours or no treatment. C, WT and *Nmp4*^{-/-} MSPCs were treated individually or in combination with salubrinal and tunicamycin, for 6 hours as indicated and the indicated proteins were measured by immunoblot. Quantification of eIF2α~P was conducted using ImageJ software. Values feature the lane number in the immunoblot, with the first lane on the left designated as lane 1, followed by quantification of eIF2α~P in parentheses: 1(1); 2(1); 3(1.6); 4(3.3); 5(0.6); 6(0.8); 7(1.3); 8(2.4). D, Levels of 40S and 60S ribosomal subunits were measured as in panel A with the exception that MgCl₂ was omitted in the lysis and sucrose gradients. E, Total DNA and total RNA lysates were quantified from WT and *Nmp4*^{-/-} MSPCs. F, The 45S rRNA and *Rps6* and *Rpl11* mRNAs were measured by qRT-PCR in WT and *Nmp4*^{-/-} MSPCs.

6.4 Deletion of *Nmp4* sensitizes MSPCs to chronic ER stress

In the UPR, expression of *Gadd34* is induced transcriptionally via ATF4 and translationally in response to eIF2 α ~P (55). Consistent with this idea, over a 8-fold increase in the levels of *Gadd34* transcript was observed upon treatment of WT cells with tunicamycin (Figure 28A). A similar induction of *Gadd34* mRNA was also observed upon tunicamycin treatment of *Nmp4*^{-/-} cells; however, given that *Nmp4*-deleted cells have much higher basal levels of *Gadd34* transcripts, there was about a 4-fold increase in *Nmp4*^{-/-} cells exposed to tunicamycin compared to similarly stress WT MSPCs. Analysis of *Gadd34* mRNA levels also resulted in a statistically significant two-way ANOVA for genotype x treatment interactions. These patterns of induction of GADD34 protein were also observed in the WT and *Nmp4*^{-/-} cells (Figure 28B). Together these results are consistent with the idea that NMP4 serves to lower *Gadd34* transcription expression during both basal and stressed conditions.

Upon ER stress in WT cells there was induced eIF2 α ~P, with a maximum around 6 hours of tunicamycin treatment. By 9 hours of ER stress, increased expression of endogenous *Gadd34* led to feedback dephosphorylation of eIF2 α ~P (Figure 28B). The greater levels of GADD34 protein in the *Nmp4*^{-/-} cells culminated in minimal induction of eIF2 α ~P during ER stress, which led to lowered levels of ATF4 expression and largely sustained protein synthesis during tunicamycin treatment (Figure 28B and C). Of interest, *Nmp4*^{-/-} cells showed a sharp reduction in the amounts of CReP protein. Despite being designated a constitutively expressed targeting subunit for PPc1 dephosphorylation of eIF2 α ~P, *Crep* expression was reported to be sharply reduced upon over-expression of GADD34, suggesting that there can be cross-regulation between the *Crep* and *Gadd34* genes.

mTORC1 activity and expression of *c-Myc* was next measured in the MSPCs subjected to ER stress. Consistent with prior reports (92), mTORC1 was repressed by

ER stress in WT cells as illustrated by lowered phosphorylation of RPS6 during the time course of tunicamycin treatment (Figure 28B). A similar reduction in RPS6 phosphorylation during ER stress also occurred in the *Nmp4*-deleted cells. Of note are the total RPL11 levels, as well as RPS6, that were increased in the *Nmp4*^{-/-} cells independent of ER stress, which further supports the idea that there are increased amounts of ribosomes upon deletion of *Nmp4*. Levels of c-MYC protein were higher in *Nmp4*^{-/-} cells compared to WT in the absence of stress (Figure 28B). However, with longer exposure to ER stress the *Nmp4*-deleted cells showed some lowering of c-MYC protein.

Phosphorylation of eIF2 α can provide for protection against acute ER stress (36,93,94). Given that *Nmp4*^{-/-} cells exhibit elevated *Gadd34* expression concomitant with lower eIF2 α ~P, the viability of WT and *Nmp4*-deleted cells were measured after exposure to tunicamycin for up to 24 hours. WT cells were largely resistant to ER stress, with only a modest 10% reduction in cell viability as measured by MTT assay (Figure 29A). By comparison, *Nmp4*^{-/-} cells showed a striking sensitivity to the ER stress, culminating in a 60% reduction of cells by 24 hours of tunicamycin treatment. Furthermore, there was increased caspase 3/7 activity in the *Nmp4*-deleted cells upon ER stress, which was absent in similarly treated WT cells (Figure 29B). Finally, the role of increased *Gadd34* expression in the sensitization of *Nmp4*^{-/-} cells to acute ER stress was addressed. The WT and *Nmp4*-deleted cells were treated with tunicamycin in the presence or absence of salubrinal (Figure 29C). Salubrinal treatment provided for cell resistance to tunicamycin in the *Nmp4*^{-/-} cells. Furthermore, combination treatment with torin, a potent small molecule inhibitor of mTORC1 (95), did not significantly alter the sensitivity of the *Nmp4*^{-/-} cells to the ER stress. These findings indicate that increased *Gadd34* expression resulting from loss of *NMP4* in MSPCs renders cells more sensitive to acute ER stress.

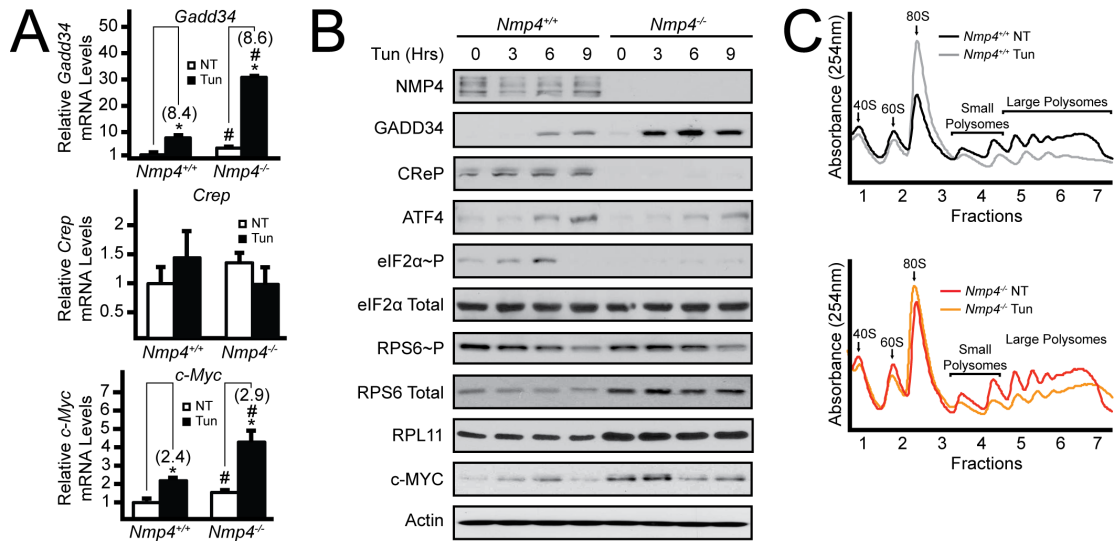


Figure 27. Deletion of *Nmp4* facilitates maintenance of global translation during activation of the UPR. A, *Gadd34*, *Crep*, and *c-Myc* mRNAs were measured by qRT-PCR in WT and *Nmp4^{-/-}* MSPCs that were treated with tunicamycin for 6 hours or left untreated. B, WT and *Nmp4^{-/-}* MSPCs were treated with tunicamycin for 3, 6, or 9 hours or left untreated and the indicated proteins were measured by immunoblot. C, Lysates were collected from WT and *Nmp4^{-/-}* MSPCs treated with tunicamycin for 6 hours or left untreated and equal amounts of total RNA were layered on top of 10-50% sucrose gradients, followed by ultracentrifugation and analysis of whole-lysate polysome profiles at 254 nm.

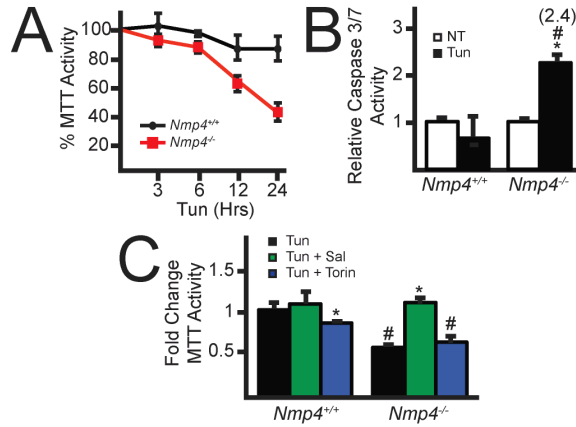


Figure 28. Deletion of *Nmp4* sensitizes MSPCs to pharmacological induction of ER stress. A, Equal numbers of MSPCs were cultured for 24 hours, followed by treatment with or without tunicamycin for up to an addition 24 hours. MTT activity was measured by the conversion of tetrazolium to formazan. B, Caspase 3/7 activity was measured in MSPCs treated with tunicamycin for 24 hours, or no ER stress. C, MTT activity was measured in the MSPCs treated with tunicamycin or combined treatment with either salubrinal or torin.

CHAPTER 7. DISCUSSION

7.1 Differential translation control of *Gadd34* and *Crep*

This thesis addresses the nature of uORFs that facilitate preferential translation in response to eIF2 α -P and the roles that these regulatory elements play in cell adaptation to stress. Levels of GADD34 and CReP expression are critical for determining the amounts of eIF2 α -P and expression of the two paralogs has previously been shown to be differentially regulated in response to ER stress (5,40,72). The 5'-leaders of *Gadd34* and *Crep* mRNAs contain two uORFs, with uORF2 in each serving as the dominant inhibitory element that is suggested to contribute to translational control (11,30). Defined here are the central regulatory features by which each of the uORF2 sequences direct translational control of *Gadd34* and *Crep*. As illustrated in a model presented in Figure 29A, *Gadd34* uORF2 serves as an efficient barrier to downstream CDS translation in basal conditions. Central to this low level of downstream translation reinitiation is an inhibitory Pro-Pro-Gly sequence juxtaposed to the termination codon in *Gadd34* uORF2. However during ER stress, eIF2 α -P facilitates a bypass of *Gadd34* uORF2 due, in part, to a poor start codon context, allowing for ribosome initiation at the *Gadd34* CDS (Figure 29A). It is important to note that only a small portion of ribosomes bypass the *Gadd34* uORF2 during ER stress, as deletion of the uORF2 led to over 10-times more luciferase activity as compared to the WT during thapsigargin treatment (Figure 6C). This level of bypass ensures that there is appropriate expression of GADD34 protein during feedback control of the ISR, which protects against premature restoration of translation during periods of ER stress.

Whereas the uORFs in *Crep* have some physical and functional similarities with *Gadd34*, there are also several significant differences. Regarding similarities, both *Gadd34* and *Crep* have two uORFs of comparable spatial arrangements, with uORF2 having a major repressing function on downstream CDS translation and uORF1

displaying a modest dampening role (Figure 9D). Furthermore, ribosomes are suggested to bypass uORF2 in both *Crep* and *Gadd34*, although the bypass occurs to a greater degree in *Gadd34* (Figure 29A and B). The critical difference between *Gadd34* and *Crep* lies in the ability of *Crep* uORF2 to facilitate more ribosome reinitiation at the downstream CDS. By comparing expression of *Crep-Luc* between WT and Δ uORF2 constructs in the absence of stress (Figure 8C), it is estimated that upwards of 12% of the ribosomes that translate uORF2 reinitiate at the *Crep* CDS. Using a similar comparison for *Gadd34-Luc* (Figure 6C), it is estimated that less than 3% of ribosomes translating uORF2 reinitiate at the *Gadd34* CDS. Together the modest bypass of uORF2 during ER stress and efficient ribosome reinitiation allow for constitutive ribosome translation of the *Crep* CDS. It is also of note that efficient reinitiation at the *Crep* CDS occurs with an uORF2 of longer length-52 codons, which appears to differ with the suggested models whereby uORFs only a few codons in length are necessary for appreciable ribosome reinitiation at a downstream CDS (10).

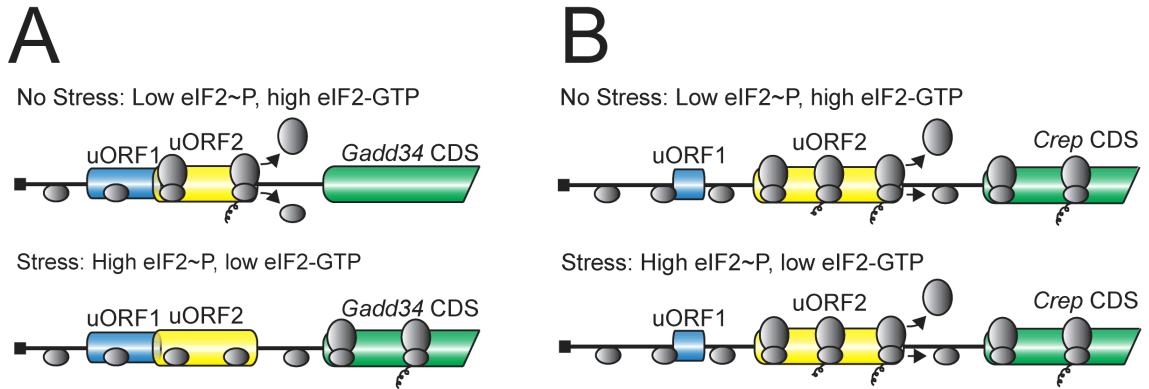


Figure 29. Models for *Gadd34* and *Crep* translational control. A, Model for *Gadd34* translational control. In the absence of stress, low eIF2 α ~P, and high eIF2-GTP, ribosomes scan the 5'-leader of the *Gadd34* mRNA and initiate translation at *Gadd34* uORF2. After translation of uORF2, terminating ribosomes are precluded from translation reinitiation downstream and are suggested to dissociate from the mRNA. In the presence of stress, eIF2 α ~P, and low eIF2-GTP levels allows for some scanning ribosome to bypass the *Gadd34* uORF2 in part due to poor start codon context, and instead initiate translation at the *Gadd34* CDS. B, Model for *Crep* translational control. In the presence or absence of stress, ribosomes scan the 5'-leader of the *Crep* mRNA and initiate translation at the *Crep* uORF2. After translation of uORF2, a portion of the terminating ribosomes resume scanning and initiate translation downstream at the *Crep* CDS. It is noted that during stress and high eIF2 α ~P, a small portion of ribosomes can bypass the uORF2 and initiate translation at *Crep* CDS. Together these processes are suggested to lead to *Crep* translation independent of eIF2 α ~P.

7.2 Roles of uORFs in regulating the ISR and cellular resistance to stress

Both GADD34 and CReP are responsible for directing PP1c to dephosphorylate eIF2 α -P. As the amount of eIF2 α -P can dictate the levels of global and gene-specific translation, regulation of GADD34 and CReP expression is central for maintaining protein homeostasis and health of the cell. This thesis shows that alteration of the regulatory features in *Gadd34* uORF2 results in significant changes in protein synthesis and cell vitality both basally and during ER stress (Figure 11). Of note, deletion of *Gadd34* uORF2 resulted in a dramatic increase in GADD34 expression, which then lowered levels of both eIF2 α -P and translational control that coincided with increased sensitivity of the cells to ER stress. These results suggest that aberrant regulation of GADD34 expression alters the dynamics of the ISR, which would not allow sufficient time for stressed cells to induce ISR-target genes to alleviate stress damage before resumption of global translation. Paradoxically, functional deletion of GADD34 and chronically low levels of global translation have been previously shown to also result in increased sensitivity of cells to ER stress (96), which further emphasizes the importance of the mechanisms regulating GADD34 and CReP expression in the timing and magnitude of ISR induction. Interestingly, mice deleted for *Gadd34* are resistant to renal toxicity upon ER stress treatment, suggesting that in tissues there are further complexities to the dynamics of the ISR (87). The mechanisms underlying differential regulation of *Gadd34* and *Crep* translation also have implications for the utility of emerging drugs to modulate the ISR and its control of cell adaptation to intracellular and extracellular stresses (74,89,97).

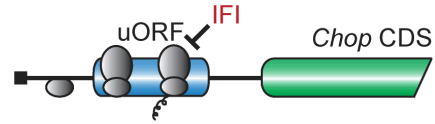
7.3 Translation control of *Chop* through a ribosomal elongation stall

Chop expression is suggested to be critical for transitioning the transcriptome from a stress alleviation program to one of programmed cell death (49,50,67,75,87,98).

The 5'-leader of *Chop* mRNA contains an inhibitory uORF that is suggested to contribute to *Chop* translation control through a Bypass mechanism (12,37). This thesis characterizes the features of the *Chop* uORF that serve to repress downstream translation during basal conditions and facilitate preferential translation in response to eIF2 α -P and the role that these regulatory elements play in cell viability. As illustrated in the model presented in Figure 30, the *Chop* uORF functions to block downstream CDS translation in basal conditions. Central to this low level of downstream translation is an inhibitory Ile-Phe-Ile sequence that efficiently stalls elongating ribosomes, thus promoting low levels of translation reinitiation at the CDS. During ER stress, however, eIF2 α -P facilitates a ribosomal bypass due in part, to its poor start codon context, and allows for ribosome initiation at the downstream *Chop* CDS (Figure 30).

While the Ile-Phe-Ile sequence of the *Chop* uORF appears to be important for the stall of elongating ribosomes during translation of the *Chop* uORF, the molecular basis underlying this ribosomal stall is not yet fully understood. The codon encoding the second Ile in the Ile-Phe-Ile sequence is a less frequently used codon, but individual alanine substitutions at each of the Ile-Phe-Ile positions were not sufficient to alleviate the elongation stall. Rather simultaneous substitution of each of the codon positions to alanine reduced the inhibitory elongation stall. Ribosome profiling analysis of ribosome stalls genome-wide indicates that the mere presence of an Ile-Phe-Ile sequence does not appear to be sufficient for stalling ribosomes (6). However, in-frame fusions of a portion of the *Chop* uORF containing the Ile-Phe-Ile sequence are suggested to be sufficient to stall ribosomes even when embedded into larger coding sequences, suggesting that short uORFs or placement of the Ile-Phe-Ile sequence in the 5'-leader of the mRNA are not obligate. These findings suggest that other features of the *Chop* uORF can also be contributors, such as additional RNA sequences or the encoded polypeptide residues flanking the Ile-Phe-Ile encoded in the *Chop* uORF.

No Stress: Low eIF2~P, High eIF2-GTP levels



Stress: High eIF2~P, Low eIF2-GTP levels

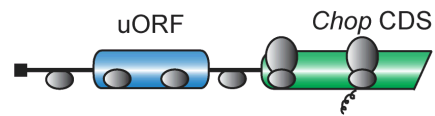


Figure 30. Model for *Chop* translational control. In the absence of stress, low eIF2 α ~P, and high eIF2-GTP, ribosomes scan the 5'-leader of the *Chop* mRNA and initiate translation at the *Chop* uORF. During translation of the uORF, elongating ribosomes are stalled at an Ile-Phe-Ile sequence, as depicted by the IFI sequence and black bar adjacent to the elongating ribosome in the uORF. The ribosome stall would preclude ribosome reinitiation downstream at the *Chop* CDS. In the presence of stress, and induced eIF2 α ~P, there would be lower levels of eIF2-GTP that would allow scanning ribosomes to bypass the *Chop* uORF in part due to its poor start codon context, and instead initiate translation at the *Chop* CDS.

7.4 Role of uORFs in regulating cell viability

Induced CHOP expression during eIF2 α -P serves to promote programmed cell death when ISR signaling slated to alleviate stress damage is insufficient to restore cellular homeostasis. The data in this thesis shows that loss of the *Chop* uORF-mediated translation control results in a significant increase in CHOP levels, along with lowered cell viability upon exposure to ER stress. With the enhanced levels of CHOP protein, the *Chop* Δ uORF cells displayed a different pattern of CHOP expression during a time course of thapsigargin treatment (Figure 16). There was higher basal expression of CHOP protein in the *Chop* Δ uORF cells that was accompanied by enhanced translation as judged by the association of *Chop* mRNA with heavy polysomes (Figures 12A and 16B). Of note, overexpression of CHOP resulted in decreased induction of *Chop* gene transcription upon ER stress (Figure 16C and D) and overexpressed CHOP displayed increased turnover (Figure 16E). As a consequence, both the transcriptional downregulation and protein destabilization would contribute to the decrease in CHOP protein levels detected in the *Chop* Δ uORF cells following 6 hours of thapsigargin treatment (Figure 16A). Previous reports have suggested that CHOP can serve to autorepress its own transcription by CHOP heterodimerization with and inhibition of the positive transcriptional activity of C/EBP β (79). This suggests that in addition to ISR feedback dephosphorylation of eIF2 α -P by GADD34 (40), additional autoregulatory mechanisms also serve to control CHOP levels and activity as a part of the ISR. It should be emphasized that even with the lowered *Chop* mRNA and increased CHOP protein turnover, there was a significant enhancement of CHOP protein both basally and with the addition of ER stress in the Δ uORF *Chop* cells. This finding highlights that translational expression of CHOP is a major feature in its regulated expression.

Elevated translational expression of CHOP in the Δ uORF *Chop* cells resulted in significant mRNA increases from the CHOP target genes *Atf5* and *Bim* (Figure 17A).

However, only upon addition of ER stress was there significant differences in cell viability between those cells expressing WT levels of CHOP and overexpressed CHOP (Figure 17B). This is consistent with an earlier report that forced expression of CHOP upregulated mRNA expression of downstream target genes, but required an ER stress stimulus to induce apoptosis (88). Interestingly, there was substantial *Bim* expression independent of stress in the Δ uORF *Chop* cells, whereas *Atf5* is largely induced by stress. The presence of both CHOP and ATF4 has been previously shown to be required for maximal *Atf5* expression and both CHOP and ATF4 bind to the *Atf5* promoter (15,67,88). These results argue for the requirement of additional stress-induced transcription factors to promote maximal expression of pro-apoptotic genes such as *Atf5* and that *Atf5* and its pattern of expression is paramount in the observed stress-induced cell death. These findings also indicate that misregulation of *Chop* expression does not cause a substantial increase in apoptosis in unstressed cells, but rather pre-programs the transcriptome to alter the timing and magnitude of the change in cell fate to apoptosis after stress and the induction of the ISR. It is noted that the levels of CHOP protein levels expressed in Δ uORF *Chop* cells were highly elevated at 1 and 3 hours of ER stress, but became diminished at 6 hours. The consequential reduced MTT activity and increased caspase 3/7 activity of Δ uORF *Chop* cells was readily detectable by 6 hours of ER stress. These findings suggest that during early exposure to ER stress, CHOP protein levels achieved a critical level and duration of expression that triggered a program of gene expression directing substantial death of the Δ uORF *Chop* cells.

7.5 Translation control of *Eprs* through non-canonical initiation codons

The mechanisms by which uORFs with non-canonical initiation codons modulate gene expression in response to eIF2 α -P are also addressed in this thesis. Previously,

identification of uORFs was largely viewed as being dependent on the presence of an AUG initiation codon in the 5'-leader of a given mRNA. Recent ribosomes profiling evidence has suggested that this mechanism of uORF identification has vastly underestimated the number of functional uORFs and that uORFs with non-canonical initiation codons can also be translated and serve regulatory roles in gene expression (4,6,83). The 5'-leader of the glutamyl-prolyl-tRNA synthetase gene *Eprs* contains five non-canonical initiation codons that are divided between three uORFs. This thesis determined the regulatory features by which the uORFs direct translation control of *Eprs* and promote increased EPRS protein expression in response to diverse cellular stresses.

As illustrated in the model presented in Figure 31, translation initiation at either CUG2, encoded in uORF1, or the uORF2 UUG reduce basal translation initiation at the *Eprs* CDS. uORF1 overlaps out-of-frame with the *Eprs* CDS and translation of uORF1 results in translation termination 3' of the start codon for *Eprs* (Figure 31). Additionally, only ~25% of the ribosomes that translate uORF2 reinitiate at the downstream *Eprs* initiation codon, thereby dampening basal *Eprs* expression (Figure 22). Central to the *Eprs* mechanism of translation control are the non-canonical initiation codons for the two functional uORFs. Replacement of either CUG2 or UUG1 with an AUG initiation codon resulted in over a 60% decrease in luciferase activity (Figures 21 and 22). The presence of the CUG and UUG initiation codons allows for a portion of the scanning ribosomes to bypass the uORFs, at least in part due to their non-canonical initiation codons, and instead initiate translation at the *Eprs* CDS during basal conditions. eIF2 α -P further facilitates bypass of the uORFs and allows for an increase in *Eprs* expression in response to stress. This modulation of ribosome bypass ensures appropriate expression of EPRS protein to perform its function as a dual function aminoacyl tRNA

synthetase, and allows for increased EPRS expression upon cellular stress and changes in demand for appropriately charged aminoacyl-tRNAs.

Another gene recently identified as containing a functional uORF with a non-canonical initiation codon is that of *Gadd45g*, which regulates cell growth and apoptosis (4). Expression of *Gadd45g* is controlled by an overlapping out-of-frame uORF that has a CUG initiation codon. The presence of the uORF was shown to be required for the induction in *Gadd45g* expression during cellular stress, suggesting that the uORF serves as a barrier to downstream translation during nonstressed conditions that is bypassed due to its noncanonical initiation codon during eIF2 α -P (4). Also recently described is the model of translation control for *Bip* (*Grp78/Hspa5*) that participates in protein folding in the ER (33). The 5'-leader of the *Bip* mRNA features two uORFs: a short 5'-proximal uORF and a subsequent overlapping out-of-frame uORF that are both encoded by non-canonical initiation codons. *Bip* translational control is suggested to be dependent on these two uORFs as well as internal ribosome entry sequences (IRES), which likely function in conjunction to facilitate *Bip* translation during cellular stress (33,99,100). The recent characterization of the *Eprs*, *Gadd45g*, and *Bip* models of translation control emphasizes that uORFs with non-canonical initiation codons can serve as significant regulators of preferential translation during cellular stress.

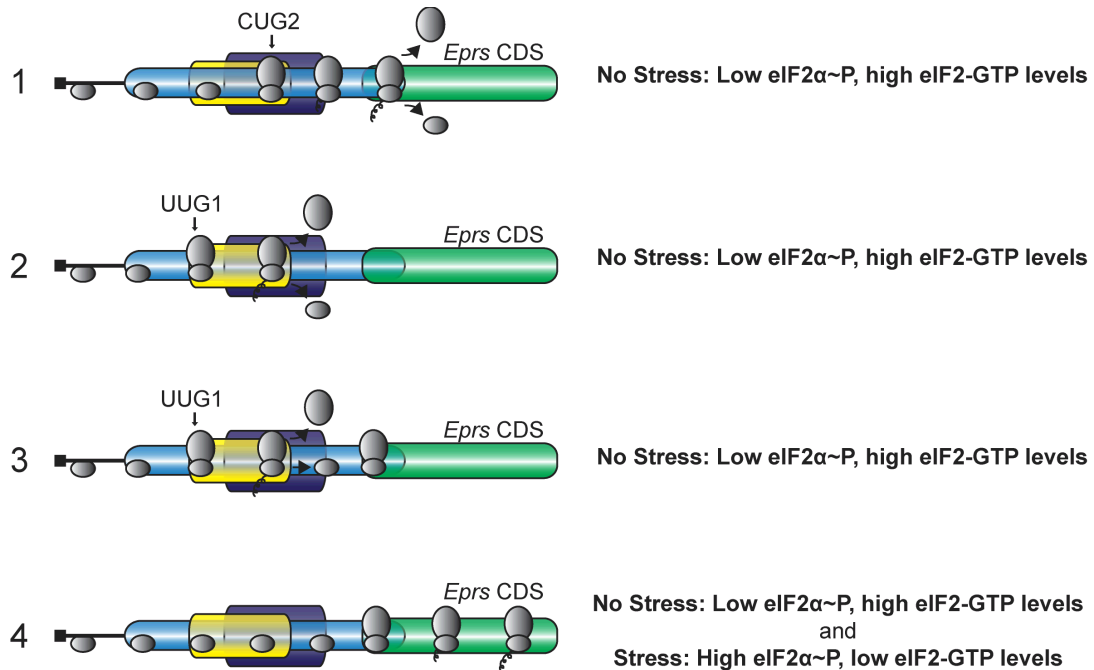


Figure 31. Model for *Eprs* translational control. *Eprs* translation control involves bypass of two inhibitory uORFs with non-canonical initiation codons. In the absence of stress, low levels of eIF2 α -P, and high eIF2-GTP, ribosomes scan the 5'-leader of the *Eprs* mRNA and initiate translation at CUG2, encoded in uORF1, or UUG1, encoded in uORF2. uORF1 overlaps out-of-frame with the *Eprs* CDS and translation of uORF1 results in translation termination 3' of the start codon for *Eprs*. A portion of the ribosomes that translate uORF2, encoded by UUG1, terminate and are released from the *Eprs* mRNA. Alternatively, ribosomes can reinitiate at the downstream *Eprs* CDS post uORF2 translation. The presence of the CUG and UUG initiation codons allows for a portion of the scanning ribosomes to bypass the uORFs, at least in part due to their non-canonical initiation codons, and instead initiate translation at the *Eprs* CDS during basal conditions. In the presence of stress, high levels of eIF2 α -P and diminished eIF2-GTP levels are suggested to further facilitate bypass of the uORFs and allow for an increase in *Eprs* CDS translation and subsequent protein expression.

7.6 Expression of *Eprs* is induced during diverse cellular stresses

EPRS is responsible for charging of glutamyl and prolyl tRNAs with their cognate amino acids. Levels of aminoacyl tRNA synthetases are critical for translation through charging of tRNAs and modulating the available aminoacyl-tRNA pool (101,102). The data present here shows that EPRS protein expression is enhanced through an uORF-mediated translation mechanism in response to ER stress and to treatment with halofuginone, which is suggested to cause a decrease in the charged prolyl-tRNA pool (85). Lowered global protein synthesis by eIF2 α -P would help to conserve resources and allow cells to reconfigure gene expression to alleviate these stress conditions. In the case of halofuginone treatment, increased amounts of uncharged prolyl-tRNAs are suggested to directly activate GCN2 phosphorylation of eIF2 α -P (Figure 32). The eIF2 α -P would then lead to preferential translation of key ISR genes including *Atf4*, which would facilitate nutrient uptake and alter metabolism to better manage the change in tRNA charging. Of importance, eIF2 α -P would also lead to increased *Eprs* expression that would serve to diminish the toxicity of the drug (Figure 32). This model is central to the surgical stress resistance concept whereby nutrient depletion prior to surgery provides for a boost in expression of genes that would provide for subsequent protection from ischemic damage occurring during surgical procedures (84). GCN2 induction of protective patterns of gene expression is suggested not just to be restricted to nutrient depletion. For example, budding yeast exposure to high salinity results in a transient decrease in the charging of several different tRNAs, most likely due to changes in amino acid transport and/or aminoacyl tRNA synthetase expression or activity (103-105). Therefore, stresses not directly linked to starvation for amino acids can change the status of tRNA charging and activate GCN2 and the ISR.

Halofuginone directly inhibits the prolyl-tRNA charging function of EPRS and expression of *Eprs* in the ISR is suggested to diminish the toxicity of halofuginone

treatment. However, expression of *Eprs* and other aminoacyl-tRNA synthetases are induced by eIF2 α -P and the ISR in response to diverse environmental stresses (42). One benefit of enhanced levels of aminoacyl tRNA synthetase would be to rapidly restore translation in the feedback regulation of the ISR. In addition to their role in regulating translation through tRNA charging, aminoacyl tRNA synthetases are also suggested to serve a role in proofreading to prevent tRNA charging with damaged amino acids, thereby ensuring translation fidelity and proper protein folding and function (106,107). Finally, aminoacyl tRNA synthetases can serve other functions unrelated to tRNA charging. EPRS, for example, functions in the GAIT complex (gamma-interferon activated inhibitor of translation) to repress translation of a class of inflammatory mRNAs in immune cells (108).

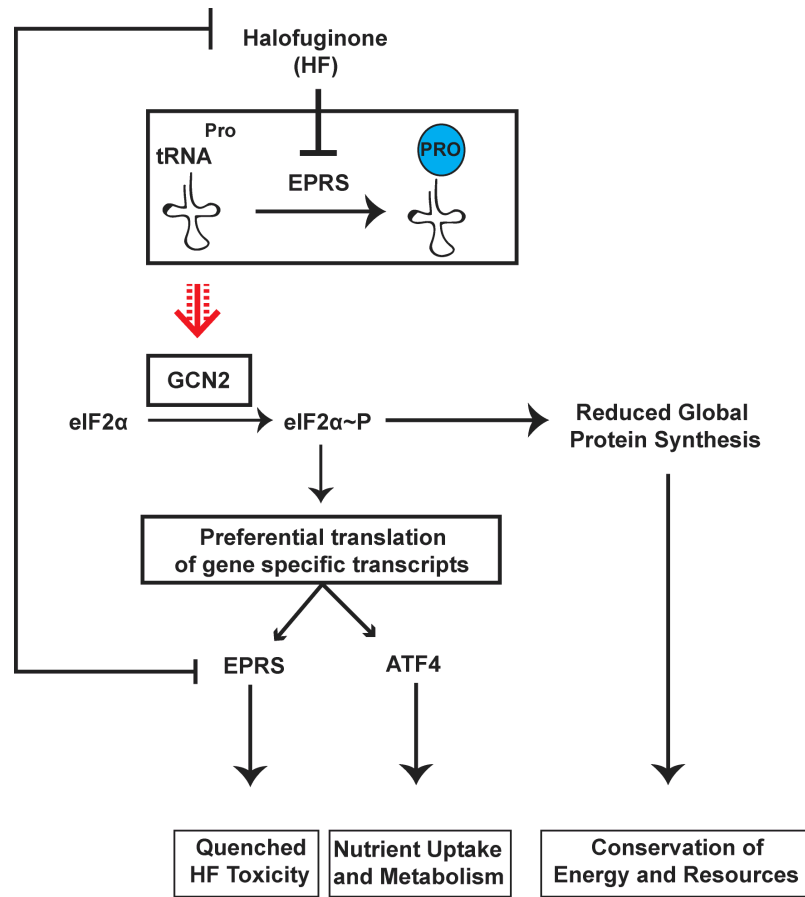


Figure 32. Model depicting gene regulation downstream of the eIF2 kinase GCN2 during halofuginone treatment. With the accumulation of uncharged tRNA^{Pro} during halofuginone treatment, activated GCN2 phosphorylates eIF2α and decreases global mRNA translation initiation. Coincident with a decrease in overall translation, mRNA encoding ATF4 is subject to preferential translation, ultimately leading to an increase in ATF4 downstream targets central to stress remediation. Also subject to preferential translation during eIF2α~P is mRNA encoding EPRS. During halofuginone treatment, *Eprs* is preferentially translated and the resulting increase in its expression is suggested to quench chronic drug toxicity.

7.7 NMP4 regulates protein synthesis through transcriptional repression of *Gadd34*

This thesis also shows transcriptional regulation of those mRNAs that are preferentially translated during cellular stress plays a significant role in cellular and protein homeostasis. That data presented here indicates that NMP4 represses *Gadd34* and *c-Myc* expression, and that loss of *Nmp4* culminates in increased ribosome biogenesis and protein synthesis. Translational control is central to the maintenance of cellular homeostasis and is critical for the implementation of the UPR, especially in professional secretory cells. In the UPR, eIF2 α ~P is central for resistance to acute ER stress, and premature resumption of translation can reduce cell viability (87,88,104). This idea is illustrated by the finding that pharmacological induction of ER stress resulted in decreased cell viability of *Nmp4*^{-/-} MSPCs that was ameliorated upon inhibition of GADD34 and CReP activity. Furthermore, this thesis showed that loss of *Nmp4* increases ribosome biogenesis by a process suggested to involve c-MYC, contributing to further increases in protein synthesis (Figure 33). Combined these results suggest a prominent role for NMP4-mediated dampening of translational control in the UPR, which is critical in the ability of cells to appropriately sense and respond to ER stress.

A model for NMP4-mediated regulation of *c-Myc* and *Gadd34* expression and subsequent translation control is presented in Figure 33. NMP4 serves to repress both *c-Myc* and *Gadd34* expression, helping to maintain appropriate regulation of ribosome biogenesis and translation initiation through eIF2 α ~P (Figure 33). Loss of *Nmp4* results in heightened *c-Myc* and *Gadd34* expression that contribute to increases in ribosome biogenesis and translation initiation. However, high levels of protein synthesis incurred through the loss of *Nmp4* rendered cells sensitive to acute ER stress induced by pharmacological agents, such as tunicamycin, due to an inability to appropriately regulate translation and activate some of the adaptive features of the UPR (Figure 33).

Previous work suggested that activation of the UPR plays a significant and obligatory role in bone formation through regulation of osteoblast differentiation, proliferation, and function, supporting the idea that the UPR promotes cellular homeostasis in highly secretory cells by regulating changes in gene expression and protecting cells from defects in protein folding (36,57,109). Emphasizing the importance of the key UPR regulators in secretory cells, loss of function of *Perk*, *Atf4*, *Ire1*, or *Xpb1* disrupts the health and secretory functions of osteoblasts and subsequent bone formation (57-59). This thesis shows that NMP4 also plays a role in the appropriate regulation of the UPR through repression of the expression of *Gadd34*. Loss of *Nmp4* resulted in a GADD34-mediated increase in protein synthesis basally that was largely sustained during pharmacological induction of ER stress, which then sensitized cells to the underlying stress. This finding emphasizes the role of NMP4 in maintaining the cell in a homeostatic state in which protection from proteotoxicity is balanced with the secretory requirements of the cell. In contrast to pharmacological stress, more mild, physiological stresses would likely result in maintenance of translation and some acceleration of protein secretion in the *Nmp4*^{-/-} background without the toxicities associated with sustained pharmacological induction of ER stress. Indeed, targeted deletion of *Nmp4* in mice enhances bone response to PTH and BMP2 and protects these animals from osteopenia likely through increased production and secretion of factors that facilitate bone formation (62).

The regulated expression and activity of NMP4 in response to pharmacological and physiological stresses also likely plays a role in NMP4-mediated regulation of ribosome biogenesis and the UPR. *Nmp4* mRNA was reported to be expressed in all major organs analyzed, although there were two distinct transcripts that were differentially expressed by a mechanism suggested to involve alternative mRNA splicing (110). Transcription of *Nmp4* is also mediated through the activity of two alternative

promoters that both respond to PTH treatment and result in the production of *Nmp4* mRNAs with different transcription start sites (111). Collectively, these regulatory mechanisms result in the production of multiple NMP4 protein isoforms, some of which contain an in-frame N-terminal extension, and all of which contain Cys₂His₂ zinc finger binding domains, which can range from five to eight in number (110-112). While multiple NMP4 protein isoforms were observed, an appreciable change in the pattern of NMP4 expression in response to pharmacological induction of the UPR was not detected (Figure 27B). This suggests that protein modifications identified in NMP4 (113,114) or availability of NMP4 interacting proteins (110) may play a role in regulating the localization and activity of NMP4 in response to cellular cues to modulate protein production and secretion (115).

Of note is the decrease in CReP protein expression that was observed upon loss of *Nmp4* and overexpression of *Gadd34*. Despite being designated a constitutively expressed targeting subunit for PPc1 dephosphorylation of eIF2 α -P, *Crep* expression was also shown in this thesis to be sharply reduced upon deletion of the *Gadd34* uORF that resulted in GADD34 over-expression. This suggests an unexplored cross-regulation between the *Crep* and *Gadd34* genes. The changes in ribosome biogenesis and eIF2 α -P described herein emphasize the importance of regulation of NMP4 in *Gadd34* and *c-Myc* expression in the maintenance of cellular homeostasis and provides a better understanding of the processes that maintain appropriate levels of protein synthesis in highly secretory tissues.

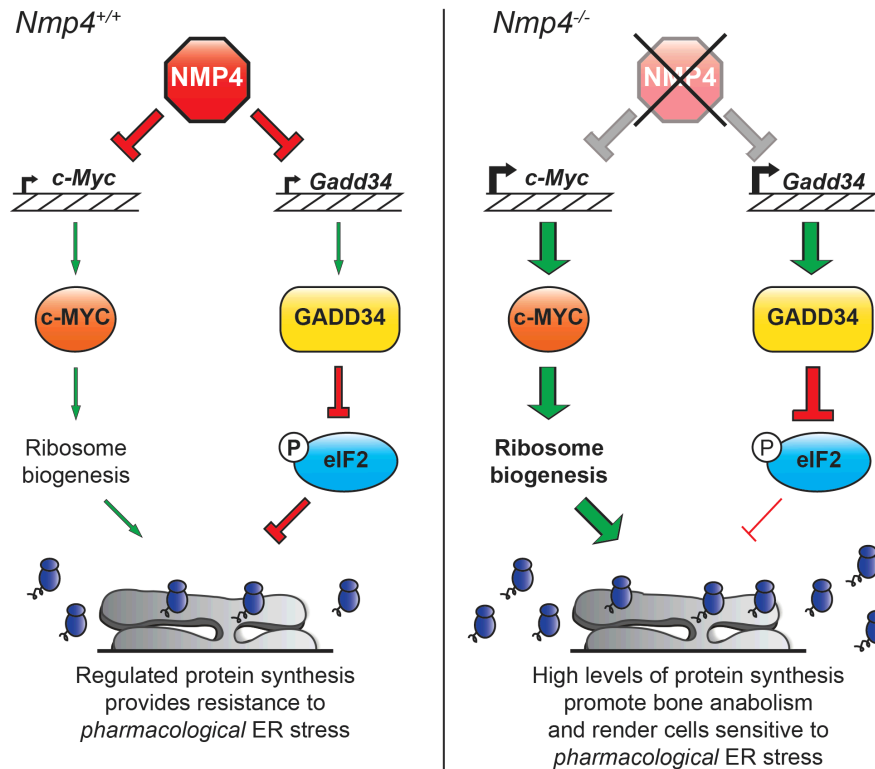


Figure 33. Model for NMP4 regulation of ribosome biogenesis and the UPR.

NMP4 serves to dampen transcriptional expression of *c-Myc* and *Gadd34* that are important for regulation of ribosome biogenesis and eIF2 α -P and the UPR, respectively. ER stress and induction of the UPR in *Nmp4*^{+/+} cells results in decreased protein synthesis that promotes stress alleviation, partially through the regulated expression of *c-Myc* and *Gadd34*. However, in *Nmp4*^{-/-} cells there are high levels of *c-Myc* and *Gadd34* expression and subsequent elevation of ribosome biogenesis and translation initiation through GADD34-mediated dephosphorylation of eIF2 α -P. As a consequence, heightened levels of synthesized proteins slated to be retained in the cytosol and those directed into the ER for secretion are maintained during pharmacological induction of the UPR, thwarting stress adaptation that renders cells sensitive to the acute ER stress. Loss of *Nmp4* has also been shown to increase bone anabolism in mice, which is likely due, at least in part, to increased c-MYC and GADD34-mediated protein synthesis and secretion.

7.8 The link between uORF-mediated translation regulation and mRNA abundance

The changes in gene expression that are incurred through uORF-mediated translation regulation are not surprisingly also dependent on mRNA abundance. The three major regulators of mRNA abundance, transcription, mRNA processing, and mRNA degradation, thus play major roles in uORF-mediated regulation of ISR induced preferential translation (116-118). For example, *Atf4* expression is potently induced during endoplasmic reticulum stress, but there are only low levels of *Atf4* expression during UV irradiation (117,119). Both conditions induce robust eIF2 α ~P and preferential translation of *Atf4* mRNA occurs with either stress (119). However, increased expression of transcriptional repressor LIP during UV irradiation was subsequently shown to result in increased LIP binding to the *Atf4* promoter, thereby repressing *Atf4* transcription. Lowered levels *Atf4* mRNA available for translation during UV stress thus results in negligible ATF4 protein and transcription activity. This illustrates that *Atf4* mRNAs with identical 5'-leaders and uORF configurations have sharply different induction capabilities in response to different stress conditions despite having comparable levels of eIF2 α ~P (117).

Translation of *Atf5*, which encodes a bZIP transcriptional activator, is additionally controlled by the Delayed translation reinitiation mechanism (15,120). Expression of *Atf5* features two different mRNA isoforms (118). The more abundant transcript, *Atf5 α* , contains two uORFs that serve to promote preferential translation during cellular stress (15,120). *Atf5 β* encodes the same *Atf5* CDS, but contains an alternative 5'-leader that does not contain any uORFs and is not translationally regulated in a stress-dependent manner (120). Thus, expression of *Atf5* can also be modulated through alternative promoter activity and differential production of mRNA isoforms (118). Recent genome-wide evidence has suggested that regulation of translation through mRNA splicing

extends to multiple other genes as well and plays a significant role in the presence of different 5'-leaders in mRNAs that can affect translational expression (116).

uORF translation can also result in activation of the mRNA decay pathways, thus adding another layer to the mechanisms in which uORFs can negatively regulate downstream translation (121). For example, *Chop* was recently identified in a genome-wide screen as a target of the nonsense mediated mRNA decay (NMD) pathway, that recognizes the presence of a premature termination codon (78). Depletion of the NMD machinery from cells results in the stabilization of *Chop* mRNA levels (122). *Chop* mRNA half-life was also increased more than two-fold in cells in which the *Chop* uORF AUG had been mutated (Figure 16). Combined, these studies suggest that the presence of an uORF can also serve to repress expression of the CDS through mechanisms involving mRNA decay. Furthermore, changes in the selection of mRNAs that contain uORFs for degradation during different cellular stress conditions likely also serve to regulate the ISR induced changes in gene expression.

7.9 Evolutionary conservation of uORF-mediated translation mechanisms

Regulation of translation initiation through eIF2 α ~P is largely conserved among eukaryotes (19,47). With this in mind, it is not surprising that uORF-mediated translation control schemes that rely on eIF2 α ~P are also conserved. For example, the uORF-mediated translational control mechanism for cell fate regulator *Ibtka* is suggested to be largely conserved among mammals (Figure 34A) (5). Interestingly, the *Homo sapien Ibtka* mRNA has four uORFs, but only the two key uORFs that confer *Ibtka* translational control are consistently conserved among other mammals (Figure 34A) (5). This suggests that those uORFs that are retained throughout species likely maintain functional significance. This idea is emphasized in genome-wide analyses of uORF conservation that suggest that selection for uORF length, amino acid sequence, and

uORF position are not conserved between species (123,124). However, the presence of an uORF and the regulatory nature of the uORF(s) is suggested to be retained (7,123-125).

An example in which the regulatory function of an uORF is retained, but the specific features of that uORF are variable throughout species is the inhibitory uORF located in the 5'-leader of *Gadd34* mRNA (30,126). The 5'-leaders of the *Drosophila melanogaster* and *Mus musculus* *Gadd34* transcripts each contain two uORFs, with the first uORF considered to be largely dispensable for *Gadd34* translation control (Figure 34B) (30,126). However, the basis for the inhibitory functions of uORF2 is different between the two species. The uORF2 in *D. melanogaster* overlaps out-of-frame with the *Gadd34* CDS and is considered to be inhibitory by promoting uORF translation termination 3' of the start codon for the *Gadd34* coding region (126). By comparison, *M. musculus* uORF2, which terminates 23 nucleotides upstream of the *Gadd34* CDS, prohibits reinitiating downstream due to the inefficient termination (Figures 29 and 34B).

While the inhibitory nature of the *Gadd34* uORF2 is different between *D. melanogaster* and *M. musculus*, both inhibitory uORFs are suggested to require ribosome bypass during cellular stress for preferential translation of *Gadd34* (Figure 29) (126). Bypass of the *M. musculus* inhibitory uORF2 was diminished when uORF2 was altered from its wild-type moderate start codon context to the Kozak consensus sequence (Figure 7). Since uORF2 in *D. melanogaster* is in strong Kozak consensus, additional factors may be required for bypass of uORF2 in this species (126).

In the case of *Mus musculus* *Gadd34*, the modulation of ribosome reinitiation post-uORF2 translation has resulted in a more complex mechanism of translation control. One potential outcome of this mechanism is an increased ability to fine-tune the levels of *GADD34* expression. Lower eukaryotes typically only express the GCN2 and PERK eIF2 α kinases, with some species expressing only a single kinase (19,127,128). It is

interesting to speculate that increased manipulative control of *Gadd34* has evolved in mammals as a compensatory mechanism to balance the increased number of stress signals and kinases that integrate on eIF2 α . This suggests that selective evolutionary pressure may have played a role in the development of the translation control mechanisms described herein.

Comparison of the uORF configurations among *Gcn4* mRNAs between fungal species also suggests that while the general regulatory function of uORFs were conserved, the specific uORF features and underlying model of uORF-mediated translational control can vary (129,130). Assessment of the *Gcn4* mRNA in twelve fungal species revealed that the uORFs configurations range from three to six in number and are not positionally conserved (129). Furthermore, the mechanism of *Gcn4* translation control for *Candida albicans* is reliant upon bypass of a single inhibitory uORF whereas *Gcn4* in *Saccharomyces cerevisiae* relies on a mechanism involving Delayed translation reinitiation that features four uORFs (Figure 34C) (130). These findings suggest that even among gene orthologs in different species that different uORF configurations and mechanisms can be implemented to achieve preferential translation in response to eIF2 α -P.

These examples of the evolutionary conservation of uORF-mediate translation control emphasize that there are multiple features of uORFs that can be combined in specific ways to generate uORFs of similar functions in regulation of translation. Furthermore, the proper composition and position of uORFs and their features are critical for uORF-mediated translation control mechanisms that direct regulated gene expression for optimal adaptation to environmental stress. Key tenants of the uORF-mediated translation control mechanisms described here are also applicable to genome-wide assessments of translation in which the specific features of uORFs are used to accurately predict the patterns of translation control for a given mRNA.

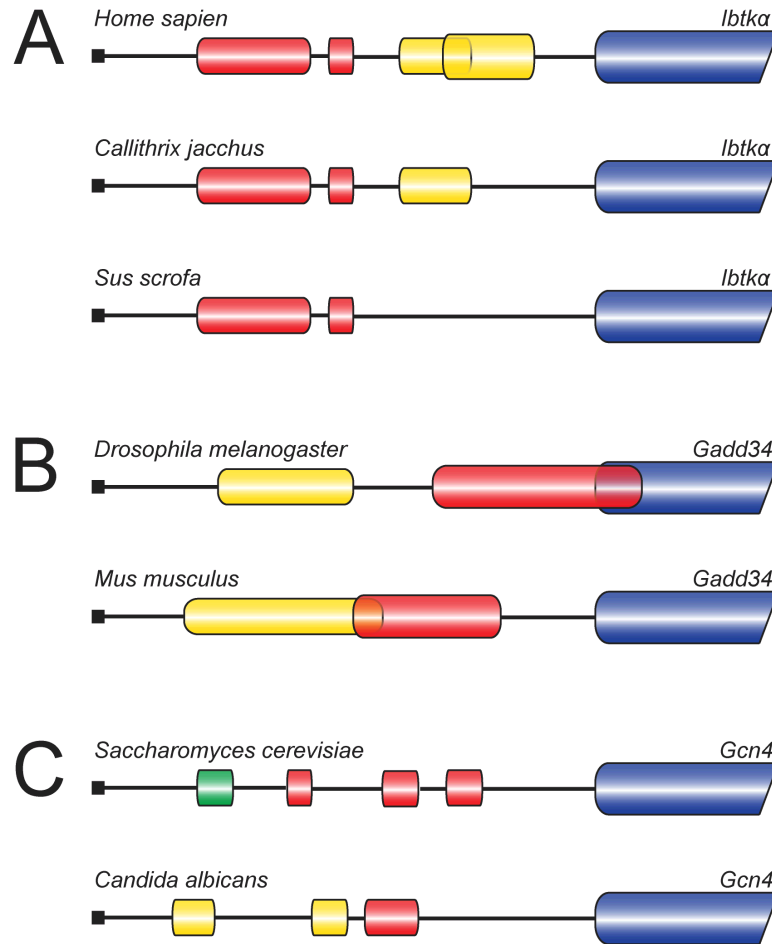


Figure 34. uORF mechanisms of translation control are evolutionarily conserved.

A, Illustration of the *Ibtka* 5'-leader in multiple species including: *Homo sapien*, *Callithrix jacchus*, and *Sus scrofa*. Translation of *Ibtka* mRNA is regulated by a bypass mechanism. The inhibitory uORFs 1 and 2 (red bars) repress *Ibtka* CDS translation during nonstressed conditions. The inhibitory effects of uORF1 and 2 are overcome during eIF2 α -P, facilitating the preferential translation of *Ibtka* (blue bar). uORFs3 and 4 (yellow bars) are considered to be dispensable for *Ibtka* translation control and are not conserved between species. B, Depiction of the 5'-leaders for *D. melanogaster* and *M. musculus* *Gadd34* mRNA. The 5'-leader of *Gadd34* mRNA in both species contains a dispensable uORF1 (yellow bar) that is largely bypassed independent of cellular stress. uORF2 (red bar) in both mRNAs is translated during basal conditions and is inhibitory to

downstream *Gadd34* CDS translation. uORF2 in *D. melanogaster* overlaps out-of-frame with the *Gadd34* CDS (blue bar) and promotes ribosome dissociation from the mRNA 3' of the initiation codon of the *Gadd34* CDS. *M. musculus* uORF contains an inhibitory Pro-Pro-Gly sequence juxtaposed to the uORF2 termination codon that promotes inefficient termination that increases ribosome dissociation from the mRNA. During cellular stress, the inhibitory uORF2 in either *D. melanogaster* or *M. musculus* are bypassed resulting in increased translation initiation at the *Gadd34* CDS and increased *Gadd34* expression. Bypass of *M. musculus* uORF2 relies upon its moderate start codon context, whereas bypass of *D. melanogaster* uORF2 may rely upon additional factors. C, Illustration of the 5'-leader of *Gcn4* in fungal species *Saccharomyces cerevisiae* and *Candida albicans*. Translation control of *S. cerevisiae Gcn4* relies on a Delayed translation reinitiation model in which translation of the positive acting uORF1 (green bar) promotes translation reinitiation at downstream uORFs. Translation of the following uORFs 2, 3, and 4 (red bars) in the *S. cerevisiae Gcn4* 5'-leader are inhibitory to downstream translation by promoting ribosome dissociation from the mRNA in nonstressed conditions. During cellular stress, low ternary complex levels allow the scanning 40S ribosome to scan through the inhibitory uORFs in *Gcn4* post-uORF1 translation, resulting in translation initiation at the *Gcn4* CDS (blue bar). *C. albicans* translation control relies on a Bypass mechanism in which only uORF3 (red bar) is required for regulation of *Gcn4* expression. In nonstressed conditions, translation of uORF3 precludes the ribosome from initiating translation at the *C. albicans Gcn4* CDS, presumably through ribosome dissociation from the mRNA. During cellular stress, eIF2 α -P promotes bypass of the inhibitory uORF3, thereby facilitating an increase in translation of the *Gcn4* coding region (blue bar).

REFERENCES

1. Schwanhausser, B., Gossen, M., Dittmar, G., and Selbach, M. (2009) Global analysis of cellular protein translation by pulsed SILAC. *Proteomics* **9**, 205-209
2. Aviner, R., Geiger, T., and Elroy-Stein, O. (2013) Novel proteomic approach (PUNCH-P) reveals cell cycle-specific fluctuations in mRNA translation. *Genes & development* **27**, 1834-1844
3. Ingolia, N. T., Ghaemmaghami, S., Newman, J. R., and Weissman, J. S. (2009) Genome-wide analysis in vivo of translation with nucleotide resolution using ribosome profiling. *Science (New York, N.Y.)* **324**, 218-223
4. Gao, X., Wan, J., Liu, B., Ma, M., Shen, B., and Qian, S. B. (2015) Quantitative profiling of initiating ribosomes in vivo. *Nat Methods* **12**, 147-153
5. Baird, T. D., Palam, L. R., Fusakio, M. E., Willy, J. A., Davis, C. M., McClintick, J. N., Anthony, T. G., and Wek, R. C. (2014) Selective mRNA translation during eIF2 phosphorylation induces expression of IBTKalpha. *Mol Biol Cell* **25**, 1686-1697
6. Ingolia, N. T., Lareau, L. F., and Weissman, J. S. (2011) Ribosome profiling of mouse embryonic stem cells reveals the complexity and dynamics of mammalian proteomes. *Cell* **147**, 789-802
7. Iacono, M., Mignone, F., and Pesole, G. (2005) uAUG and uORFs in human and rodent 5'untranslated mRNAs. *Gene* **349**, 97-105
8. Calvo, S. E., Pagliarini, D. J., and Mootha, V. K. (2009) Upstream open reading frames cause widespread reduction of protein expression and are polymorphic among humans. *Proceedings of the National Academy of Sciences of the United States of America* **106**, 7507-7512
9. Kozak, M. (1989) The scanning model for translation: an update. *The Journal of cell biology* **108**, 229-241

10. Jackson, R. J., Hellen, C. U., and Pestova, T. V. (2010) The mechanism of eukaryotic translation initiation and principles of its regulation. *Nat Rev Mol Cell Biol* **11**, 113-127
11. Andreev, D. E., O'Connor, P. B., Fahey, C., Kenny, E. M., Terenin, I. M., Dmitriev, S. E., Cormican, P., Morris, D. W., Shatsky, I. N., and Baranov, P. V. (2015) Translation of 5' leaders is pervasive in genes resistant to eIF2 repression. *eLife* **4**, e03971
12. Palam, L. R., Baird, T. D., and Wek, R. C. (2011) Phosphorylation of eIF2 facilitates ribosomal bypass of an inhibitory upstream ORF to enhance CHOP translation. *The Journal of biological chemistry* **286**, 10939-10949
13. Vattem, K. M., and Wek, R. C. (2004) Reinitiation involving upstream open reading frames regulates ATF4 mRNA translation in mammalian cells. *Proc Natl Acad Sci U.S.A.* **101**, 11269-11274
14. Calkhoven, F. C., Muller, C., and Leutz, A. (2000) Translational control of C/EBPa and C/EBPb isoform expression. *Genes & development* **14**, 1920-1932
15. Zhou, D., Palam, L. R., Jiang, L., Narasimhan, J., Staschke, K. A., and Wek, R. C. (2008) Phosphorylation of eIF2 directs ATF5 translational control in response to diverse stress conditions. *The Journal of biological chemistry* **283**, 7064-7073
16. Baird, T. D., and Wek, R. C. (2012) Eukaryotic initiation factor 2 phosphorylation and translational control in metabolism. *Adv Nutr* **3**, 307-321
17. Kozak, M. (1987) Effects of intercistronic length on the efficiency of reinitiation by eucaryotic ribosomes. *Molecular and cellular biology* **7**, 3438-3445
18. Kozak, M. (2001) Constraints on reinitiation of translation in mammals. *Nucleic acids research* **29**, 5226-5232
19. Hinnebusch, A. G. (2005) Translational regulation of GCN4 and the general amino acid control of yeast. *Annual review of microbiology* **59**, 407-450

20. Miller, P. F., and Hinnebusch, A. G. (1988) Sequences that surround the stop codons of upstream open reading frames in *GCN4* mRNA determine their distinct functions in translational control. *Genes and Development* **8**, 1217-1225
21. Cuchalova, L., Kouba, T., Herrmannova, A., Danyi, I., Chiu, W. L., and Valasek, L. (2010) The RNA recognition motif of eukaryotic translation initiation factor 3g (eIF3g) is required for resumption of scanning of posttermination ribosomes for reinitiation on *GCN4* and together with eIF3i stimulates linear scanning. *Molecular and cellular biology* **30**, 4671-4686
22. Skabkin, M. A., Skabkina, O. V., Hellen, C. U., and Pestova, T. V. (2013) Reinitiation and other unconventional posttermination events during eukaryotic translation. *Molecular cell* **51**, 249-264
23. Poyry, T. A., Kaminski, A., Connell, E. J., Fraser, C. S., and Jackson, R. J. (2007) The mechanism of an exceptional case of reinitiation after translation of a long ORF reveals why such events do not generally occur in mammalian mRNA translation. *Genes & development* **21**, 3149-3162
24. Kolupaeva, V. G., Unbehauen, A., Lomakin, I. B., Hellen, C. U., and Pestova, T. V. (2005) Binding of eukaryotic initiation factor 3 to ribosomal 40S subunits and its role in ribosomal dissociation and anti-association. *RNA (New York, N.Y.)* **11**, 470-486
25. Zinoviev, A., Hellen, C. U., and Pestova, T. V. (2015) Multiple mechanisms of reinitiation on bicistronic calicivirus mRNAs. *Molecular cell* **57**, 1059-1073
26. Law, G. L., Raney, A., Heusner, C., and Morris, D. R. (2001) Polyamine regulation of ribosome pausing at the upstream open reading frame of S-adenosylmethionine decarboxylase. *The Journal of biological chemistry* **276**, 38036-38043

27. Col, B., Oltean, S., and Banerjee, R. (2007) Translational regulation of human methionine synthase by upstream open reading frames. *Biochimica et biophysica acta* **1769**, 532-540
28. Grant, C. M., and Hinnebusch, A. G. (1994) Effect of sequence context at stop codons on efficiency of reinitiation in GCN4 translational control. *Molecular and cellular biology* **14**, 606-618
29. Abastado, J. P., Miller, P. F., and Hinnebusch, A. G. (1991) A quantitative model for translational control of the GCN4 gene of *Saccharomyces cerevisiae*. *The New biologist* **3**, 511-524
30. Lee, Y. Y., Cevallos, R. C., and Jan, E. (2009) An upstream open reading frame regulates translation of GADD34 during cellular stresses that induce eIF2alpha phosphorylation. *The Journal of biological chemistry* **284**, 6661-6673
31. Raveh-Amit, H., Maissel, A., Poller, J., Marom, L., Elroy-Stein, O., Shapira, M., and Livneh, E. (2009) Translational control of protein kinase Ceta by two upstream open reading frames. *Molecular and cellular biology* **29**, 6140-6148
32. Kozak, M. (1986) Point mutations define a sequence flanking the AUG initiator codon that modulates translation by eukaryotic ribosomes. *Cell* **44**, 283-292
33. Starck, S. R., Tsai, J. C., Chen, K., Shodiya, M., Wang, L., Yahiro, K., Martins-Green, M., Shastri, N., and Walter, P. (2016) Translation from the 5' untranslated region shapes the integrated stress response. *Science (New York, N.Y.)* **351**, aad3867
34. Kozak, M. (1989) Context effects and inefficient initiation at non-AUG codons in eucaryotic cell-free translation systems. *Molecular and cellular biology* **9**, 5073-5080
35. Hinnebusch, A. G. (2014) The scanning mechanism of eukaryotic translation initiation. *Annual review of biochemistry* **83**, 779-812

36. Walter, P., and Ron, D. (2011) The unfolded protein response: from stress pathway to homeostatic regulation. *Science (New York, N.Y.)* **334**, 1081-1086
37. Jousse, C., Bruhat, A., Carraro, V., Urano, F., Ferrara, M., Ron, D., and Fafournoux, P. (2001) Inhibition of CHOP translation by a peptide encoded by an open reading frame localized in the chop 5'UTR. *Nucleic acids research* **29**, 4341-4351
38. Lu, P. D., Harding, H. P., and Ron, D. (2004) Translation reinitiation at alternative open reading frames regulates gene expression in an integrated stress response. *The Journal of cell biology* **167**, 27-33
39. Harding, H. P., Zhang, Y., Scheuner, D., Chen, J. J., Kaufman, R. J., and Ron, D. (2009) Ppp1r15 gene knockout reveals an essential role for translation initiation factor 2 alpha (eIF2alpha) dephosphorylation in mammalian development. *Proceedings of the National Academy of Sciences of the United States of America* **106**, 1832-1837
40. Novoa, I., Zeng, H., Harding, H. P., and Ron, D. (2001) Feedback inhibition of the unfolded protein response by GADD34-mediated dephosphorylation of eIF2alpha. *The Journal of cell biology* **153**, 1011-1022
41. Abastado, J. P., Miller, P. F., Jackson, B. M., and Hinnebusch, A. G. (1991) Suppression of ribosomal reinitiation at upstream open reading frames in amino acid-starved cells forms the basis of GCN4 translational control. *Molecular and cellular biology* **11**, 486-496
42. Harding, H. P., Zhang, Y., Zeng, H., Novoa, I., Lu, P. D., Calton, M., Sadri, N., Yun, C., Popko, B., Paules, R., Stojdl, D. F., Bell, J. C., Hettmann, T., Leiden, J. M., and Ron, D. (2003) An integrated stress response regulates amino acid metabolism and resistance to oxidative stress. *Molecular cell* **11**, 619-633

43. Mascarenhas, C., Edwards-Ingram, L. C., Zeef, L., Shenton, D., Ashe, M. P., and Grant, C. M. (2008) Gcn4 is required for the response to peroxide stress in the yeast *Saccharomyces cerevisiae*. *Mol Biol Cell* **19**, 2995-3007
44. Natarajan, K., Meyer, M. R., Jackson, B. M., Slade, D., Roberts, C., Hinnebusch, A. G., and Marton, M. J. (2001) Transcriptional profiling shows that Gcn4p is a master regulator of gene expression during amino acid starvation in yeast. *Molecular and cellular biology* **21**, 4347-4368
45. Hinnebusch, A. G., and Natarajan, K. (2002) Gcn4p, a master regulator of gene expression, is controlled at multiple levels by diverse signals of starvation and stress. *Eukaryot Cell* **1**, 22-32
46. Harding, H. P., Novoa, I., Zhang, Y., Zeng, H., Wek, R., Schapira, M., and Ron, D. (2000) Regulated translation initiation controls stress-induced gene expression in mammalian cells. *Molecular cell* **6**, 1099-1108
47. Sonenberg, N., and Hinnebusch, A. G. (2009) Regulation of translation initiation in eukaryotes: mechanisms and biological targets. *Cell* **136**, 731-745
48. Pisarev, A. V., Kolupaeva, V. G., Pisareva, V. P., Merrick, W. C., Hellen, C. U., and Pestova, T. V. (2006) Specific functional interactions of nucleotides at key -3 and +4 positions flanking the initiation codon with components of the mammalian 48S translation initiation complex. *Genes & development* **20**, 624-636
49. Zinszner, H., Kuroda, M., Wang, X. Z., Batchvarova, N., Lightfoot, R. T., Remotti, H., Stevens, J. L., and Ron, D. (1998) CHOP is implicated in programmed cell death in response to impaired function of the endoplasmic reticulum. *Genes & development* **12**, 982-995
50. Rutkowski, D. T., Arnold, S. M., Miller, C. N., Wu, J., Li, J., Gunnison, K. M., Mori, K., Sadighi Akha, A. A., Raden, D., and Kaufman, R. J. (2006) Adaptation to ER

- stress is mediated by differential stabilities of pro-survival and pro-apoptotic mRNAs and proteins. *PLoS Biol* **4**, e374
51. Hussain, T., Llacer, J. L., Fernandez, I. S., Munoz, A., Martin-Marcos, P., Savva, C. G., Lorsch, J. R., Hinnebusch, A. G., and Ramakrishnan, V. (2014) Structural changes enable start codon recognition by the eukaryotic translation initiation complex. *Cell* **159**, 597-607
 52. Pestova, T. V., and Kolupaeva, V. G. (2002) The roles of individual eukaryotic translation initiation factors in ribosomal scanning and initiation codon selection. *Genes and Development* **16**, 2906-2922
 53. Shi, Y., Vattem, K. M., Sood, R., An, J., Liang, J., Stramm, L., and Wek, R. C. (1998) Identification and characterization of pancreatic eukaryotic initiation factor 2 alpha-subunit kinase, PEK, involved in translational control. *Molecular and cellular biology* **18**, 7499-7509
 54. Harding, H. P., Zhang, Y., and Ron, D. (1999) Protein translation and folding are coupled by an endoplasmic-reticulum-resident kinase. *Nature* **397**, 271-274
 55. Ma, Y., and Hendershot, L. M. (2003) Delineation of a negative feedback regulatory loop that controls protein translation during endoplasmic reticulum stress. *The Journal of biological chemistry* **278**, 34864-34873
 56. Connor, J. H., Weiser, D. C., Li, S., Hallenbeck, J. M., and Shenolikar, S. (2001) Growth arrest and DNA damage-inducible protein GADD34 assembles a novel signaling complex containing protein phosphatase 1 and inhibitor 1. *Molecular and cellular biology* **21**, 6841-6850
 57. Saito, A., Ochiai, K., Kondo, S., Tsumagari, K., Murakami, T., Cavener, D. R., and Imaizumi, K. (2011) Endoplasmic reticulum stress response mediated by the PERK-eIF2(alpha)-ATF4 pathway is involved in osteoblast differentiation induced by BMP2. *The Journal of biological chemistry* **286**, 4809-4818

58. Tohmonda, T., Miyauchi, Y., Ghosh, R., Yoda, M., Uchikawa, S., Takito, J., Morioka, H., Nakamura, M., Iwawaki, T., Chiba, K., Toyama, Y., Urano, F., and Horiuchi, K. (2011) The IRE1alpha-XBP1 pathway is essential for osteoblast differentiation through promoting transcription of Osterix. *EMBO reports* **12**, 451-457
59. Murakami, T., Saito, A., Hino, S., Kondo, S., Kanemoto, S., Chihara, K., Sekiya, H., Tsumagari, K., Ochiai, K., Yoshinaga, K., Saitoh, M., Nishimura, R., Yoneda, T., Kou, I., Furuichi, T., Ikegawa, S., Ikawa, M., Okabe, M., Wanaka, A., and Imaizumi, K. (2009) Signalling mediated by the endoplasmic reticulum stress transducer OASIS is involved in bone formation. *Nature cell biology* **11**, 1205-1211
60. Jang, W. G., Kim, E. J., Kim, D. K., Ryoo, H. M., Lee, K. B., Kim, S. H., Choi, H. S., and Koh, J. T. (2012) BMP2 protein regulates osteocalcin expression via Runx2-mediated Atf6 gene transcription. *The Journal of biological chemistry* **287**, 905-915
61. Karsenty, G. (2008) Transcriptional control of skeletogenesis. *Annual review of genomics and human genetics* **9**, 183-196
62. Childress, P., Stayrook, K. R., Alvarez, M. B., Wang, Z., Shao, Y., Hernandez-Buquer, S., Mack, J. K., Grese, Z. R., He, Y., Horan, D., Pavalko, F. M., Warden, S. J., Robling, A. G., Yang, F. C., Allen, M. R., Krishnan, V., Liu, Y., and Bidwell, J. P. (2015) Genome-Wide Mapping and Interrogation of the Nmp4 Antianabolic Bone Axis. *Molecular endocrinology (Baltimore, Md.)* **29**, 1269-1285
63. Childress, P., Philip, B. K., Robling, A. G., Bruzzaniti, A., Kacena, M. A., Bivi, N., Plotkin, L. I., Heller, A., and Bidwell, J. P. (2011) Nmp4/CIZ suppresses the response of bone to anabolic parathyroid hormone by regulating both osteoblasts and osteoclasts. *Calcified tissue international* **89**, 74-89

64. Robling, A. G., Childress, P., Yu, J., Cotte, J., Heller, A., Philip, B. K., and Bidwell, J. P. (2009) Nmp4/CIZ suppresses parathyroid hormone-induced increases in trabecular bone. *Journal of cellular physiology* **219**, 734-743
65. UCSC Genome Bioinformatics. <http://genome.ucsc.edu>
66. Jiang, H. Y., Wek, S. A., McGrath, B. C., Lu, D., Hai, T., Harding, H. P., Wang, X., Ron, D., Cavener, D. R., and Wek, R. C. (2004) Activating transcription factor 3 (ATF3) is integral to the eIF2 kinase stress response. *Molecular and cellular biology* **24**, 1365-1377
67. Teske, B. F., Fusakio, M. E., Zhou, D., Shan, J., McClintick, J. N., Kilberg, M. S., and Wek, R. C. (2013) CHOP induces activating transcription factor 5 (ATF5) to trigger apoptosis in response to perturbations in protein homeostasis. *Mol Biol Cell* **24**, 2477-2490
68. Teske, B. F., Baird, T. D., and Wek, R. C. (2011) Methods for analyzing eIF2 kinases and translational control in the unfolded protein response. *Methods Enzymol* **490**, 333-356
69. Fang, P., Spevak, C. C., Wu, C., and Sachs, M. S. (2004) A nascent polypeptide domain that can regulate translation elongation. *Proceedings of the National Academy of Sciences of the United States of America* **101**, 4059-4064
70. Wang, Z., and Sachs, M. S. (1997) Ribosome stalling is responsible for arginine-specific translation attenuation in *Neurospora crassa*. *Molecular and cellular biology* **17**, 4904-4913
71. Wang, Z., and Sachs, M. S. (1997) Arginine-specific regulation mediated by the *Neurospora crassa* arg-2 upstream open reading frame in a homologous, cell-free in vitro translation system. *Journal of Biological Chemistry* **272**, 255-261
72. Jousse, Oyadomari, S., Novoa, I., Lu, P. D., Zhang, H., Harding, H. P., and Ron, D. (2003) Inhibition of a constitutive translation initiation factor 2a phosphatase,

- CREP*, promotes survival of stressed cells. *The Journal of cell biology* **163**, 767-775
73. Gutierrez, E., Shin, B. S., Woolstenhulme, C. J., Kim, J. R., Saini, P., Buskirk, A. R., and Dever, T. E. (2013) eIF5A promotes translation of polyproline motifs. *Molecular cell* **51**, 35-45
 74. Tsaytler, P., Harding, H. P., Ron, D., and Bertolotti, A. (2011) Selective inhibition of a regulatory subunit of protein phosphatase 1 restores proteostasis. *Science (New York, N.Y.)* **332**, 91-94
 75. Rutkowski, D. T., and Kaufman, R. J. (2007) That which does not kill me makes me stronger: adapting to chronic ER stress. *Trends Biochem Sci* **32**, 469-476
 76. Ma, Y., Brewer, J. W., Diehl, J. A., and Hendershot, L. M. (2002) Two distinct stress signaling pathways converge upon the *CHOP* promoter during the mammalian unfolded protein response. *J Mol Biol* **318**, 1351-1365
 77. Fawcett, T. W., Martindale, J. L., Guyton, K. Z., Hai, T., and Holbrook, N. J. (1999) Complexes containing activating transcription factor (ATF)/cAMP-responsive-element-binding-protein (CREB) interact with the CCAAT/enhancer-binding protein (C/EBP)-ATF composite site to regulate Gadd153 expression during the stress response. *Biochemical Journal* **339**, 135-141
 78. Mendell, J. T., Sharifi, N. A., Meyers, J. L., Martinez-Murillo, F., and Dietz, H. C. (2004) Nonsense surveillance regulates expression of diverse classes of mammalian transcripts and mutes genomic noise. *Nature genetics* **36**, 1073-1078
 79. Fawcett, T. W., Eastman, H. B., Martindale, J. L., and Holbrook, N. J. (1996) Physical and functional association between GADD153 and CCAAT/enhancer-binding protein beta during cellular stress. *Journal of Biological Chemistry* **271**, 14285-14289

80. Ron, D., and Habener, J. F. (1992) CHOP, a novel developmentally regulated nuclear protein that dimerizes with transcription factors C/EBP and LAP and functions as a dominant negative inhibitor of gene transcription. *Genes & development* **6**, 439-453
81. Ubeda, M., Wang, X. Z., Zinszner, H., Wu, I., Habener, J. F., and Ron, D. (1996) Stress-induced binding of the transcriptional factor CHOP to a novel DNA control element. *Molecular and cellular biology* **16**, 1479-1489
82. Puthalakath, H., O'Reilly, L. A., Gunn, P., Lee, L., Kelly, P. N., Huntington, N. D., Hughes, P. D., Michalak, E. M., McKimm-Breschkin, J., Motoyama, N., Gotoh, T., Akira, S., Bouillet, P., and Strasser, A. (2007) ER stress triggers apoptosis by activating BH3-only protein Bim. *Cell* **129**, 1337-1349
83. Lee, S., Liu, B., Lee, S., Huang, S. X., Shen, B., and Qian, S. B. (2012) Global mapping of translation initiation sites in mammalian cells at single-nucleotide resolution. *Proceedings of the National Academy of Sciences of the United States of America* **109**, E2424-2432
84. Peng, W., Robertson, L., Gallinetti, J., Mejia, P., Vose, S., Charlip, A., Chu, T., and Mitchell, J. R. (2012) Surgical stress resistance induced by single amino acid deprivation requires Gcn2 in mice. *Sci Transl Med* **4**, 118ra111
85. Keller, T. L., Zocco, D., Sundrud, M. S., Hendrick, M., Edenius, M., Yum, J., Kim, Y. J., Lee, H. K., Cortese, J. F., Wirth, D. F., Dignam, J. D., Rao, A., Yeo, C. Y., Mazitschek, R., and Whitman, M. (2012) Halofuginone and other febrifugine derivatives inhibit prolyl-tRNA synthetase. *Nat Chem Biol* **8**, 311-317
86. Zhou, H., Sun, L., Yang, X. L., and Schimmel, P. (2013) ATP-directed capture of bioactive herbal-based medicine on human tRNA synthetase. *Nature* **494**, 121-124

87. Marciniak, S. J., Yun, C. Y., Oyadomari, S., Novoa, I., Zhang, Y., Jungreis, R., Nagata, K., Harding, H. P., and Ron, D. (2004) CHOP induces death by promoting protein synthesis and oxidation in the stressed endoplasmic reticulum. *Genes & development* **18**, 3066-3077
88. Han, J., Back, S. H., Hur, J., Lin, Y. H., Gildersleeve, R., Shan, J., Yuan, C. L., Krokowski, D., Wang, S., Hatzoglou, M., Kilberg, M. S., Sartor, M. A., and Kaufman, R. J. (2013) ER-stress-induced transcriptional regulation increases protein synthesis leading to cell death. *Nature cell biology* **15**, 481-490
89. Boyce, M., Bryant, K. F., Jousse, C., Long, K., Harding, H. P., Scheuner, D., Kaufman, R. J., Ma, D., Coen, D. M., Ron, D., and Yuan, J. (2005) A selective inhibitor of eIF2alpha dephosphorylation protects cells from ER stress. *Science (New York, N.Y.)* **307**, 935-939
90. van Riggelen, J., Yetil, A., and Felsher, D. W. (2010) MYC as a regulator of ribosome biogenesis and protein synthesis. *Nature reviews. Cancer* **10**, 301-309
91. Iadevaia, V., Liu, R., and Proud, C. G. (2014) mTORC1 signaling controls multiple steps in ribosome biogenesis. *Seminars in cell & developmental biology* **36**, 113-120
92. Preston, A. M., and Hendershot, L. M. (2013) Examination of a second node of translational control in the unfolded protein response. *Journal of cell science* **126**, 4253-4261
93. Scheuner, D., Song, B., McEwen, E., Liu, C., Laybutt, R., Gillespie, P., Saunders, T., Bonner-Weir, S., and Kaufman, R. J. (2001) Translational control is required for the unfolded protein response and in vivo glucose homeostasis. *Molecular cell* **7**, 1165-1176

94. Harding, H. P., Zhang, Y., Bertolotti, A., Zeng, H., and Ron, D. (2000) Perk is essential for translational regulation and cell survival during the unfolded protein response. *Molecular cell* **5**, 897-904
95. Thoreen, C. C., Kang, S. A., Chang, J. W., Liu, Q., Zhang, J., Gao, Y., Reichling, L. J., Sim, T., Sabatini, D. M., and Gray, N. S. (2009) An ATP-competitive mammalian target of rapamycin inhibitor reveals rapamycin-resistant functions of mTORC1. *The Journal of biological chemistry* **284**, 8023-8032
96. Novoa, I., Zhang, Y., Zeng, H., Jungreis, R., Harding, H. P., and Ron, D. (2003) Stress-induced gene expression requires programmed recovery from translational repression. *The EMBO journal* **22**, 1180-1187
97. Das, I., Krzyzosiak, A., Schneider, K., Wrabetz, L., D'Antonio, M., Barry, N., Sigurdardottir, A., and Bertolotti, A. (2015) Preventing proteostasis diseases by selective inhibition of a phosphatase regulatory subunit. *Science (New York, N.Y.)* **348**, 239-242
98. Osowski, C. M., and Urano, F. (2010) The binary switch between life and death of endoplasmic reticulum-stressed beta cells. *Current opinion in endocrinology, diabetes, and obesity* **17**, 107-112
99. Cho, S., Park, S. M., Kim, T. D., Kim, J. H., Kim, K. T., and Jang, S. K. (2007) BiP internal ribosomal entry site activity is controlled by heat-induced interaction of NSAP1. *Molecular and cellular biology* **27**, 368-383
100. Kim, Y. K., and Jang, S. K. (2002) Continuous heat shock enhances translational initiation directed by internal ribosomal entry site. *Biochemical and biophysical research communications* **297**, 224-231
101. Ibba, M., and Soll, D. (2000) Aminoacyl-tRNA synthesis. *Annual review of biochemistry* **69**, 617-650

102. Ling, J., Reynolds, N., and Ibba, M. (2009) Aminoacyl-tRNA synthesis and translational quality control. *Annual review of microbiology* **63**, 61-78
103. Zaborske, J. M., Narasimhan, J., Jiang, L., Wek, S. A., Dittmar, K. A., Freimoser, F., Pan, T., and Wek, R. C. (2009) Genome-wide analysis of tRNA charging and activation of the eIF2 kinase Gcn2p. *The Journal of biological chemistry* **284**, 25254-25267
104. Bernales, S., Papa, F. R., and Walter, P. (2006) Intracellular signaling by the unfolded protein response. *Annu Rev Cell Dev Biol* **22**, 487-508
105. Narasimhan, J., Staschke, K. A., and Wek, R. C. (2004) Dimerization is required for activation of eIF2 kinase Gcn2 in response to diverse environmental stress conditions. *The Journal of biological chemistry* **279**, 22820-22832
106. Bullwinkle, T. J., Reynolds, N. M., Raina, M., Moghal, A., Matsa, E., Rajkovic, A., Kayadibi, H., Fazlollahi, F., Ryan, C., Howitz, N., Faull, K. F., Lazazzera, B. A., and Ibba, M. (2014) Oxidation of cellular amino acid pools leads to cytotoxic mistranslation of the genetic code. *eLife* **3**
107. Bullwinkle, T., Lazazzera, B., and Ibba, M. (2014) Quality control and infiltration of translation by amino acids outside of the genetic code. *Annual review of genetics* **48**, 149-166
108. Mukhopadhyay, R., Jia, J., Arif, A., Ray, P. S., and Fox, P. L. (2009) The GAIT system: a gatekeeper of inflammatory gene expression. *Trends Biochem Sci* **34**, 324-331
109. Wei, J., Sheng, X., Feng, D., McGrath, B., and Cavener, D. R. (2008) PERK is essential for neonatal skeletal development to regulate osteoblast proliferation and differentiation. *Journal of cellular physiology* **217**, 693-707
110. Nakamoto, T., Yamagata, T., Sakai, R., Ogawa, S., Honda, H., Ueno, H., Hirano, N., Yazaki, Y., and Hirai, H. (2000) CIZ, a zinc finger protein that interacts with

- p130(cas) and activates the expression of matrix metalloproteinases. *Molecular and cellular biology* **20**, 1649-1658
111. Alvarez, M., Shah, R., Rhodes, S. J., and Bidwell, J. P. (2005) Two promoters control the mouse Nmp4/CIZ transcription factor gene. *Gene* **347**, 43-54
 112. Thunyakitpisal, P., Alvarez, M., Tokunaga, K., Onyia, J. E., Hock, J., Ohashi, N., Feister, H., Rhodes, S. J., and Bidwell, J. P. (2001) Cloning and functional analysis of a family of nuclear matrix transcription factors (NP/NMP4) that regulate type I collagen expression in osteoblasts. *Journal of bone and mineral research : the official journal of the American Society for Bone and Mineral Research* **16**, 10-23
 113. Sharma, K., D'Souza, R. C., Tyanova, S., Schaab, C., Wisniewski, J. R., Cox, J., and Mann, M. (2014) Ultradeep human phosphoproteome reveals a distinct regulatory nature of Tyr and Ser/Thr-based signaling. *Cell reports* **8**, 1583-1594
 114. Mertins, P., Yang, F., Liu, T., Mani, D. R., Petyuk, V. A., Gillette, M. A., Clauser, K. R., Qiao, J. W., Gritsenko, M. A., Moore, R. J., Levine, D. A., Townsend, R., Erdmann-Gilmore, P., Snider, J. E., Davies, S. R., Ruggles, K. V., Fenyo, D., Kitchens, R. T., Li, S., Olvera, N., Dao, F., Rodriguez, H., Chan, D. W., Liebler, D., White, F., Rodland, K. D., Mills, G. B., Smith, R. D., Paulovich, A. G., Ellis, M., and Carr, S. A. (2014) Ischemia in tumors induces early and sustained phosphorylation changes in stress kinase pathways but does not affect global protein levels. *Molecular & cellular proteomics : MCP* **13**, 1690-1704
 115. Feister, H. A., Torrungruang, K., Thunyakitpisal, P., Parker, G. E., Rhodes, S. J., and Bidwell, J. P. (2000) NP/NMP4 transcription factors have distinct osteoblast nuclear matrix subdomains. *Journal of cellular biochemistry* **79**, 506-517
 116. Floor, S. N., and Doudna, J. A. (2016) Tunable protein synthesis by transcript isoforms in human cells. *eLife* **5**

117. Dey, S., Savant, S., Teske, B. F., Hatzoglou, M., Calkhoven, C. F., and Wek, R. C. (2012) Transcriptional repression of ATF4 gene by CCAAT/enhancer-binding protein beta (C/EBPbeta) differentially regulates integrated stress response. *The Journal of biological chemistry* **287**, 21936-21949
118. Hansen, M. B., Mitchelmore, C., Kjaerulff, K. M., Rasmussen, T. E., Pedersen, K. M., and Jensen, N. A. (2002) Mouse *ATF5*: Molecular cloning of two novel mRNAs, genomic organization, and odorant sensory neuron localization. *Genomics* **80**, 344-350
119. Dey, S., Baird, T. D., Zhou, D., Palam, L. R., Spandau, D. F., and Wek, R. C. (2010) Both transcriptional regulation and translational control of ATF4 are central to the integrated stress response. *The Journal of biological chemistry* **285**, 33165-33174
120. Watatani, Y., Ichikawa, K., Nakanishi, N., Fujimoto, M., Takeda, H., Kimura, N., Hirose, H., Takahashi, S., and Takahashi, Y. (2008) Stress-induced translation of ATF5 mRNA is regulated by the 5'-untranslated region. *The Journal of biological chemistry* **283**, 2543-2553
121. Gardner, B. M., Pincus, D., Gotthardt, K., Gallagher, C. M., and Walter, P. (2013) Endoplasmic reticulum stress sensing in the unfolded protein response. *Cold Spring Harbor perspectives in biology* **5**, a013169
122. Gardner, L. B. (2008) Hypoxic inhibition of nonsense-mediated RNA decay regulates gene expression and the integrated stress response. *Molecular and cellular biology* **28**, 3729-3741
123. Fritsch, C., Herrmann, A., Nothnagel, M., Szafranski, K., Huse, K., Schumann, F., Schreiber, S., Platzer, M., Krawczak, M., Hampe, J., and Brosch, M. (2012) Genome-wide search for novel human uORFs and N-terminal protein extensions using ribosomal footprinting. *Genome research* **22**, 2208-2218

124. Neafsey, D. E., and Galagan, J. E. (2007) Dual modes of natural selection on upstream open reading frames. *Molecular biology and evolution* **24**, 1744-1751
125. Johnstone, T. G., Bazzini, A. A., and Giraldez, A. J. (2016) Upstream ORFs are prevalent translational repressors in vertebrates. *The EMBO journal*
126. Malzer, E., Szajewska-Skuta, M., Dalton, L. E., Thomas, S. E., Hu, N., Skaer, H., Lomas, D. A., Crowther, D. C., and Marciniak, S. J. (2013) Coordinate regulation of eIF2alpha phosphorylation by PPP1R15 and GCN2 is required during *Drosophila* development. *Journal of cell science* **126**, 1406-1415
127. Olsen, D. S., Jordan, B., Chen, D., Wek, R. C., and Cavener, D. R. (1998) Isolation of the gene encoding the *Drosophila melanogaster* homolog of the *Saccharomyces cerevisiae* GCN2 eIF-2alpha kinase. *Genetics* **149**, 1495-1509
128. Pomar, N., Berlanga, J. J., Campuzano, S., Hernandez, G., Elias, M., and de Haro, C. (2003) Functional characterization of *Drosophila melanogaster* PERK eukaryotic initiation factor 2alpha (eIF2alpha) kinase. *European journal of biochemistry / FEBS* **270**, 293-306
129. Cvijovic, M., Dalevi, D., Bilsland, E., Kemp, G. J., and Sunnerhagen, P. (2007) Identification of putative regulatory upstream ORFs in the yeast genome using heuristics and evolutionary conservation. *BMC bioinformatics* **8**, 295
130. Sundaram, A., and Grant, C. M. (2014) A single inhibitory upstream open reading frame (uORF) is sufficient to regulate *Candida albicans* GCN4 translation in response to amino acid starvation conditions. *RNA (New York, N.Y.)* **20**, 559-567

CURRICULUM VITAE

Sara Kathryn Young

Education

Indiana University, Ph.D., Biochemistry and Molecular Biology, 2016

Indiana University, B.S., Biology, 2010

Honors, Awards, and Fellowships

2011-2012 I.U. School of Medicine University Fellowship

2009-2010 Undergraduate Capstone Research Honors Scholar, Indiana University

2009 Women in Science Conference, Best Undergraduate Poster Presentation
in the Natural Sciences Category, Indiana University

2006-2010 Arts and Sciences Indiana Scholars Award

2006-2007 Indiana Scholars Award

2006-2007 Integrated Freshman Learning Experience (IFLE) Undergraduate
Research Scholar, Indiana University

Research and Training Experience

2011-2016 Graduate Fellow, I.U. School of Medicine, Indianapolis, IN

2010-2011 Post-baccalaureate research assistant, Dept. of Biology, Indiana
University, Bloomington, IN

2009-2010 Undergraduate Capstone Research Honors Scholar, Dept. of Biology,
Indiana University

2007-2009 Undergraduate research assistant, Dept. of Biology, Indiana University

2006-2007 Integrated Freshman Learning Experience (IFLE) Undergraduate
Research Scholar, Dept. of Biology, Indiana University

Teaching Experience and Scholarly Activities

- 2014-2015 Coordinator, Central Dogma Research Journal Club, I.U. School of
Medicine
- 2012 Graduate Teaching Assistant, G716 Molecular Biology and Genetics, I.U.
School of Medicine

Publications

- Young S.K.**, Shao Y., Bidwell J.P., and R.C. Wek. 2016. NMP4 is a novel regulator of ribosome biogenesis and controls the Unfolded Protein Response via repression of *Gadd34*. *J. Biol. Chem.* In press.
- Young S.K.**, Baird T.D., and R.C. Wek. 2016. Translation regulation of the glutamyl-prolyl-tRNA synthetase gene *Eprs* through bypass of uORFs with non-canonical initiation codons. *J. Biol. Chem.* In press.
- Young S.K.**, Palam L.R., Wu C., Sachs M.S., and R.C. Wek. 2015. Ribosome elongation stall directs gene-specific translation and regulates cell homeostasis in the integrated stress response. *J. Biol. Chem.* 291(12): 6546-6558.
- Young S.K.**, Willy J.A., Wu C., Sachs M.S., and R.C. Wek. 2015. Ribosome reinitiation directs gene-specific translation and regulates the integrated stress response. *J. Biol. Chem.* 290(47): 28257-28271.
- Willy J.A., **Young S.K.**, Stevens J.L., Masuoka H.C., and R.C. Wek. 2015. CHOP links endoplasmic reticulum stress to NF- κ B activation in the pathogenesis of nonalcoholic steatohepatitis. *Mol. Biol. Cell.* 26(12): 2190-2204.
- Gao R., Chen S., Kobayashi M., Yu H., Zang Y., Wan Y., **Young S.K.**, Soltis A., Yu M., Vemula S., Fraenkel E., Cantor A., Antipin Y., Xu Y., Yoder M.C., Wek R.C., Ellis S.R., Kapur R., Zhu X., and Y. Liu. 2015. Bmi1 promotes erythroid development through regulating ribosome biogenesis. *Stem. Cells.* 33(3): 925-938.

Bashey F., **Young S.K.**, Hawlena H., and C.M. Lively. 2012. Spiteful interactions between sympatric natural isolates of *Xenorhabdus bovienii* benefit kin and reduce virulence. *J. Evol. Biol.* 25(3): 431-437.

Bashey F., Reynolds C., Sarin T., and **S.K. Young**. 2011. Virulence and competitive ability in an obligately killing parasite. *Oikos*. 120: 1539-1545.